

UC San Diego

UC San Diego Electronic Theses and Dissertations

Title

Radiocarbon Distribution in Atlantic Water Masses Over the Last 20 kyr - Results from a South Atlantic Sediment Depth Transect

Permalink

<https://escholarship.org/uc/item/8pg610zh>

Author

Munson, Jenna

Publication Date

2021

Peer reviewed|Thesis/dissertation

UNIVERSITY OF CALIFORNIA SAN DIEGO

**Radiocarbon Distribution in Atlantic Water Masses Over the Last 20 kyr -
Results from a South Atlantic Sediment Depth Transect**

A dissertation submitted in partial satisfaction of the requirements for the degree Doctor of
Philosophy

in

Oceanography

by

Jenna Marie Munson

Committee in Charge:

Professor Christopher Charles, Chair
Assistant Professor Sarah Aarons
Professor Carolyn Kurle
Professor Jennifer MacKinnon
Professor Richard Norris

2021

Copyright
Jenna Marie Munson, 2021
All rights reserved

This Dissertation of Jenna Marie Munson is approved, and it is acceptable in quality and form for publication on microfilm and electronically.

University of California San Diego

2021

TABLE OF CONTENTS

Dissertation Approval Page.....	iii
Table of Contents	iv
List of Tables.....	vi
List of Figures	vii
Acknowledgements.....	ix
Vita.....	xi
Abstract of the Dissertation.....	xii
Chapter 1: Introduction.....	1
Radiocarbon water mass reconstructions.....	2
Changes in water mass geometry in the past ocean.....	3
Organization of the dissertation.....	3
References.....	9
Chapter 2: A detailed test of the “depth transect” approach to paleoceanographic studies from a suite of sediment cores from the southeastern Atlantic.....	10
Abstract.....	11
Introduction.....	12
Materials and Methods.....	13
Results.....	15
Stratigraphic Correlation.....	15
Sequence of Events.....	21
Discussion.....	22
Summary and Conclusions.....	28
References.....	30
Chapter 3: A core top assessment from the southeastern Atlantic for the planktonic/benthic foraminiferal radiocarbon proxy.....	49
Abstract.....	50
Introduction.....	52
Core Locations and Oceanographic Setting.....	53
Materials and Methods.....	56
Results.....	58
Discussion.....	61
Summary and Conclusions.....	64
Acknowledgements.....	66
References.....	67

Chapter 4: Water mass distribution from the past 20,000 years reconstructed from radiocarbon and stable isotopes in the southeastern Atlantic.....	77
Abstract.....	78
Introduction.....	79
Materials and Methods.....	82
Results.....	84
Discussion.....	89
Summary and Conclusions.....	96
Acknowledgements.....	97
References.....	98

LIST OF TABLES

Table 2.1. Piston cores measured for bulk density, planktonic foraminiferal $\delta^{18}\text{O}$, and planktonic and benthic foraminiferal $\delta^{13}\text{C}$ and radiocarbon spanning the late glacial to present.....	33
Table 3.1. Core type, depth, core top radiocarbon ages, and core depth to the LGM.....	69
Table 4.1 Samples used from each core for radiocarbon and stable isotope measurements.....	100
Table 4.2 ^{14}C ages and distance to the LGM (as a proxy for sedimentation rate).....	101

LIST OF FIGURES

Figure 2.1. The Atlantic map is from <i>Prange et al.</i> , 2004 and depicts the Atlantic SST response to the meltwater perturbation in the present-day experiment. Two additional maps depict our study site, the cores sampled, and the water depth (m) they were collected from.....	34
Figure 2.2. Bulk density (g/cm ³) plotted versus core depth.....	35
Figure 2.3. Planktonic $\delta^{18}\text{O}$ and $\delta^{13}\text{C}$ of <i>G. bulloides</i> or <i>O. universa</i> plotted versus core depth. Black circles indicate intervals that were radiocarbon dated.....	38
Figure 2.4. <i>G. bulloides</i> $\delta^{18}\text{O}$ plotted versus <i>G. bulloides</i> $\delta^{13}\text{C}$ from core 31, spanning the late glacial to 15.0 kyr BP.....	41
Figure 2.5. Stacked bulk density (g/cm ³) and <i>G. bulloides</i> $\delta^{18}\text{O}$ from cores 17, 54, 27, 45, and 31.....	42
Figure 2.6. Calendar age and sedimentation rate for core 27 are plotted on its depth scale.....	44
Figure 2.7. $\delta^{18}\text{O}$ profiles from cores 21, 23, 27, 31, 45, 43, and 52 are plotted versus calendar age.....	45
Figure 2.8. Density profiles from cores 13, 25, 29, 39, 43, 45, and 52 plotted on a calendar age scale.	46
Figure 2.9 Bulk density z-scores for cores 13, 25, 29, 39, 43, 45, and 52; planktonic $\delta^{18}\text{O}$; benthic $\delta^{13}\text{C}$; temperature records from Greenland and Antarctica; and atmospheric $\Delta^{14}\text{C}$ are plotted versus calendar age.....	47
Figure 3.1. Weight % organic carbon of bulk sediment from core tops, dissolved inorganic carbon $\delta^{13}\text{C}$, $\delta^{13}\text{C}$ of benthic foraminifera, water column salinity values, $\delta^{18}\text{O}$ values from the benthic foraminifera, and predicted foraminiferal $\delta^{18}\text{O}$ values.....	70
Figure 3.2. Benthic minus planktonic ^{14}C ages from cores tops.....	72
Figure 3.3. $\Delta^{14}\text{C}$ values of benthic foraminifera, $\Delta^{14}\text{C}$ of dissolved inorganic carbon, Silica (μmol), and Salinity data.....	73
Figure 3.4. Abundance data (#/gram) for <i>O. universa</i> , <i>G. bulloides</i> , and mixed benthics from the present to the LGM for four cores: 31, 45, 54, and 17.....	75
Figure 4.1. Stacked density profiles of seven cores spanning the density high to low transition plotted with calendar age.....	102

Figure 4.2. Downcore $\delta^{13}\text{C}$ and bulk density values plotted versus depth in core for cores 31, 45, 27, and 17.....	103
Figure 4.3. <i>Globigerina bulloides</i> $\delta^{18}\text{O}$ values plotted versus depth in core.....	104
Figure 4.4. Modern and Last Glacial Maximum benthic foraminifera $\delta^{18}\text{O}$ values plotted versus core water depth (m).....	105
Figure 4.5. Benthic $\delta^{13}\text{C}$ values from, modern LGM, 15.2 kyr, and 13.7 kyr datasets.....	107
Figure 4.6. $\Delta^{14}\text{C}$ values measured on <i>O. universa</i> plotted relative to the atmosphere from the 15.2 kyr, 13.7 kyr, and modern datasets.....	108
Figure 4.7. Benthic minus planktonic ^{14}C dates plotted versus the water depth of the core.	109
Figure 4.8. Calendar age plotted versus <i>depth in core</i> for two planktonic species, <i>O. universa</i> and <i>G. bulloides</i> of core 27.....	110
Figure 4.9. Reconstructed modern and LGM benthic minus planktonic ^{14}C ages.....	111

ACKNOWLEDGEMENTS

I would like to thank Christopher Charles for his guidance and support as my advisor. He has an incredible capacity for critical thinking and is always available and willing to offer help and advice. I would also like to thank other faculty who have provided advice and guidance: Jeff Severinghaus, Lynne Talley, Joel Norris, and Neil Driscoll.

I want to thank all of the members of the Charles lab through the years I have been here. Kim Cobb and Stephanie Mumma were here when I arrived and helped me learn how to work in the lab and on the mass spec. Other paleo students who came to Scripps at the same time: Takuro Kobashi, Vasilli Petreknko, Tabitha Hensley and Melissa Headly were great friends and helpful colleagues. In addition, the climate group (Heather Graven, Vas, Takuro, Neil Gordon, and Melissa) was helpful and supportive and I enjoyed studying and coursework with them. Ross Beaudette, the Sevrinhaus lab technician, was always willing to lend a hand and help with any equipment fixes. The Charles Lab group got bigger with the addition of Patrick Rafter and Lydia Roach - they were an enjoyable addition and made tedious foraminifera picking and late-night mass spectrometer runs go by faster. I also thank the radiocarbon team at Lawrence Livermore for their guidance preparing and analyzing my samples: Michael Kashgarian, Tom Guilderson, and their lab technicians.

Most of the cores used in this project were collected during the MelVan 09 cruise off the coast of Africa with Niall Slowey's team from the University of Texas. They took the 12 hour overnight shifts and were helpful and accommodating of me when I made trip to Texas to sample them.

I have made incredible friends at Scripps and appreciate their support, friendship, and making my time in San Diego memorable. Melissa Headly and Christine Whitcraft were wonderful friends

and I am thankful we were given the opportunity to go through grad school together. Evan Solomon made my time in my office in Sverdrup memorable and fun – I appreciated his quirky wit and wry commentary. Other friends I'd like to thank are Jenna Hill, Tabitha Hensely, Brian Hopkinson, Roman DeJesus, Travis Meador, Roberta Hansman, Mike Vardaro, and Andrew King,

Lastly, I want to thank my aunt, Marcia Sessa lives in San Diego and was always ready to pamper me with dinners, or time relaxing on her patio when I needed that. My brother moved to San Diego towards the end of my time at Scripps and I am so thankful for that extra time I got to spend with him. I loved our family traditions of Thanksgiving at T-29, I am thankful my family was always willing to come out and visit. Lastly, I want to thank my husband Gregory Dick. He was one of the first people I met at Scripps and he has been a constant source of steady love and support.

VITA

2000 Bachelor of Science, University of Minnesota, Duluth

2001-2008 Research Assistant, University of California San Diego

2002-2004 Teaching Assistant, Department of Earth Science, University of California
San Diego

2002-2006 Lawrence Livermore National Laboratory Student Employee Fellow

2007 Master of Science, University of California San Diego

2021 Doctor of Philosophy, University of California San Diego

PUBLICATIONS

- Lynch-Stieglitz, J., W.B. Curry, D.W. Oppo, U.N. Ninneman, C.D. Charles, and J.M. Munson.
Meridional overturning circulation in the south Atlantic at the last glacial maximum.
Geochemistry, Geophysics, Geosystems, 7, Q10N03, doi:10.1029/2005GC001226 (2006).
- Jablonski, Sarah, Ellen Mccray, Jenna Munson, and Dann Blackwood, 2002. Geochemical
Sediment Analysis Procedures: U.S. Geological Survey Open-File Report 02-371

FIELD OF STUDY

Major Field: Oceanography

Studies in Paleoclimatology
Professors Christopher Charles and Richard Norris

ABSTRACT OF THE DISSERTATION

Radiocarbon Distribution in Atlantic Water Masses Over the Last 20 kyr - Results From a South Atlantic Sediment Depth Transect

by

Jenna Marie Munson

Doctor of Philosophy in Oceanography

University of California San Diego, 2021

Professor Christopher Charles, Chair

We present radiocarbon results from a geographically constrained depth transect of sediment cores from water depths spanning 400-3500 meters in the southeastern Atlantic. The distribution of radiocarbon is a tracer of the ventilation history of mid-depth water and can delineate water of North Atlantic versus Southern sources. Coexisting benthic and planktonic foraminifera pairs in the sedimentary record have been used to reconstruct past changes in ventilation, yet the fidelity of the method has been called in to question due to potential problems

and biases. Thus, before interpretation of past changes to the ocean's interior can be made, it is important to assess the validity of using benthic/planktonic pairs to distinguish the essential features of modern seawater radiocarbon distribution. Here we present radiocarbon and stable isotope results from twenty-seven high sedimentation rate modern samples from the southeastern Atlantic, an area where the seafloor intersects all the principal water masses involved in the thermohaline circulation of the Atlantic. We use two cosmopolitan planktonic species, from different habitats, and with a ^{14}C age of less than 2000 years and find several consistent trends; it is these consistent trends that provide quantitative insight to the benthic-planktonic radiocarbon method. In all cases, the *G. bulloides* ^{14}C ages are older than *O. universa*. However, this age offset between *O. universa* and *G. bulloides* is not consistent at all water depths – the ages diverge significantly in the 2000-1500 water depth range, in parallel with the shifts in sedimentary organic carbon %. This inter-species variability is large enough to overwhelm any possible radiocarbon differences in deep water masses (benthic foraminifera). Clearly, even among the most abundant taxa, planktonic foraminifera do not provide an interchangeable chronological reference for the benthic foraminiferal radiocarbon. Restricting the analysis to planktonic foraminifera that are most likely to be “surface dwelling”—in our case, *O. universa*—results in a benthic-planktonic radiocarbon depth profile that bears the same structure as modern seawater nutrient profiles (especially dissolved silica) in the region. However, benthic-planktonic radiocarbon depth profile does not reproduce the features of the closest dissolved inorganic carbon $\Delta^{14}\text{C}$ (modern seawater) profile. In particular, with respect to modern DIC $\Delta^{14}\text{C}$ measurements, the benthic-planktonic depth profile gives the impression of significantly “older” water bathing mid depth sediments (600-800 meters) and abyssal depth sediments

(greater than 2500 meters). The consistency of the trends with water depth provides a measure of the fidelity of the method for reconstructions over the interval since the last glacial maximum.

Chapter 1

Introduction

The last 20,000 years was punctuated by several abrupt changes in the global climate and deep-ocean systems. We know these climate events involved a reorganization of the thermohaline circulation (e.g. Boyle and Keigwin, 1987; Keigwin et al. 1991; Sarnthein et al. 1994), yet how the mid-depth of the Atlantic changed during these events is still unresolved.

Because all the principal water masses involved in the thermohaline circulation of the Atlantic are found in the mid-depths of the southeastern Atlantic, this is an ideal location to track changes in the configuration of water masses. Here they are present in a layer-cake structure; southern source, northward-flowing Antarctic Bottom Water (AABW) fills the deep basin, overlain by northern-source, southward-flowing North Atlantic Deep Water (NADW), which is overlain by southern source, northward flowing Antarctic Intermediate Water (AAIW). This interleaving of three principle water masses at this location, make it ideal for examining the changing dominance of northern versus southern source waters in the Atlantic during the late Pleistocene.

Various nutrient proxies such as benthic foraminiferal $\delta^{13}\text{C}$, Cd/Ca, and sedimentary neodymium isotopes have been used to reconstruct the distribution of water masses involved in thermohaline circulation over abrupt climate changes (*Sarnthein et al.*, 1994; *Boyle and Keigwin*, 1985; *Piotrowsi et al.*, 2005). However, these proxies cannot discern rates of overturning, whereas radiocarbon is a powerful tracer for tracking changes in both the geometry and ventilation history of major water masses. Thus far, most radiocarbon data from the LGM and deglacial is currently concentrated in the western North Atlantic.

Detailed radiocarbon and stable isotope measurements along a depth-transect in the southeastern Atlantic will help constrain specific circulation patterns over the abrupt climate events at the LGM and through the deglacial period. This depth transect approach has been

used to reconstruct past water columns using oxygen (*Lynch Stieglitz et al.*, 2006) and carbon isotopes (*Curry and Oppo*, 2005; *Sarnthein et al.*, 1994). While stable isotopes can provide useful information about water mass changes, radiocarbon offers the ability to discern rates of overturning. The challenge with using radiocarbon is that the age of the global ocean is less than 1000 years and the radiocarbon age of deep and intermediate water masses varies within any ocean basin by a maximum of about 500 years. For radiocarbon to be useful, correlation within a few hundred years of discrete stratigraphic markers needs to be achieved between cores. We achieved this in a small subset of cores taken from the southeastern Atlantic where AAIW, NADW, and AABW are found stacked on top of each other.

The overarching goal of this dissertation was to reconstruct the ventilation history of mid-depth water in the Atlantic Ocean and track changes in the distribution of water masses through time. This was accomplished by measuring radiocarbon of benthic foraminifera at discrete intervals corresponding to known climatic events, such as the last glacial maximum (LGM) and the Bolling-Allerod. Our strategy for reconstructing past water column changes involved a number of steps. First, collect a large number of cores, from a small geographic location, that intersect all the principle water masses involved in the thermohaline circulation of the Atlantic. Second, provide guidelines for the validity of stacking these cores based on sedimentological and chronological data points (chapter 2). Third, use modern, radiocarbon-dated core tops to assess the validity of the paired benthic minus planktonic method for reconstructing past water column structure (chapter 3). Fourth, we were able to determine guidelines for the paired benthic-planktonic method and apply them to our subset of cores aligned at the LGM and deglacial (chapter 4). Overall, these results filled in a data gap for

information from the southeastern Atlantic about the water column configuration at the LGM.

Chapter 2: A detailed test of the "depth transect" approach to paleoceanographic studies from a suite of sediment cores from the southeastern Atlantic.

We limited core sampling to a small geographic area, where surface processes should be uniform. Therefore, density (as a proxy for carbonate versus silica composition) and planktonic isotopic records (recording surface ocean variability) should correlate among cores. Once cores are correlated using these records, benthic radiocarbon and stable isotope analysis – recording the deep-water signal at the water depth of the core, can be used to interpret the changing water column in this area and the linkage between past ocean circulation and climate.

We analyzed sixteen cores using radiocarbon dating and stable isotope and density measurements. Although at first glance there were a number of sedimentological disturbances, we found that careful, individual analysis of cores, at the time horizons of interest, allowed us to compile a robust dataset. This allowed the construction of a basic sequence of oceanographic events for the southeast Atlantic at the Last Glacial Maximum (LGM) and through the deglacial.

In seven of the sixteen cores analyzed, we were able to show stratigraphic and chronological convergence to within a few hundred years of each other at both the LGM and at the onset of the Bolling-Allerod. These cores were well-dated and well-resolved - sampled at 5 or 10 cm intervals. All cores share four prominent stratigraphic markers: a $\delta^{18}\text{O}$ and $\delta^{13}\text{C}$ high immediately preceding a rapid shift to lower values, the $\delta^{18}\text{O}$ and $\delta^{13}\text{C}$ low immediately following this shift, as well as a prominent density high and low on each end of an abrupt

density shift. These stratigraphic markers coincide with known world-wide climatic changes from the Last Glacial Maximum (LGM) through the deglacial period – the LGM being identified at our $\delta^{18}\text{O}$ and $\delta^{13}\text{C}$ high. Decreasing $\delta^{18}\text{O}$ values after the LGM indicate an abrupt warming. Two other stratigraphic markers were a prominent density high (average age 14,552 years BP), followed by an abrupt shift to a density low – a transition coincident with the onset of the Bolling-Allerod (BA) at 14,550 years BP.

Only seven of sixteen cores analyzed were tightly correlated enough to be useful in constructing a sequence of events between cores. Nine of our cores had sedimentological disturbances and had to be culled out. This highlights the importance of carefully scrutinizing each individual core at each interval of interest, which requires a large number of planktonic radiocarbon dates to accept or reject certain section of each core. We found interpolation of dates cannot be made too far between dated points, and that stratigraphic correlation did not necessarily mean chronological correlation. We were able to use less than half of our initial cores, signifying future *depth transect approach* studies need to start with a large number of cores to find a meaningful subset. Our culled dataset of seven cores allowed us to construct a basic sequence of oceanographic events for the southeast Atlantic. Details of the changing deep-water geometry during these oceanographic and climatic events are presented in Chapter 4.

Chapter 3: *A core top assessment from the southeastern Atlantic for the planktonic/benthic foraminiferal radiocarbon proxy*

To track deep-water distribution, paired benthic/planktonic radiocarbon dates have been used in other studies. Planktonic foraminifera are assumed to be reflecting surface radiocarbon values, which are in equilibrium with the atmosphere, and therefore can be used

to determine the calendar age of the sediment sample. Benthic foraminifera are dated to obtain the radiocarbon signal from the water-depth the core was sampled at. By subtracting the planktonic radiocarbon age from the benthic radiocarbon age, the result is the “age” of the water mass the benthic foraminifera were living in. The idea behind this method is southern and northern sources waters, AAIW, AABW, and NADW each have a unique radiocarbon signature to differentiate them from each other. Bottom dwelling foraminifera would record the radiocarbon “age” of the water mass they are bathed in. Modern ocean high-latitude southern source waters (AAIW and AABW) have lower initial radiocarbon levels than North Atlantic source waters (NADW) due to not having time to fully equilibrate with the atmosphere before sinking. For example, AAIW is approximately 250 years older than NADW. This method has been called into question because of possible problems such as reworking, bioturbation, secondary calcite contamination of samples, and the validity of planktonic species actually recording the true calendar age of the sample.

Before using paired benthic/planktonic radiocarbon dated foraminifera to track past changes in the water column structure in the southeast Atlantic, it is important to examine modern, core-top sediments to ensure they are faithfully recording the modern ocean conditions. We analyzed 38 core-tops, spanning 400-3500 meters, and after analysis of core-top radiocarbon and stable isotope data from individual cores, we culled these 38 to a subset of 27 cores with a planktonic radiocarbon age less than 1800 years. This subset of 27, well-dated core tops from a small geographic area offers a test to determine the validity of the benthic/planktonic radiocarbon method.

Although *G. bulloides* has been used in other studies for the benthic/planktonic paired method, and thus, was assumed to reflect the calendar age of the sample, (Roark *et al.*, 2003;

Schefuss et al., 2005) we found a consistent age offset between *O. universa* and *G. bulloides*. In all cases, *G. bulloides* radiocarbon age was older than the *O. universa* age from the same sample, and in some cases, older than the dated benthic foraminifera – the age offset being large enough to overwhelm any benthic radiocarbon differences. Both species are planktonic foraminifera, but *O. universa* is more surface-dwelling than *G. bulloides*, and therefore, we conclude, it is more faithfully recording surface signals. By using *O. universa* as our planktonic radiocarbon data point, we were able to show a reconstructed water column profile similar to modern seawater nutrient profiles (especially dissolved silica) in the region. Our reconstructed water column profile does not follow the nearest dissolved inorganic carbon $\Delta^{14}\text{C}$ (modern seawater) profile as well as it does the silica profile. We find that the nearest dissolved inorganic carbon $\Delta^{14}\text{C}$ measurements are too far away from our site to be reflecting the unique water column structure of our area, bounded to the north and west by the Walvis Ridge and the continental margin to the East. We conclude that the consistent trends between 27 dated, modern core-tops accurately reflects the radiocarbon distribution in our geographically constrained field area. This knowledge allows us to use this method to examine changes in the water column from the LGM through the deglacial.

Chapter 4: Water mass distribution from the past 20,000 years reconstructed from radiocarbon and stable isotopes in the southeastern Atlantic

We used both radiocarbon and stable isotope measurements to reconstruct water column configurations over two climatic transitions identified in our cores – the close of the LGM and the BA transition. Although our cores were well-dated and had tight stratigraphic alignment, we found uncoupled $\delta^{13}\text{C}$ and $\Delta^{14}\text{C}$ results during the deglacial period – which led to the conclusion these sections of the cores were sedimentologically disturbed. This leads us

to conclude all results using the benthic-planktonic paired radiocarbon method need to be verified with benthic $\delta^{13}\text{C}$ and only interpreted where there were foraminifera abundance peaks. Both of these conditions were met for our subset of seven LGM intervals– they were stratigraphically and chronologically aligned – the planktonic radiocarbon dates were within 280 years of each other for all seven cores and had *G. bulloides* abundance peaks.

Our LGM results fill in a void of data from the South Atlantic during this important climatic period. Unlike Pa/Th data that suggest vigorous overturning of the NADW during the LGM, our radiocarbon results indicate the deep Atlantic filled with southern-source waters at the close of the LGM. This is in agreement with North Atlantic $\delta^{13}\text{C}$, Cd/Ca, and Zn/Ca records and south Atlantic Nd records.

References

- Boyle, E. A., and L. D. Keigwin (1985), Comparison of Atlantic and Pacific paleochemical records for the last 215,000 years - changes in deep ocean circulation and chemical inventories, *Earth and Planetary Science Letters*, 76(1-2), 135-150.
- Boyle, E.A. and L.D. Keigwin (1987), North Atlantic thermohaline circulation during the last 20,000 years: link to high latitude surface temperature, *Nature* 330:35-40.
- Curry, W. B., and D. W. Oppo (2005), Glacial water mass geometry and the distribution of delta C-13 of Sigma CO2 in the western Atlantic Ocean, *Paleoceanography*, 20(1).
- Keigwin, L.D., G.A. Jones, S.J. Lehman, and E.A. Boyle (1991), Deglacial meltwater discharge, North Atlantic deep circulation, and abrupt climate change, *J. Geophys. Res.* 96: 16811-16826.
- Lynch-Stieglitz, J., William B. Curry, Delia W. Oppo, Ulysses S. Ninneman, Christopher D. Charles, Jenna Munson (2006), Meridional overturning circulation in the South Atlantic at the last glacial maximum, *Geochemistry Geophysics Geosystems*, 7, 14.
- Piotrowski, A. M., Steven L. Goldstein, Sidney R. Hemming, Richard G. Fairbanks (2005), Temporal relationships of carbon cycling and ocean circulation at glacial boundaries, *Science*, 307(5717), 1933-1938.
- Roark, E. B., Lynn Ingram, John Southon, James P. Kennett (2003), Holocene foraminiferal radiocarbon record of paleocirculation in the Santa Barbara Basin, *Geology*, 31(4), 379-382.
- Sarnthein, M., Kyaw Winn, Simon J. A. Jung, Jean-Claude Duplessy, Laurent Labeyrie, Helmut Erlenkeuser, Gerald Ganssen (1994), Changes in east Atlantic deepwater circulation over the last 30,000 years: Eight time slice reconstructions. *Paleoceanography*, 9(2), 209-267.
- Schefuß, E., Stefan Schouten, Ralph R. Schneider (2005), Climatic controls on central African hydrology during the past 20,000 years, *Nature*, 437(7061), 1003-1006.

Chapter 2

A detailed test of the "depth transect" approach to paleoceanographic studies from
a suite of sediment cores from the southeastern Atlantic

Abstract

Sediment core depth transects allow for the reconstruction of past water column $\delta^{13}\text{C}$, $\delta^{18}\text{O}$, and $\Delta^{14}\text{C}$ structure. In order for this method to valid, common surficial proxies must be chronologically tied to one another to within a few hundred years. We present a suite of seven well-dated, high resolution cores from the southeastern Atlantic spanning water depths from 1000 to 3000 meters. These seven were culled from a set of sixteen cores using sedimentary indices and radiocarbon data from various horizons. Stratigraphic and chronological convergence was achieved in these cores to within a few hundred years of each other. Bulk density and benthic and planktonic $\delta^{13}\text{C}$, $\delta^{18}\text{O}$, and $\Delta^{14}\text{C}$ data from this well-dated and correlated set of cores thus allow construction of a basic sequence of oceanographic events for the southeast Atlantic.

Introduction

One often-used paleoceanographic strategy for reconstructing the past behavior of the interior of the ocean is to build “depth transects” of sediment cores (e.g. *Curry and Lohmann, 1983*). If cores are taken down the slope of a rise or continental margin, the sediment (or sedimentary tracers) derived from the surface ocean should be in common among all cores, allowing only the deep-water processes—carbonate dissolution, organic matter remineralization, or changes in the geometry of deep-water tracers, for example—to be highlighted. This approach has been useful for understanding the deep ocean controls on bulk sediment properties (*Curry et al., 1988; Farrell and Prell, 1989*), and, in some cases, depth transects have, in effect, served as means for constructing “paleo-CTDs” from robust sediment tracers such as oxygen (*Lynch Stieglitz et al., 2006*) and carbon isotopes (*Curry and Oppo, 2005; Sarnthein et al., 1994*).

In principle, given the proper sedimentary sequences, this approach could also be extended to the potentially more powerful and sensitive geochronological tracers, such as radiocarbon. However, this application has not yet been realized because the age range of the global ocean is less than 1000 years and the radiocarbon age of deep and intermediate water masses varies within any ocean basin by a maximum of about 500 years. Thus, the depth transect approach for reconstructing radiocarbon in the interior of the ocean depends critically on the ability to make chronological ties among cores to within a few hundred years. Conventional wisdom suggests that such requirements might be difficult to achieve: obtaining undisturbed sequences in a collection of cores from any slope or continental margin is bound to be complicated by the possibilities of downslope transport and the generally limited areas of the

seafloor intersecting the depth ranges of interest. Nevertheless, some continental margins around the world could potentially yield appropriate sedimentary sequences.

The purpose of this paper is to present a suite of sixteen piston cores spanning 1000 to 3000 meters from the southeastern Atlantic as a more explicit test of the “depth transect” approach for mapping radiocarbon in the past ocean. The ultimate goal is to arrive at a meaningful interpretation of the benthic foraminiferal radiocarbon and $\delta^{13}\text{C}$ measurements in terms of changing water column geometry from the LGM through the deglaciation. However, this goal can only be accomplished if the material used is from well-dated, highly resolved, and undisturbed sections of core. We outline the nature of the material and potential problems and biases found in the southeastern Atlantic sediments. We show that stratigraphic and chronological convergence can be achieved in a small subset of these cores. By identifying and eliminating the problematic sections of cores, we are able to cull a set of sequences that are free from sedimentological disturbances. These observations establish the opportunities (however limited) for building paleo-CTD casts of radiocarbon in the region over the last deglaciation. Through multiple replication of sedimentary climate proxy variables and multiple replication of radiocarbon dates at various horizons, these exercises also allow construction of basic sequence of oceanographic events for the southeast Atlantic. This dataset will form the basis for paleoceanographic water column reconstructions and examining linkages between climate and past ocean circulation.

Materials and Methods

Cores are from the northern Cape Basin south of the Walvis Ridge (figure 2.1). The cores presented in this chapter were taken from water depths ranging from 1002 to 3092 meters and are from an area defined by the boundaries: 10°32.26'E, 11°44.5'E and 20°4.99'S,

21°18.53'S. Bulk density $\delta^{18}\text{O}$, $\delta^{13}\text{C}$, and radiocarbon from planktonic and benthic foraminifera were measured from sixteen piston cores spanning the late glacial to present (table 3.1). Bulk density measurements (g/cm^3) were made with a GeoTek Multi-Sensor Core Logger (MSCL) aboard the R/V Melville at one to four centimeter intervals. *Bulk Density* and *Depth in Core* graphs for each core are shown in figures 2.2a-c. Stable isotopes were measured on the planktonic foraminifera *Globigerina bulloides* (*Orbulina universa* for cores 13, 19, and 48) and the benthic species *planulina* at five or ten centimeter intervals. All *G. bulloides* were from the 250-425 μm size fraction and are plotted with *Depth in Core* in figures 2.3a-c.

A prominent feature of our stable isotope data is the remarkable covariance between the *G. bulloides* $\delta^{18}\text{O}$ and $\delta^{13}\text{C}$ records- a signal not seen in other south Atlantic planktonic stable isotope records, which include *G. bulloides* (Schneider, 1992 and Hodell et al., 2003) and *O. universa* data (ODP 1079, Munson & Charles, unpublished data). This covariance is observed up until the onset of global ice volume changes, which cause a decrease in the $\delta^{18}\text{O}$, but not in the $\delta^{13}\text{C}$ (observed in core 31 at 1.57 meters *depth in core*). The *G. bulloides* $\delta^{18}\text{O}$ is plotted versus *G. bulloides* $\delta^{13}\text{C}$ from core 31 data spanning the late glacial to 15.0 kyr BP in figure 2.4.

Planulina were from all size fractions and each sample analyzed weighed between 150 to 190 μg . Isotopic analyses were performed using a common acid-bath Carousel-48 automation carbonate preparation device coupled to a Finnigan MAT 252 mass spectrometer. Estimated analytical precision, deduced from the concurrent measurement of 24 NBS-19 standards, was 0.05 and 0.07 per mil for $\delta^{13}\text{C}$ and $\delta^{18}\text{O}$, respectively. Radiocarbon measurements were made on mixed epifaunal benthic foraminifera, *G. bulloides*, and *O. universa*. The benthic foraminifera were from all size fractions and the analyzed planktonic foraminifera were from the >250 μm size fraction. Planktonic radiocarbon ages were converted to calendar age BP using the Fairbanks

(2005) calibration (*Fairbanks et al.*, 2005) assuming a reservoir age correction of 400 years. Radiocarbon dated intervals from each core are plotted as diamonds on the density and stable isotope graphs in figures 2.2 and 2.3. Radiocarbon measurements were made at the Center for Accelerator Mass Spectrometry at Lawrence Livermore National Laboratory. Foraminifera tests were sonicated in a .0001N HCl solution; planktonic foraminifera were sonicated briefly to avoid having the shells explode, whereas benthic foraminifera were sonicated for 1 minute. The HCl was then pipetted off and the samples were dried, weighed, and graphitized. Sample sizes varied between two and eight mg. The $\delta^{13}\text{C}$ of the samples used for radiocarbon analysis was not measured, but assigned a $^{13}\text{C}/^{12}\text{C}$ ratio of 1.5‰ for planktonic samples, and 0‰ for the benthic samples to correct for the mass-dependent fractionation.

Results

Stratigraphic correlation

Planktonic stable isotope records provide a general overview of the sedimentary sequences analyzed. The depth in core to the first maximum in $\delta^{18}\text{O}$ (the last ice age interval) ranges from 70 cm to 200 cms, suggesting that average sedimentation rates are on the order of 5-10 cms/kyr. Though explicit lithological determinations were not made for all the cores, visual inspection of the samples suggest a variable mixture of biogenic and nonbiogenic components, with carbonate becoming progressively more dominant in the deeper (more offshore) cores. Bulk density values in these sediments reflect this variability in bulk lithology—high densities correspond to high concentrations of carbonate (*ODP initial report 177*).

All the cores share the same general features over the Last Glacial Maximum (LGM) to recent interval in the sedimentary variables we measured. There are four prominent stratigraphic markers seemingly apparent in all the cores: a $\delta^{18}\text{O}$ and $\delta^{13}\text{C}$ high immediately preceding a rapid

shift to lower values, the $\delta^{18}\text{O}$ and $\delta^{13}\text{C}$ low immediately following this shift, as well as a prominent density high and low on each end of an abrupt density shift (located at approximately 2.1, 1.8, 1.65, and 1.45 meters in core 31, respectively). The stable isotope sampling resolution ranges between five and twenty centimeters, whereas the density measurements have a resolution between one and four centimeters. Comparison of cores with ten centimeter and greater stable isotope resolution indicates all four parameters could be stratigraphically consistent between cores (following the stratigraphic order of core 31 above), but smaller-scale analysis of cores 17, 25, 27, 39, and 54 with five centimeter stable isotope resolution and one to two centimeter density resolution can provide a more definitive answer to this question.

Benthic foraminiferal isotopic records would not be expected to exhibit common signals among these cores, given that the water depth varies from zones dominated by several different deep and intermediate water masses. However, the planktonic isotopic records are driven by variability in the surface ocean, and, therefore, these records should correlate with one another among cores (at least to the extent that the horizontal footprint of this cluster of cores is small enough to sample the same surface ocean environment everywhere). Furthermore, any fluctuations in density profiles that are a product of increased opal concentration in the core—ultimately, a measure of increased diatom productivity—should also correlate among cores. Five well-dated, representative cores from various depths are stacked in figure 2.5. Cores were placed on a common sediment depth scale by maximizing the correlation between planktonic stable isotope and density profiles; these are plotted on the *depth in core* scale of core 31 (chosen as a “benchmark” core because of its relatively high and relatively constant sedimentation rate through this interval). In general, correlations among cores are quite strong, as one would

expect. For example, core 54 is significantly correlated (at the 99% confidence interval) with both cores 31 and 27.

However, our correlation exercise establishes a natural test of the sensitivity of radiocarbon in these cores. If it is true the surface-derived proxy variables record climatic phenomena synchronously among cores, then the apparent stratigraphic alignment should produce a tight cluster of radiocarbon ages for each major distinctive horizon (at least, within the constraints imposed by the sampling resolution.) Three prominent stratigraphic intervals that we have dated intensively are marked with arrows in figure 2.5: The average age at the $\delta^{18}\text{O}$ high from *G. bulloides* measurements of twelve cores is 19,653 yrs with a standard deviation of 1121 yrs. The average age and standard deviation from *O. universa* measurements of ten cores is 15,044 yrs, 596 yrs, at the density high and 14,013 years, 555 years, at the density low. The span in ages at each stratigraphic point is outside the variability attributed to sampling resolution, indicating that within our dataset there are invalid planktonic radiocarbon dates, presumably because of sedimentological disturbances. This exercise demonstrates that, while high stratigraphic correlation among less sensitive tracers may be seemingly achieved, chronological correlation is another matter: each core may have small-scale sedimentological features--i.e. hiatuses truncations, or expanded sections-- that result in part of, or the entire core not being informative for the purposes of building a paleo CTD. As a result, each core must be scrutinized individually for potential problems.

The observations from core 27 illustrate the kind of problems that may arise. Radiocarbon dates for this core are plotted with depth in figure 2.6 along with the corresponding sedimentation rate determined between dated points (data for all cores is plotted in Table 2.1). The observations from two separate planktonic foraminiferal species, *O. universa* and *G.*

bulloides, tend to suggest disparate depth/age trends. As demonstrated more completely in Chapter 2, these two species generally exhibit differences in their history of relative abundance in this region of the South Atlantic, and coexisting radiocarbon dates suggest substantial age offsets between the two species. Specifically, abundance studies indicate peak *O. universa* numbers in modern sediments that decrease asymptotically through the interval of interest here. *G. bulloides* abundances are low in modern sediments and peak during the early deglaciation interval. Meanwhile in core-top and down-core samples, *G. bulloides* almost invariably has an older ^{14}C age than *O. universa*.

Armed with these observations, one can offer a credible explanation for the sedimentological anomalies in the early deglaciation section of core 27. Between approximately .6 and .7 meters appears to be a mixing zone above and below a stratigraphic truncation where *O. universa* abundance counts indicate an interval of constant numbers. Therefore mixing will cause the *O. universa* ^{14}C ages to appear older than the actual age of the interval. On the other hand, because the abundance of *G. bulloides* peaks during the early deglaciation, these will dominate the ^{14}C age at the mixing zone and there may not be an observed age reversal – only a decrease of sedimentation rate. This example illustrates the necessity for screening all portions of the sedimentary sequence.

Given the disturbances evident in the radiocarbon dates, it would not be appropriate to assign calendar ages to the whole core based on a few radiocarbon tie points. However, we can assign an age scale to portions of the core where there is sufficient radiocarbon coverage and where there is both stratigraphic and chronological agreement among 3 or more cores. This “majority rules” procedure is as follows: Twelve cores were radiocarbon dated at the first $\delta^{18}\text{O}/\delta^{13}\text{C}$ maximum and had a *G. bulloides* ^{14}C age spread of 4,900 years. These planktonic

ages, along with changes in sedimentation rate and stratigraphic features, were used to disqualify five of the twelve dated points. Core 37 dated radiocarbon dead and core 54's *G. bulloides* date was older than the mixed benthic date. Core 25 did not have enough material to date *G. bulloides*, but the mixed benthics dated to 18,493 calendar years BP. This date is younger than the average planktonic date, indicating sedimentological problems at this interval. Two other cores were dated whose calendar age fell approximately 2000 years from the mean for the dataset. Core 17 dated young (17,492 calendar years BP) and core 39 dated old (22,394 calendar years BP) compared to the average of 19,641 calendar years BP. These two cores were therefore discarded, leaving seven cores whose *G. bulloides* calendar ages were tightly constrained to within 570 years of each other. Figure 2.7 plots cores (31, 45, 43, 27, 23, 21, and 52). The late glacial sediment truncation found in cores 43 and 21 is apparent in the later than expected isotope jump, but we are confident that the radiocarbon dated interval for these cores is not affected, and is thus from the same time horizon as the rest of the dataset. By whittling down from twelve to these seven cores, we have a dataset whose matching $\delta^{18}\text{O}$ and $\delta^{13}\text{C}$ stratigraphic points are within 570 years of each other, a spread of dates to be expected with the ten centimeter stable isotope sampling resolution. This dataset, and its accompanying benthic ^{14}C dates, is explored further in chapter 3 where the water column structure from this point in time is resolved.

The same exercise can be applied to the deglacial sediment density shift (to low values) where there is radiocarbon coverage both before and after the shift. *O. universa* dates for eleven cores were examined for this interval. Three of the cores -27, 21 and 17 - had sedimentological disturbances during this interval which were apparent from the down core radiocarbon age reversals, planktonic stable isotope data, and marked decreases in sedimentation rate. Core 23

had a sedimentation hiatus at this interval, which could be responsible for the dissimilar density structure of core 23 when compared to the rest of the dataset. Lastly, core 54's density structure is offset approximately 2000 years young compared to the other cores. These five cores were therefore not used in constructing a chronology of events.

Plotted in figure 2.8 are the remaining seven cores over this interval with black circles indicating radiocarbon dated points. In addition to these six cores, core 29 is plotted as well. This core does not have *O. universa* dates, but displayed similar density structure as the remaining cores. These seven cores are tightly constrained by their calendar ages at prominent stratigraphic points. At the density high, the age span is from 14,490 to 14,963 years BP. Core 43 (14,963 years BP) is the one outlier from the rest of the group. Without core 43, the age span is only 162 years, spanning from 14,490 to 14,652 years BP. After the transition, there are two distinct intervals that could be construed as a density low – this can be observed in figure 2.8. At the first “step” defined as the immediate end of the abrupt shift, the ages span is 244 years ranging from 13,932 to 14,176 years BP. At the next density low interval – defined as the lowest density point before values start trending higher, the age span is 64 years ranging from 13,497 to 13,561 years. These calendar ages at the density low do not take into account the values of cores 52 or 13 – the two deepest cores in our dataset. Neither of these cores have the same abrupt transition from high to low values as the other five cores. Their differing density profiles at this interval could be a result of these deeper cores being more affected by carbonate content changes in the deep ocean as opposed to surface opal changes, or it is possible that both of these cores have sedimentological disturbances after the density high (both their density high ages match the rest of the stacked cores and fall within the tight age constraint). The stratigraphic correlation between these seven cores at three prominent intervals is 162, 244, and 64 years. This precision

is convincing evidence that both stratigraphic and chronological correlation may be achieved over the intervals of interest. Changes in the deep-water column structure over the deglacial density shift are examined using this dataset in chapter 3.

Sequence of Events

In order to compare the surface and deep-water changes observed in our dataset to other global climate events, we developed an age scale with the smaller subset of cores. The age scale is only presented to 10,000 years BP as there is no radiocarbon coverage between this time and modern sediments. Density and $\delta^{18}\text{O}$ values for these cores are plotted with calendar age in figure 2.9, along with temperature records from Greenland and Antarctica, atmospheric $\Delta^{14}\text{C}$, and benthic $\delta^{13}\text{C}$ data. Downcore benthic $\delta^{13}\text{C}$ data was only measured on the four cores presented. Three of the cores (17, 27, and 31) have flawed down-core planktonic radiocarbon dates, so these cores were matched based on density and planktonic $\delta^{18}\text{O}$ profiles and graphed using the age scale for core 45.

The density and stable isotope data presented here represents a record of changes in surface and deep-water properties in the southeastern Atlantic. An abrupt warming – indicated by a decrease in the $\delta^{18}\text{O}$ values – begins ~19,700 years BP at our study site. This occurs simultaneously with Antarctic air temperature changes reconstructed from Dome Fuji $\delta^{18}\text{O}$ and deuterium (δD) records (*Kawamura, K., et al. 2007*), which constrain the onset of warming to between 20,250 and 19,750 years BP. Following this transition, surface waters in our study area remain warm – indicated by low $\delta^{18}\text{O}$ values during Heinrich Event 1, which occurs from 17.5 to 15.0 kyrs BP. Following Heinrich Event 1, the prominent density high (average age 14,552 years BP) immediately prior to a shift to low values is coincident with the onset of the Bolling-Allerod (BA) at 14,550 years BP – a signal recorded in the GISP2 record as a temperature

maximum. Immediately following the start of the BA, our density data has an abrupt shift to lower values – the first “step” in this transition has an age span of 13,932 to 14,176 years BP and the lowest density value after this transition spans 13,497 to 13,561 years BP. During this same interval, between 13,400 and 14,100 years BP, $\delta^{13}\text{C}$ values from core 17 (2946 meters) converge with the $\delta^{13}\text{C}$ values from the three shallower cores. This convergence takes place after the initial density shift and after the onset of the Bolling-Allerod, but cannot be constrained to absolute timing with respect to the density low as the sampling resolution is too coarse in core 17.

Discussion

A cursory look at our results might indicate that sedimentological problems in mid-depth sediments from the continental margins of the southeastern Atlantic would make paleoceanographic reconstructions from this area unreliable. Although some of our cores are marked by areas of mixing, downslope transport, hiatuses in deposition, and age reversals, we have shown that both stratigraphic and chronological correlation can be achieved from a subset of cores through careful scrutiny of each individual core. After careful analysis of our initial sixteen cores, we propose a series of guidelines for applying the depth transect approach to reconstruct bottom water geometry over periods of abrupt change in the deep ocean and to produce meaningful linkages between benthic data and climatic changes. These include: ^{14}C radiocarbon dates cannot be extrapolated too far in either direction, therefore chronological ties need to be constrained for each interval of interest, stratigraphic correlation of surface variables alone cannot equate chronological correlation, and a large suite of cores must be analyzed and culled to a meaningful subset.

Sedimentation rates in our cores are variable throughout the deglacial (Table 2.1). Core 31 (1002 meters) gives no indication of compromised sequences, yet its sedimentation rate varies between 6.9 and 18.5 cm/kyr. If an age scale had been assigned to this core by interpolating between two points and assuming a constant sedimentation rate, sections of the core could be assigned a calendar age hundreds of years off the actual age. Interpolation between ages will lead to a false sense of the stratigraphic sequence; therefore, each interval of interest (i.e. the change across the BA) needs to be constrained with planktonic radiocarbon dates. Planktonic radiocarbon dates are also necessary for aligning cores as we have shown stratigraphic correlation alone leads to large age errors. Core 17 has a robust $\delta^{18}\text{O}$ and $\delta^{13}\text{C}$ profile (figure 2.3c) and one could be confident the 1.314 meter interval is the LGM, yet it dated 2,000 years earlier than the accepted LGM date for our cores. From our suite of sixteen cores, we were able to utilize seven cores at each time slice analyzed. These cores are from a region of relatively high sedimentation rate and there are no indications they would not contain reliable paleoceanographic information, yet to tightly constrain our intervals of interest to each other and a calendar age scale required using less than half the cores.

Pa/Th data from the North Atlantic indicate a near instantaneous cessation (~ 17.5 kyrs) and an abrupt resumption (~ 14.7 kyrs) of meridional overturning circulation during the deglacial period (*McManus et al.*, 2004). These changes in the deep ocean are synchronous with abrupt climate changes as well - cooler SST in the North Atlantic at 17.5 kyr and Greenland warming at 14.7 kyrs. If, for example, the Brazilian Margin set of cores from Curry and Oppo (2005) were used to examine benthic $\delta^{13}\text{C}$ changes over these transitions, and the strategy used was the same as for their glacial samples, we believe they would not accurately be reflecting the abrupt changes of the deglacial period, nor accurately aligning the benthic signal to a true calendar age.

For example, correlation between cores was made based on benthic or planktonic $\delta^{18}\text{O}$ values or radiocarbon dates. Only five of the 29 cores were radiocarbon dated and from those dates the LGM age spread was 3000 years. The actual age spread may be even larger for the remaining 24 cores that were not ^{14}C dated (as illustrated by our core 17 example). This spread in ages for one time point (the LGM), that we were able to constrain to within 570 years, would be too great to capture the abrupt MOC deglacial changes observed in the Pa/Th record. If this set of cores from the southwestern Atlantic were to be used through the deglacial, it would have to be culled to a smaller set by measuring more planktonic dates, and examining each core in detail at each climate interval of interest.

We have produced a well-dated depth transect of seven cores spanning 1100 to 3000 meters in the southeastern Atlantic. The planktonic and benthic signals recorded in these cores allow a detailed comparison of these signals and the climatic changes observed in other records. Our stacked record constrains the timing of deglacial warming in the southeastern Atlantic to approximately 19.7 kyr BP, coincident with initial warming observed in Antarctic records, but well before deglacial warming observed in Greenland records. This warming signal is apparent in our abrupt planktonic $\delta^{18}\text{O}$ shift to low values, coincident with an abrupt shift in *G. bulloides* $\delta^{13}\text{C}$ (a decrease of 1.75‰ and 1.50‰, respectively). This correlation, plotted in figure 2.4, (enriched $\delta^{18}\text{O}$ = enriched $\delta^{13}\text{C}$) is the opposite of what would be expected if it is assumed that higher $\delta^{18}\text{O}$ is found in colder, deeper thermocline waters; modern water column and stable isotope data presented in chapter 3 indicates these deeper waters are $\delta^{13}\text{C}$ depleted. This covariance is not a result of planktonic water depth, nor is it a result of seasonality (the $\delta^{18}\text{O}$ and $\delta^{13}\text{C}$ trends would be opposite) or a mass spectrometer effect which would produce a 2:1 ratio (our slope is 1.18 – figure 2.4). All our *G. bulloides* came from the 250-425 μm size fraction, and

thus size variance is not expected to explain the data, and, as mentioned above, this covariance was not found in our *Orbulina universa* analysis from ODP core 175/1079, located 10° farther north of this study site. This leaves the possibility of the covariance being a reflection of the “carbonate ion effect” in our samples. *Spero et al.* (1997) observe that the $^{13}\text{C}/^{12}\text{C}$ and $^{18}\text{O}/^{16}\text{O}$ ratios of *G. bulloides* shells decrease with increasing seawater $[\text{CO}_2^{-3}]$. The $(\delta^{18}\text{O}: \delta^{13}\text{C})$ *G. bulloides* slope was calculated to be between 0.29 and 0.33 – this slope is plotted in figure 2.4. The expected $(\delta^{18}\text{O}: \delta^{13}\text{C})$ slope for *G. bulloides* can be estimated using the change in temperature and DIC $\delta^{13}\text{C}$ values in the upper ocean – this data is plotted in figure 3.1 and give an approximate slope of -1.7, which is plotted in figure 2.4. These two vectors (the “carbonate ion effect” and the “predicted $(\delta^{18}\text{O}: \delta^{13}\text{C})$ relationship”) combined, are close to the 1:1 slope we observe in our *G. bulloides* stable isotope data.

The abrupt warming observed in our *G. bulloides* $\delta^{18}\text{O}$ data is not observed in other southeastern Atlantic records, but both the planktonic $\delta^{18}\text{O}$ and $\delta^{13}\text{C}$ indicate at our field site, located in the Benguela Upwelling Region, the initiation of Antarctic warming is synchronous with an abrupt increase in SST and a shift in the surface waters to lower $\delta^{13}\text{C}$ values. This *G. bulloides* excursion is most likely reflecting upwelling of $\delta^{13}\text{C}$ depleted water and would be expected to be accompanied by a shift in opal deposition- a relationship that is observed in eastern equatorial Pacific Ocean, where Subantarctic Mode Water upwells today (*Anderson, 2009*). This is not the case in our records – density values remain consistently high (associated with low opal) during the initial *G. bulloides* excursion from high to low values. The shift in *G. bulloides* values coincides with temperature changes in Antarctica, whereas Greenland temperatures remain constant.

The interhemispheric asynchrony (shown in figure 2.9) observed at the LGM is found during Heinrich Event 1 (H1) as well. GISP2 ice core records show the deglacial warming in Greenland started well after H1 and colder SST's are observed in the North Atlantic during H1 (*Bard, 2000*). This is in contrast to Dome Fuji records that indicate Antarctica is in the middle of its deglacial warming during H1 and hybrid-coupled climate model results predicting warming during Heinrich events in the Cape Basin (figure 2.1) when run with both present day and glacial conditions (*Prange et al. 2004*), which is observed in our cores as low $\delta^{18}\text{O}$ values.

The density profiles contain a shift from high to low values, presumed to be due to the increase in relative opal concentration observed in the Benguela Upwelling System at approximately 14.5 kyr BP (*Romero et al., 2003*) – coincident with the onset of the Bolling-Allerod warm interval found in Greenland temperature records (*Alley, 2004*). This deglacial opal pulse has been observed in other records in the tropical Atlantic and Pacific (*Bradtmiller et al., 2007; Bradtmiller et al., 2006*) and Southern Ocean (*Frank et al., 2000*) centered around 15 kyr BP and attributed to productivity, not dissolution changes. Frank hypothesized that as winter sea ice disappeared at this time, increased upwelling and decreased stratification led to a more efficient transfer of nutrients and dissolved silica to surface waters which increased productivity. Bradtmiller postulates that because this opal pulse is observed in both the Atlantic and Pacific, it is due to a reorganization of thermohaline circulation driven by Southern Ocean processes. If this were the case, our *G. bulloides* $\delta^{13}\text{C}$ and density excursions should be synchronous. This is not the case at our study site, as the *G. bulloides* $\delta^{13}\text{C}$ excursion to low values is synchronous with Antarctica air temperatures and starts much earlier than the density shift that is synchronous with Greenland air temperature. Past studies have shown synchronous increased opal deposition and a shift to low planktonic $\delta^{13}\text{C}$ values recording increased upwelling of southern source water

in the Southern Ocean and Equatorial Pacific during the last deglacial period (*Anderson et al.*, 2009; *Hayes et al.*, 2011) – a relationship that is uncoupled in our data. If the upwelled water were high in silica content and contained a low $\delta^{13}\text{C}$, opal deposition and planktonic $\delta^{13}\text{C}$ values should change together. Instead, at our site, the timing of our opal deposition pulse suggests that there were significant changes to the silica content of upwelled water during the last deglacial period.

When we do observe an opal deposition pulse in our density records, after our initial *G. bulloides* $\delta^{13}\text{C}$ excursion, it is accompanied by an influx of NSW (observed in our deep benthic $\delta^{13}\text{C}$ records). Our deep benthic $\delta^{13}\text{C}$ records show a convergence with the $\delta^{13}\text{C}$ values from the three shallower cores during this interval, indicating a deep water regime shift, also observed in North and South Atlantic $\Delta^{14}\text{C}$, Pa/Th, Nd, and $\delta^{13}\text{C}$ records (*Robinson et al.*, 2005; *McManus et al.*, 2004; *Piotrowski et al.*, 2004; *Sarnthein et al.*, 1994; and *Charles and Fairbanks*, 1992). $\Delta^{14}\text{C}$, Pa/Th, Nd, and $\delta^{13}\text{C}$ indicate during the Bolling-Allerod, the NADW intensity was at, or near Holocene levels. At this time of the NADW reinvigoration, Greenland temperatures reach their warmest values of the deglacial period.

It is curious that although our deepest benthic $\delta^{13}\text{C}$ values show a convergence with the three shallowest cores at this time, the shift in deep water values to modern levels do not take place until well after this period. After the benthic $\delta^{13}\text{C}$ divergence, the values from 2946, 1804, and 1405 meters synchronously decrease through the deglacial (the full benthic $\delta^{13}\text{C}$ records are presented in chapter 4 – here we have presented only the interval constrained by calendar ages). Whereas Charles and Fairbanks's benthic $\delta^{13}\text{C}$ record is at modern values by 14 kyr, and stay at these values through the deglacial, the benthic $\delta^{13}\text{C}$ pattern at our site suggests the full change in the deep Atlantic benthic $\delta^{13}\text{C}$ signal is not recorded at our site in conjunction with NADW

reinvigoration. The addition of benthic $\Delta^{14}\text{C}$ data over this deep ocean shift will allow us to answer if both $\Delta^{14}\text{C}$ and $\delta^{13}\text{C}$ lag other deep Atlantic records, or if this is just observed in the benthic $\delta^{13}\text{C}$ record.

Following this warming, the $\delta^{18}\text{O}$ and $\delta^{13}\text{C}$ values diverge due to a decrease in global ice volume which causes a decrease in the $\delta^{18}\text{O}$, but not in the $\delta^{13}\text{C}$. While the timing of this initial divergence is not well dated, it falls after the LGM, but before 15 kyr – following the pattern of northern hemisphere ice volume signal changes (*Imbrie et al.*, 1984)

Summary and Conclusions

Although our set of cores contain intervals of sedimentological disturbances evident in the sedimentation rate data, planktonic stable isotope profiles, and comparisons between the *O. universa* and *G. bulloides* dates, they are to be expected from such a large dataset from the continental margin. By examining each individual core and disregarding flawed sections, we have produced robust datasets at two time horizons of interest – the last glacial maximum and the Bolling-Allerod period.

Seven of our cores, ranging in depth from 1002 to 3092 meters, have been convincingly stratigraphically aligned, producing a well-dated and stacked dataset from the southeastern Atlantic that spans the LGM to the end of the Bolling-Allerod. Using this established subset of legitimate cores, additional benthic proxies such as radiocarbon can now be added to the dataset to produce paleo water column profiles from defined points in time (see chapters 3 and 4). These profiles will track changes in the water column structure in the southeast Atlantic from the LGM through the end of the deglaciation. This method has been applied successfully to other parts of the ocean, most recently by Robinson et al., 2005, who reconstructed past ventilation changes of intermediate and deep-water using corals and benthic/planktonic foraminifera pairs over the

glacial and deglacial period. This is one of the few Atlantic records to track changes through time at various depths using deep-water $\Delta^{14}\text{C}$, as opposed to tracers like Pa/Th, Nd, and $d^{13}\text{C}$, which have no built-in time clock. Robinson et al.'s results indicate significant changes to the intermediate and deep-water column structure at the last glacial maximum and throughout the Bolling-Allerod period. The dataset we presented here, from the southeastern Atlantic at these time horizons, spans the depths ranging from 1000 to 3000 meters and will be the basis for producing well-dated and credible water column reconstructions with the addition of benthic radiocarbon measurements. This will enable us to address the question of whether Southern Hemisphere processes are more important than those in the north in terms of governing the stability of global thermohaline circulation, as has been suggested by previous work (Toggweiler and Samuels, 1998; Keeling and Stephens, 2001). Additionally, well-dated $\Delta^{14}\text{C}$ data from the south Atlantic will provide coverage for modeled simulations of past ventilation changes as the only constraints thus far for these models are from the Ceara Rise, Blake Ridge, Carribean Sea, and the North Atlantic (Meissner, 2003).

References

- Alley, R.B. 2004. GISP2 Ice Core Temperature and Accumulation Data. IGBP PAGES/World Data Center for Paleoclimatology. Data Contribution Series #2004-013. NOAA/NGDC Paleoclimatology Program, Boulder CO, USA.
- Anderson, R.F., S. Ali, L. I. Bradtmiller, S. H. H. Nielsen, M. Q. Fleisher, B. E. Anderson, L. H. Burckle (2009), Wind-Driven Upwelling in the Southern Ocean and the Deglacial Rise in Atmospheric CO₂, *Science*, 323, 1443-1448).
- Bard, E., Frauke Rostek, Jean-Louis Turon, Sandra Gendreau (2000), Hydrological impact of Heinrich events in the subtropical northeast Atlantic, *Science*, 289(5483), 1321-1324.
- Bradtmiller, L. I., R. F. Anderson, M. Q. Fleisher, L. H. Burckle (2006), Diatom productivity in the equatorial Pacific Ocean from the last glacial period to the present: A test of the silicic acid leakage hypothesis, *Paleoceanography*, 21(4).
- Bradtmiller, L. I., R. F. Anderson, M. Q. Fleisher, L. H. Burckle (2007), Opal burial in the equatorial Atlantic Ocean over the last 30 ka: Implications for glacial-interglacial changes in the ocean silicon cycle, *Paleoceanography*, 22(4).
- Charles, C. D., and R. G. Fairbanks (1992), Evidence from Southern Ocean sediments for the effect of North Atlantic deep water flux on climate, *Nature*, 355(6359), 416-419.
- Curry, W. B., and G. P. Lohmann (1982), Carbon isotopic changes in benthic foraminifera from the western South Atlantic – Reconstruction of glacial abyssal circulation, *Quaternary Research*, 18(2), 218-235.
- Curry, W.B., J.C. Duplessy, L.D. Labeyrie, N.J. Shackleton (1988), Changes in the distribution of $\delta^{13}\text{C}$ of deepwater ΣCO_2 between the last glaciation and the Holocene, *Paleoceanography*, 3, 317-341.
- Curry, W. B., and D. W. Oppo (2005), Glacial water mass geometry and the distribution of delta C-13 of Sigma CO₂ in the western Atlantic Ocean, *Paleoceanography*, 20(1).
- Fairbanks, R. G., Richard A. Mortlock, Tzu-Chien Chiu, Li Cao, Alexey Kaplan, Thomas P. Guilderson, Todd W. Fairbanks, Arthur L. Bloom, Pieter M. Grootes, Marie-Josée Nadeau (2005), Radiocarbon calibration curve spanning 0 to 50,000 years BP based on paired Th-230/U-234/U-238 and C-14 dates on pristine corals, *Quaternary Science Reviews*, 24(16-17), 1781-1796.
- Farrell, J.W. and W.L. Prell (1989), Climate change and CaCO₃ preservation: An 800,000 year bathymetric reconstruction from the central equatorial Pacific Ocean, *Paleoceanography* 4 pp. 447–466.

Frank, M., R. Gersonde, M. R. Loeff, G. Bohrmann, C. C. Nürnberg, P. Kubik, M. Suter, A. Mangini (2000), Similar glacial and interglacial export bioproductivity in the Atlantic sector of the Southern Ocean: Multiproxy evidence and implications for glacial atmospheric CO₂, *Paleoceanography*, 15(6), 642-658.

Gersonde, R., D.A. Hodell, P. Blum, (1999) *Proc. ODP, Init. Repts.*, 177: College Station, TX (Ocean Drilling Program).

Hayes, C.T., R. F. Anderson, M. Q. Fleisher (2011), Opal accumulation rates in the equatorial Pacific and mechanisms of deglaciation, *Paleoceanography*, 26(12), 1207-1219.

Hodell, D. A., Kathryn A. Venz, Christopher D. Charles, Ulysses S. Ninnemann (2003), Pleistocene vertical carbon isotope and carbonate gradients in the South Atlantic sector of the Southern Ocean, *Geochemistry Geophysics Geosystems*, 4.

Imbrie J, Hays HD, Martinson DG, McIntyre A, Mix AC, Morley JJ, Pisias NG, Prell WL, Shackleton NJ (1984), The orbital theory of pleistocene climate: Support from a revised chronology of the marine $\delta^{18}\text{O}$ record". In: Berger AL et al. (eds), Milankovitch and climate. Pt 1, 269–305, Reidel Publ Co, Dordrecht.

Kawamura, Kenji, Frédéric Parrenin, Lorraine Lisiecki, Ryu Uemura, Françoise Vimeux, Jeffrey P. Severinghaus, Manuel A. Hutterli, Takakiyo Nakazawa, Shuji Aoki, Jean Jouzel, Maureen E. Raymo, Koji Matsumoto, Hisakazu Nakata, Hideaki Motoyama, Shuji Fujita, Kumiko Goto-Azuma, Yoshiyuki Fujii, Okitsugu Watanabe (2007), Northern Hemisphere forcing of climatic cycles in Antarctica over the past 360,000 years, *Nature*, 448 (7156), 912-U914.

Keeling, R. F., and B. B. Stephens (2001), Antarctic sea ice and the control of Pleistocene climate instability, *Paleoceanography*, 16(1), 20.

Lynch-Stieglitz, J., William B. Curry, Delia W. Oppo, Ulysses S. Ninneman, Christopher D. Charles, Jenna Munson (2006), Meridional overturning circulation in the South Atlantic at the last glacial maximum, *Geochemistry Geophysics Geosystems*, 7, 14.

McManus, J. F., J.-M. Gherardi, L. D. Keigwin, S. Brown-Leger, R. Francois (2004), Collapse and rapid resumption of Atlantic meridional circulation linked to deglacial climate changes, *Nature*, 428(6985), 834-837.

Meissner, K. J., A. Schmittner, A. J. Weaver, J. F. Adkins (2003), Ventilation of the North Atlantic Ocean during the Last Glacial Maximum: A comparison between simulated and observed radiocarbon ages, *Paleoceanography*, 18(2), 23.

Piotrowski, Alexander M., Steven L. Goldstein, Sidney R. Hemming, Richard G. Fairbanks (2004), Intensification and variability of ocean thermohaline circulation through the last deglaciation, *Earth and Planetary Science Letters*, 225(1-2), 205-220.

Prange, M., Gerrit Lohmann, Vanya Romanove, Martin Butzin (2004), Modelling temporal signatures of Heinrich Events: influence of the climatic background state, *Quaternary Science Reviews*, 23(5-6), 521-527.

Robinson, L. F., Jess F. Adkins, Lloyd D. Keigwin, John Southon, Diego P. Fernandez, S-L Wang, Daniel S. Scheirer (2005), Radiocarbon variability in the western North Atlantic during the last deglaciation, *Science*, 310(5753), 1469-1473.

Romero, O., G. Mollenhauer, R. R. Schneider, G. Wefer (2003), Oscillations of the siliceous imprint in the central Benguela Upwelling System from MIS 3 through to the early Holocene: the influence of the Southern Ocean, *Journal of Quaternary Science*, 18(8), 733-743.

Sarnthein, M., Kyaw Winn, Simon J. A. Jung, Jean-Claude Duplessy, Laurent Labeyrie, Helmut Erlenkeuser, Gerald Ganssen (1994), Changes in east Atlantic deepwater circulation over the last 30,000 years: Eight time slice reconstructions. *Paleoceanography*, 9(2), 209-267.

Schneider, R., A. Dahmke, A. Kölling, P. J. Müller, H. D. Schulz & G. Wefer. *Geological Society, London, Special Publications*; 1992; v. 64; p. 285-297.

Spero, H. J., et al. (1997), Effect of Seawater Carbonate Concentration on Foraminiferal Carbon and Oxygen Isotopes, *Nature*, 390, 497-500.

Toggweiler, J. R., and B. Samuels (1998), On the ocean's large-scale circulation near the limit of no vertical mixing, *Journal of Physical Oceanography*, 28(9), 1832-1852.

Zahn, R., Joachim Schönfeld, Hermann-Rudolf Kudrass, Myong-Ho Park, Helmut Erlenkeuser, Pieter Grootes (1997), Thermohaline instability in the North Atlantic during meltwater events: Stable isotope and ice-rafted detritus records from core SO75-26KL, Portuguese margin, *Paleoceanography*, 12(5), 696-710.

Table 2.1. Piston cores measured for bulk density, planktonic foraminiferal $\delta^{18}\text{O}$, and planktonic and benthic foraminiferal $\delta^{13}\text{C}$ and radiocarbon spanning the late glacial to present.

Core	Water Depth (m)	Average Sed. Rate (cm/kyr)
31	1002	12.2
29	1163	8.7
45	1405	8.9
43	1503	10.7
41	1603	11.7
39	1724	11.5
27	1804	5.1
25	1902	4.6
23	1977	6.3
54	2202	9.6
52	2343	6.4
21	2680	6
19	2816	11.3
17	2946	10
13	3092	12.2
48	3571	6

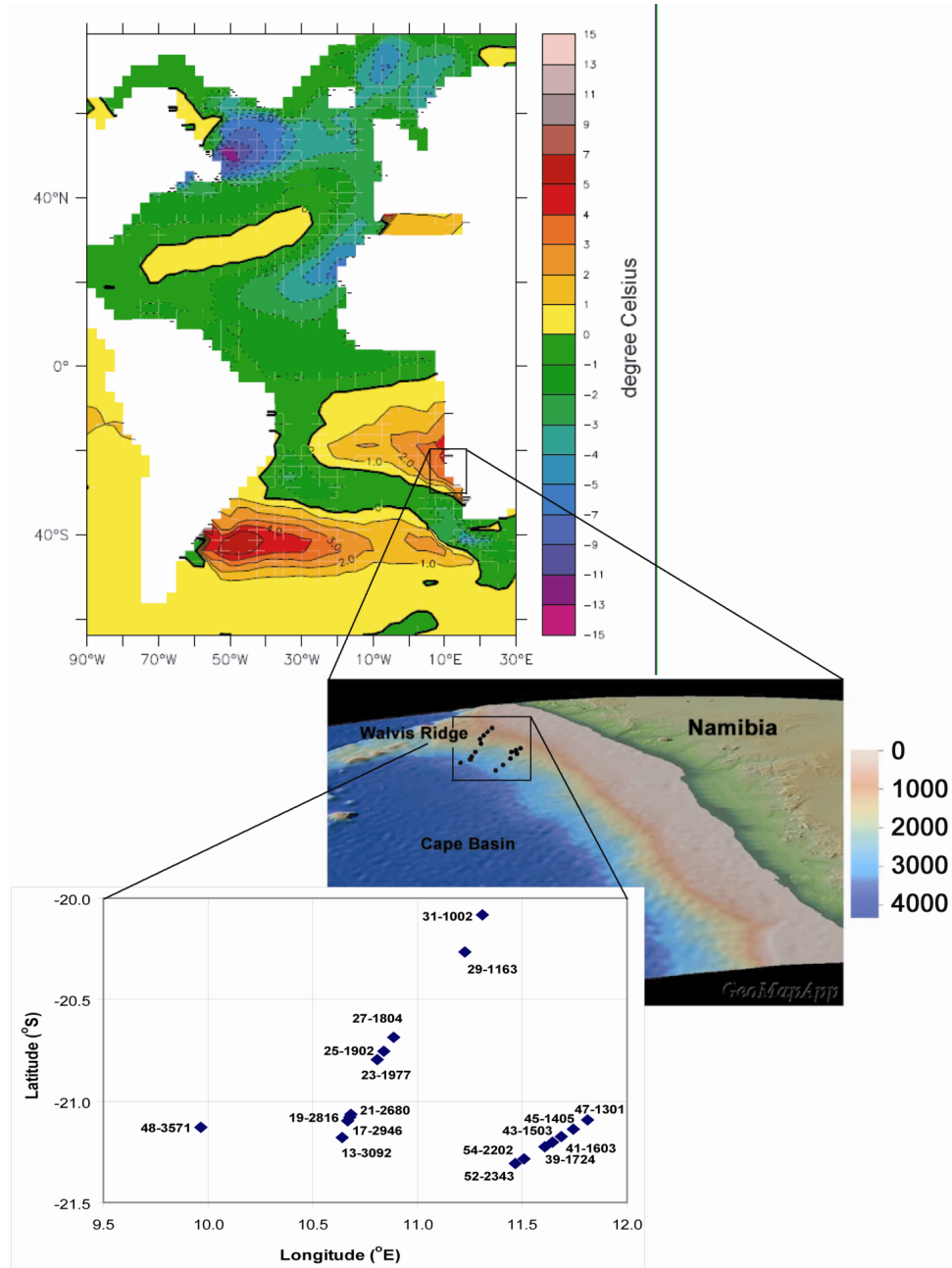


Figure 2.1. The Atlantic map is from *Prange et al.*, 2004 and depicts the Atlantic SST response to the meltwater perturbation in the present day experiment. For comparison, temperature changes suggested by proxy data from marine sediment cores for Heinrich Event 1 are marked by circles as follows: warming (violet red), temperature changes less than 70.5_C (beige), cooling (light blue), very strong (>2_C) cooling (dark blue). The proxy data near our study site is from core Geo-B 1023-5.

The two bottom maps depict our study site, the cores sampled, and the water depth (m) they were collected from.

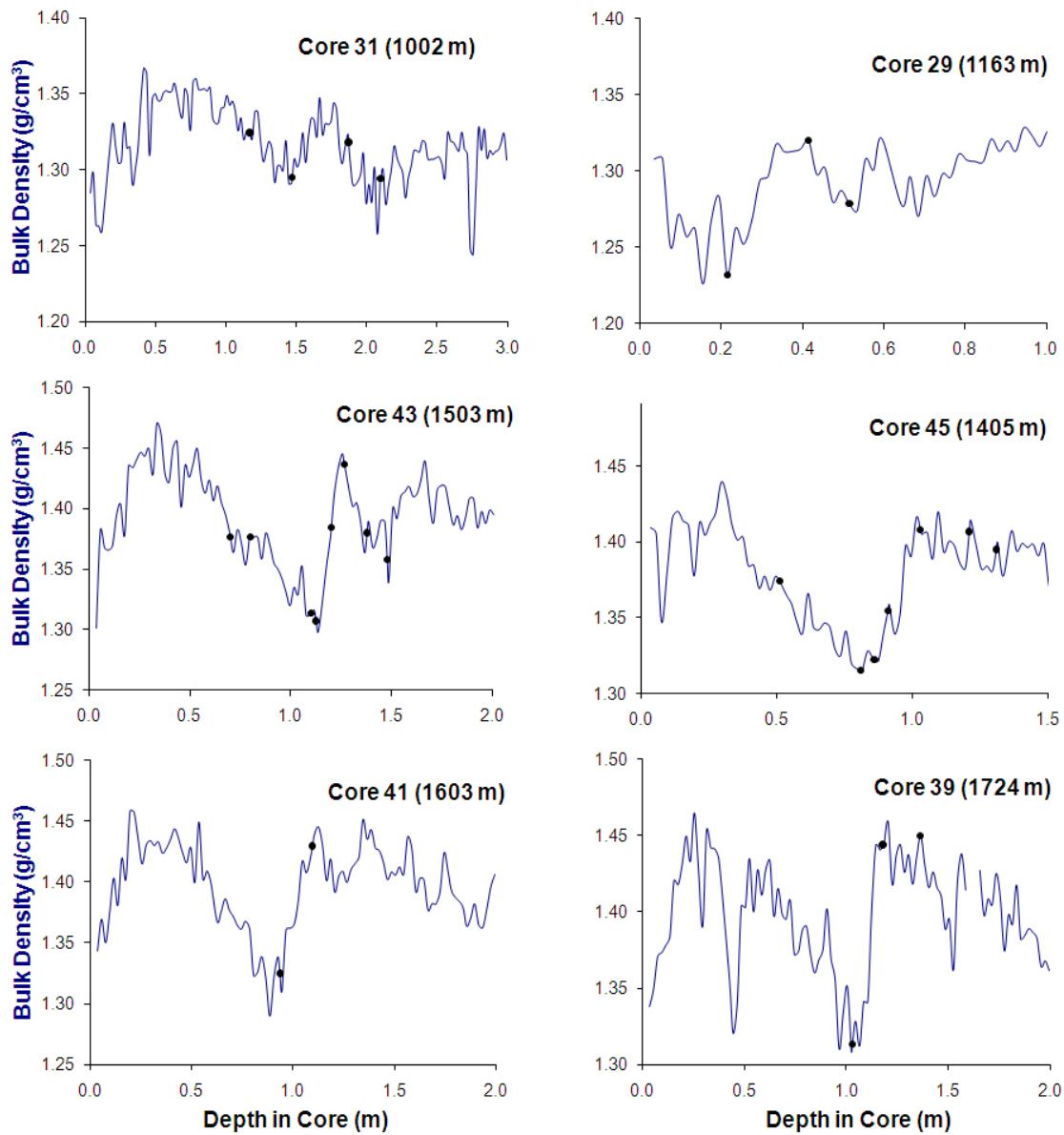


Figure 2.2. Bulk density (g/cm³) plotted versus core depth. Black circles indicate intervals that were radiocarbon dated.

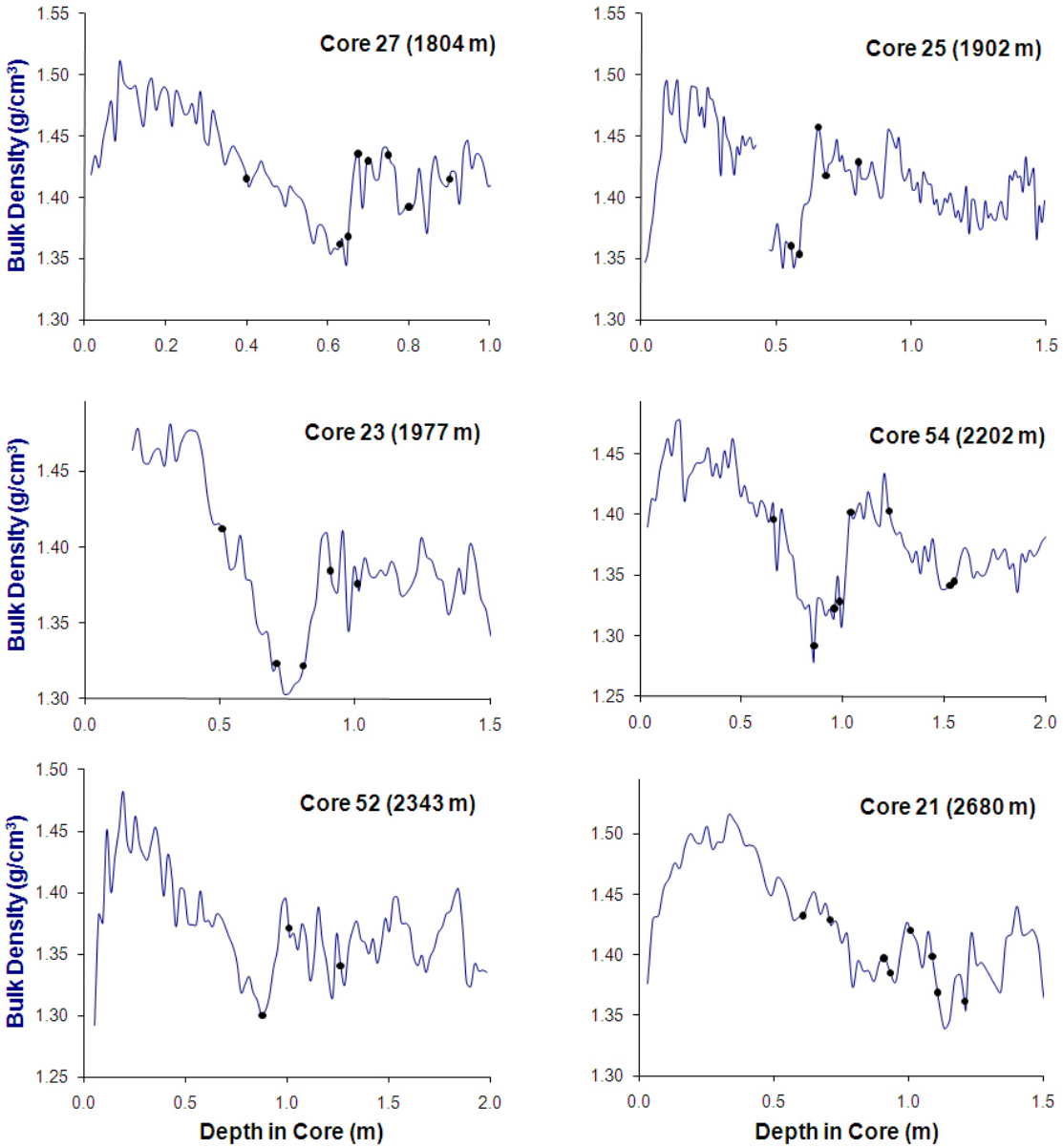


Figure 2.2. Bulk density (g/cm³) plotted versus core depth. Black circles indicate intervals that were radiocarbon dated, continued.

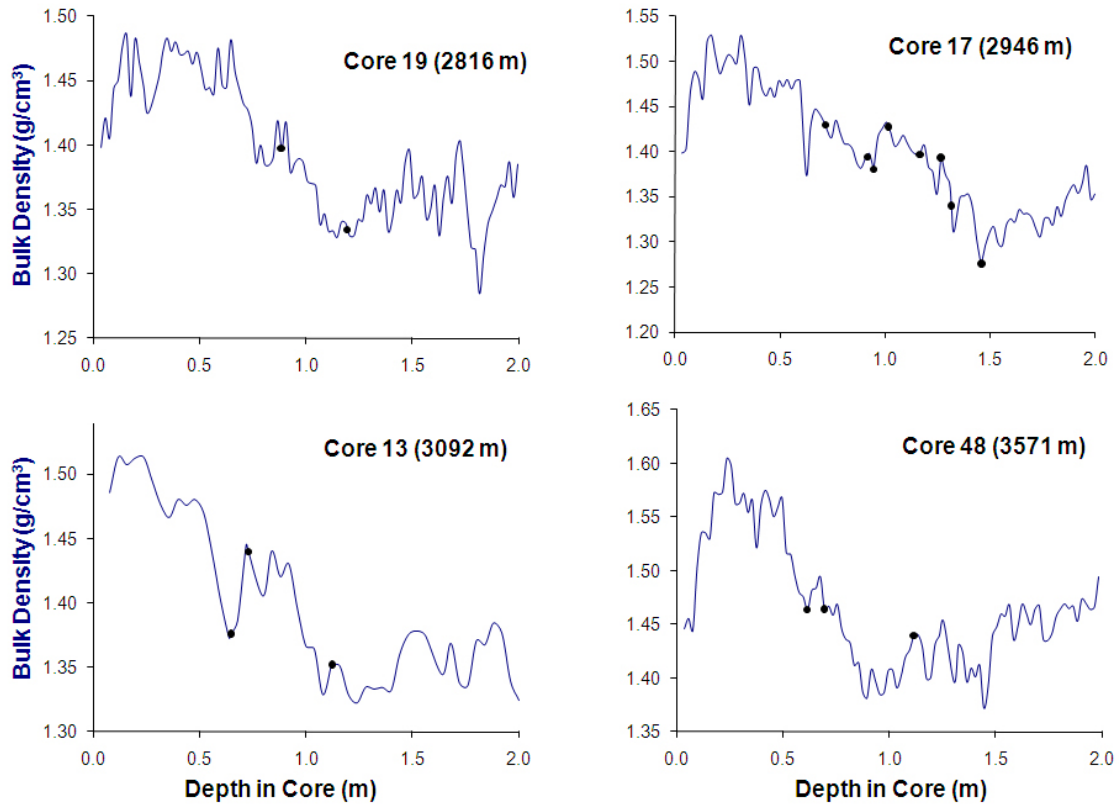


Figure 2.2. Bulk density (g/cm^3) plotted versus core depth. Black circles indicate intervals that were radiocarbon dated, continued

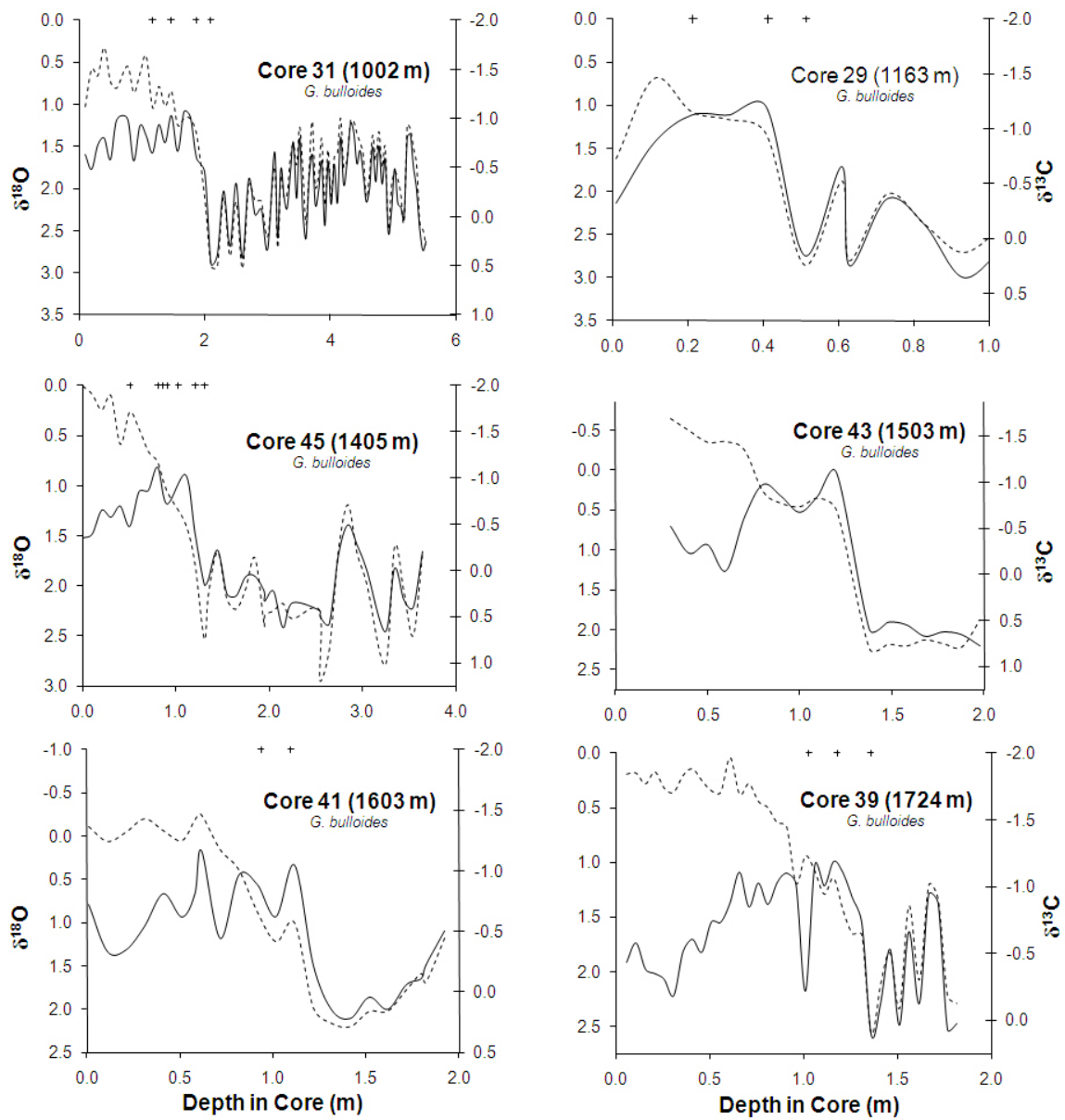


Figure 2.3. Planktonic $\delta^{18}\text{O}$ and $\delta^{13}\text{C}$ of *G. bulloides* or *O. universa* plotted versus core depth. Black hatches indicate intervals that were radiocarbon dated, continued.

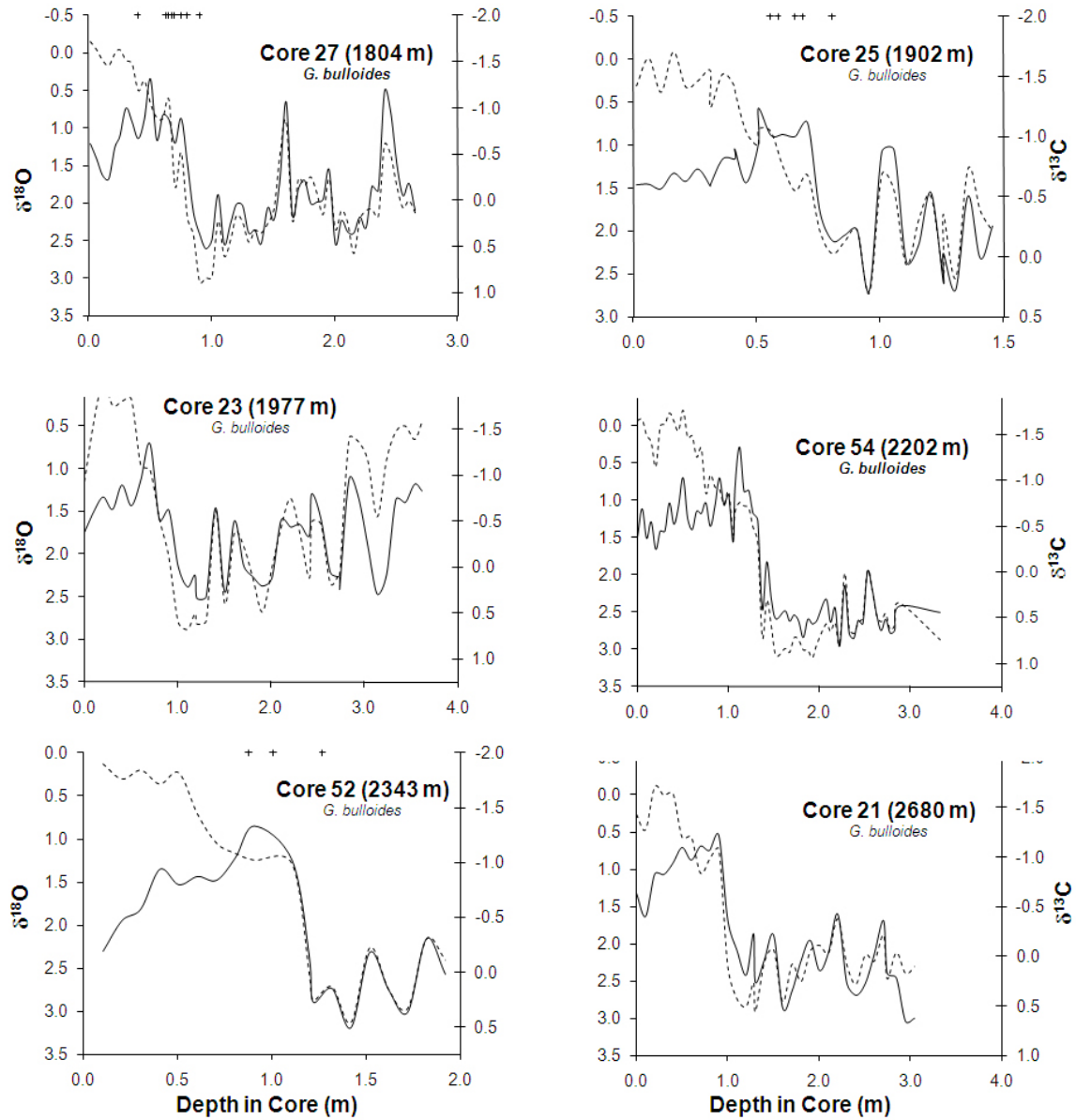


Figure 2.3. Planktonic $\delta^{18}\text{O}$ and $\delta^{13}\text{C}$ of *G. bulloides* or *O. universa* plotted versus core depth. Black hatches indicate intervals that were radiocarbon dated, continued.

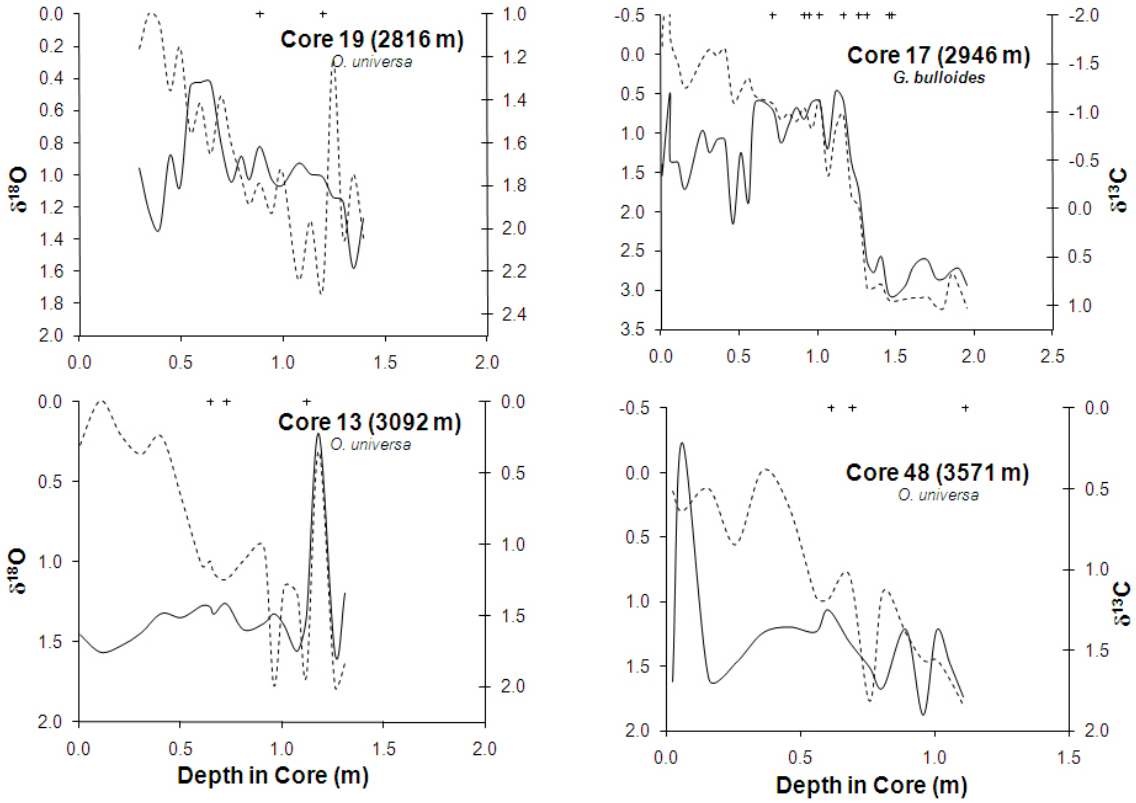


Figure 2.3. Planktonic $\delta^{18}\text{O}$ and $\delta^{13}\text{C}$ of *G. bulloides* or *O. universa* plotted versus core depth. Black hatches indicate intervals that were radiocarbon dated, continued.

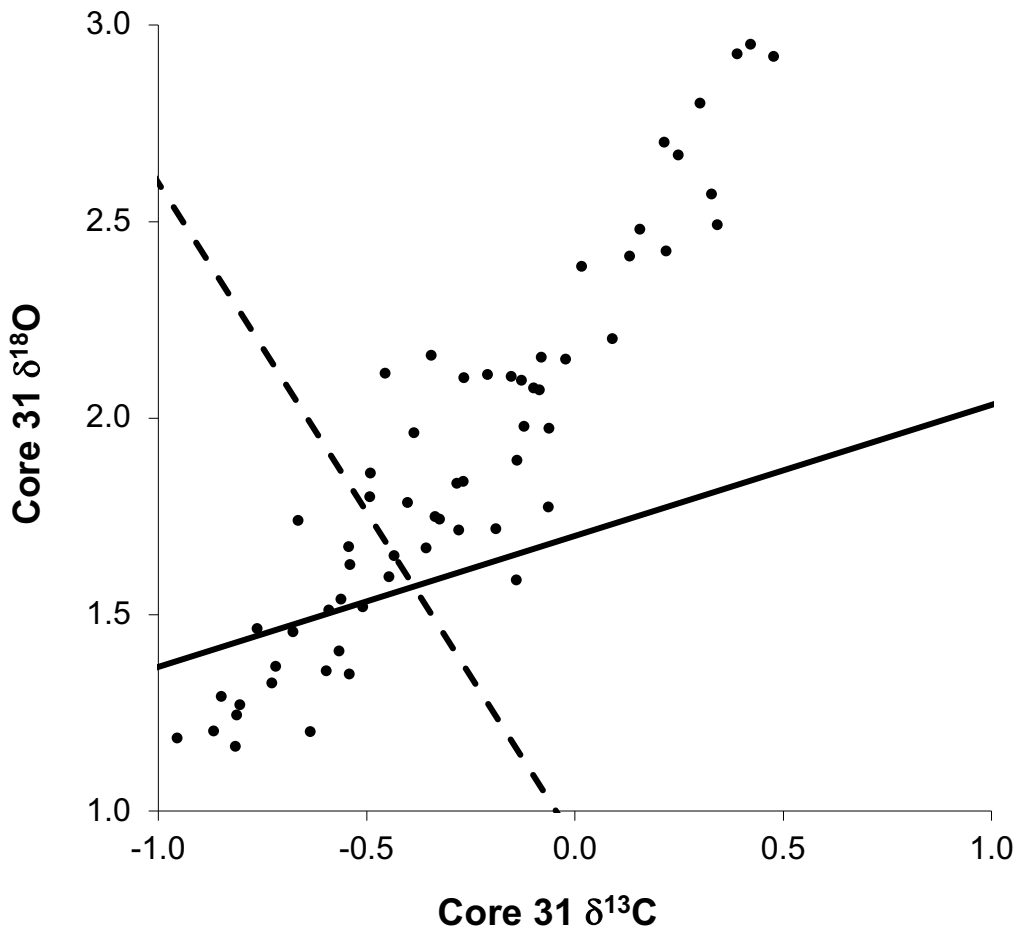
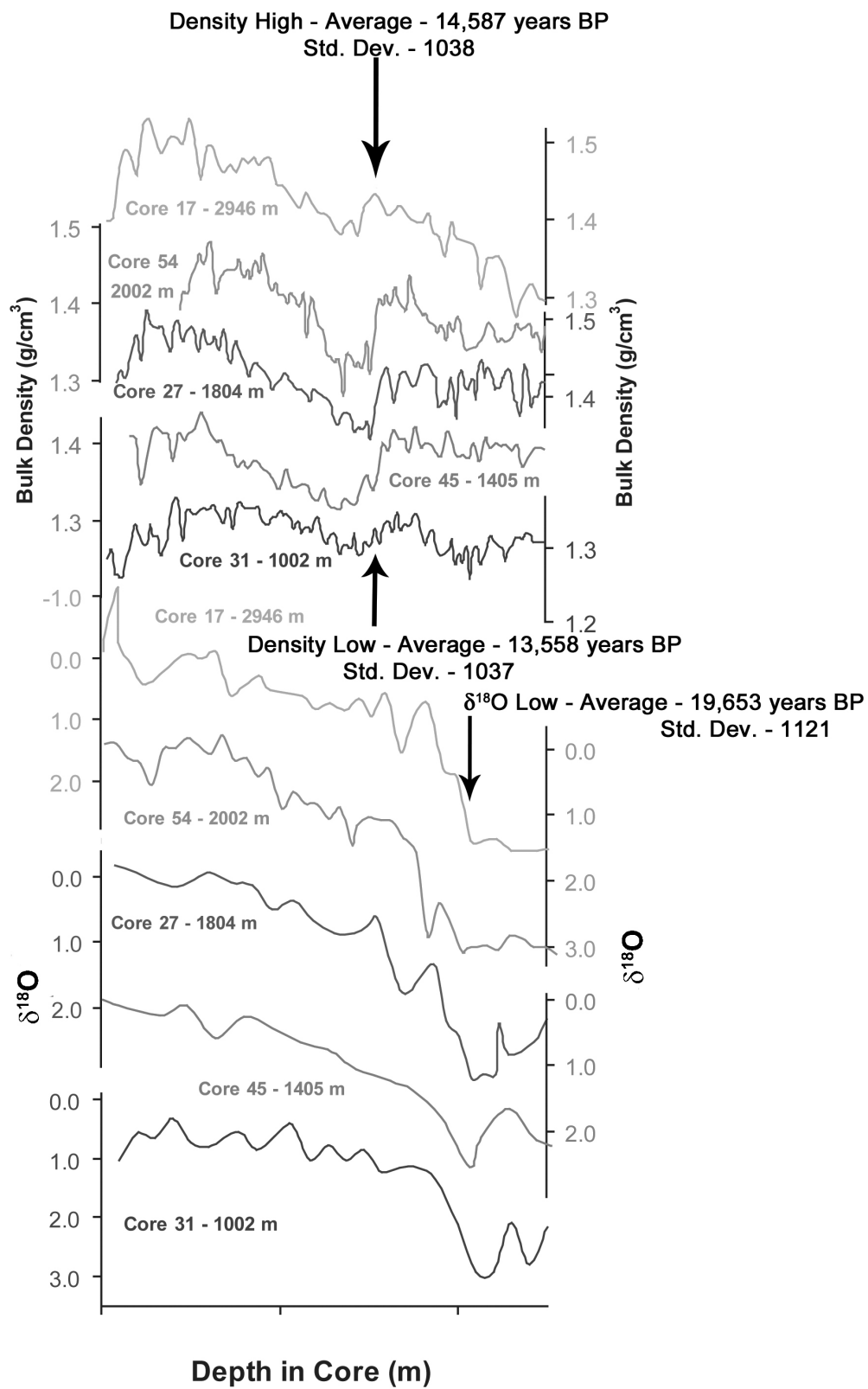


Figure 2.4. *G. bulloides* $\delta^{18}\text{O}$ plotted versus *G. bulloides* $\delta^{13}\text{C}$ from core 31, spanning the late glacial to 15.0 kyr BP. The $\delta^{18}\text{O}$: $\delta^{13}\text{C}$ slope due to the “carbonate ion effect” is plotted with a black vector and the expected $\delta^{18}\text{O}$: $\delta^{13}\text{C}$ values calculated from temperature and DIC $\delta^{13}\text{C}$ values are plotted with a dashed vector.

Figure 2.5. Stacked bulk density (g/cm^3) and *G. bulloides* $\delta^{18}\text{O}$ from cores 17, 54, 27, 45, and 31. Cores were placed on a common depth scale by maximizing the correlation between planktonic stable isotope and density profiles; these cores are plotted on the “*depth in core 31*” scale. Three prominent stratigraphic intervals are marked with arrows and the average age and standard deviation calculated from twelve cores for each point is noted.



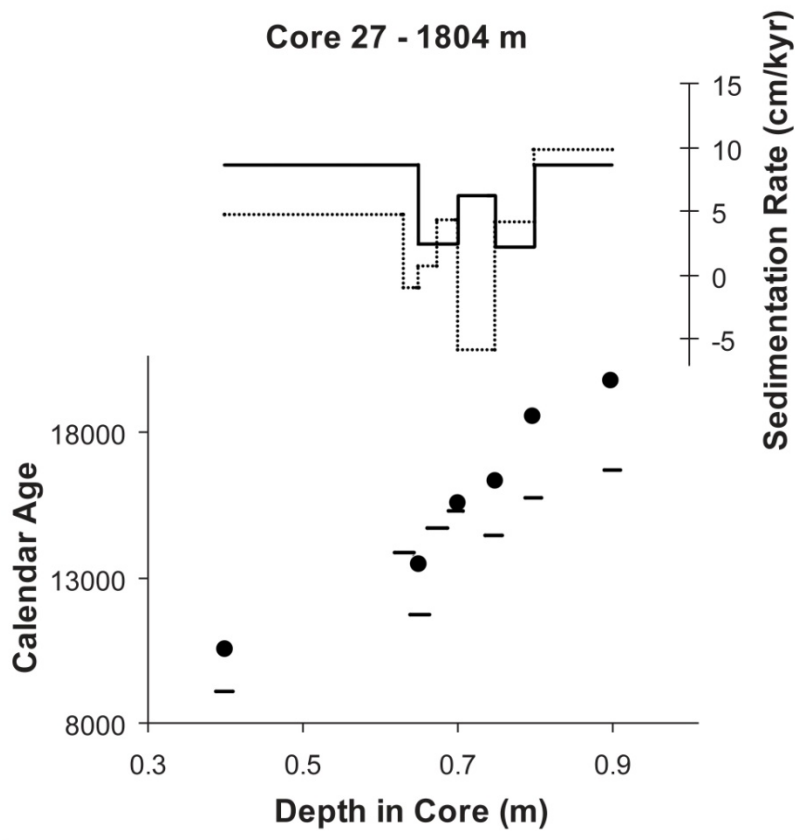


Figure 2.6. Calendar age and sedimentation rate for core 27 are plotted on its depth scale. Data for *G. bulloides* data is indicated by a solid line, whereas data for *O. universa* data is indicated by a dashed line.

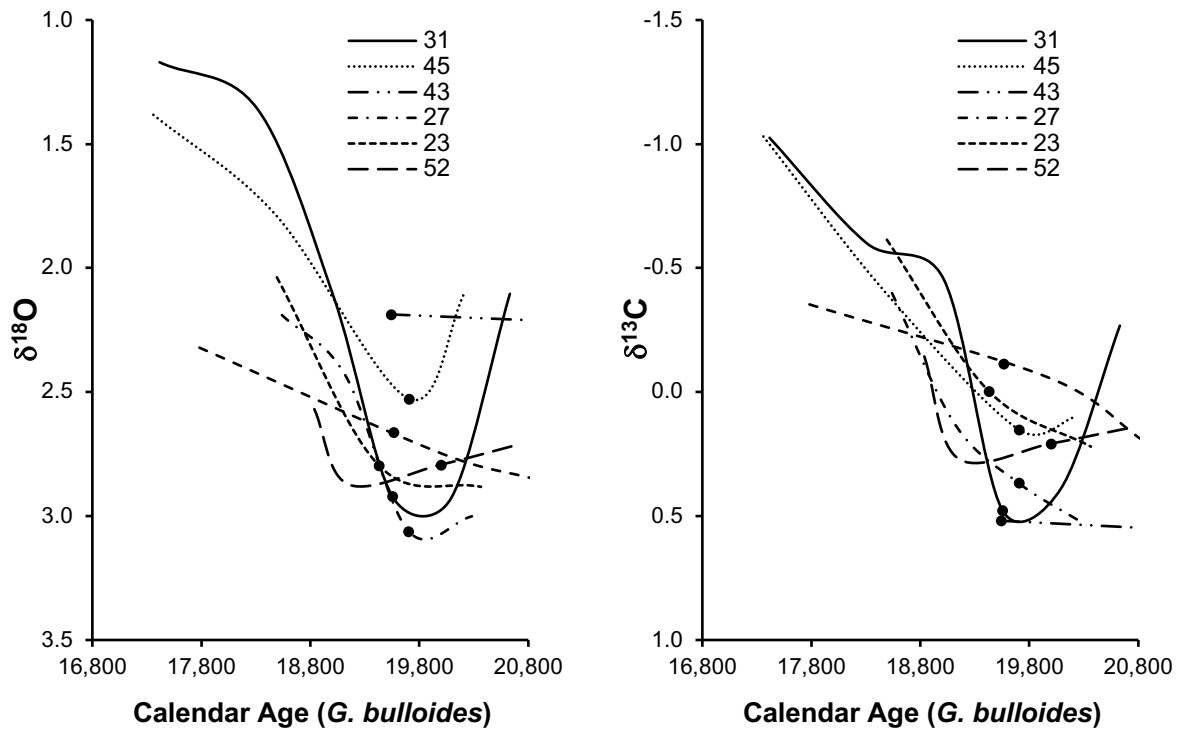


Figure 2.7. $\delta^{18}\text{O}$ profiles from cores 21, 23, 27, 31, 45, 43, and 52 are plotted versus calendar age. Black circles indicate intervals that were radiocarbon dated.

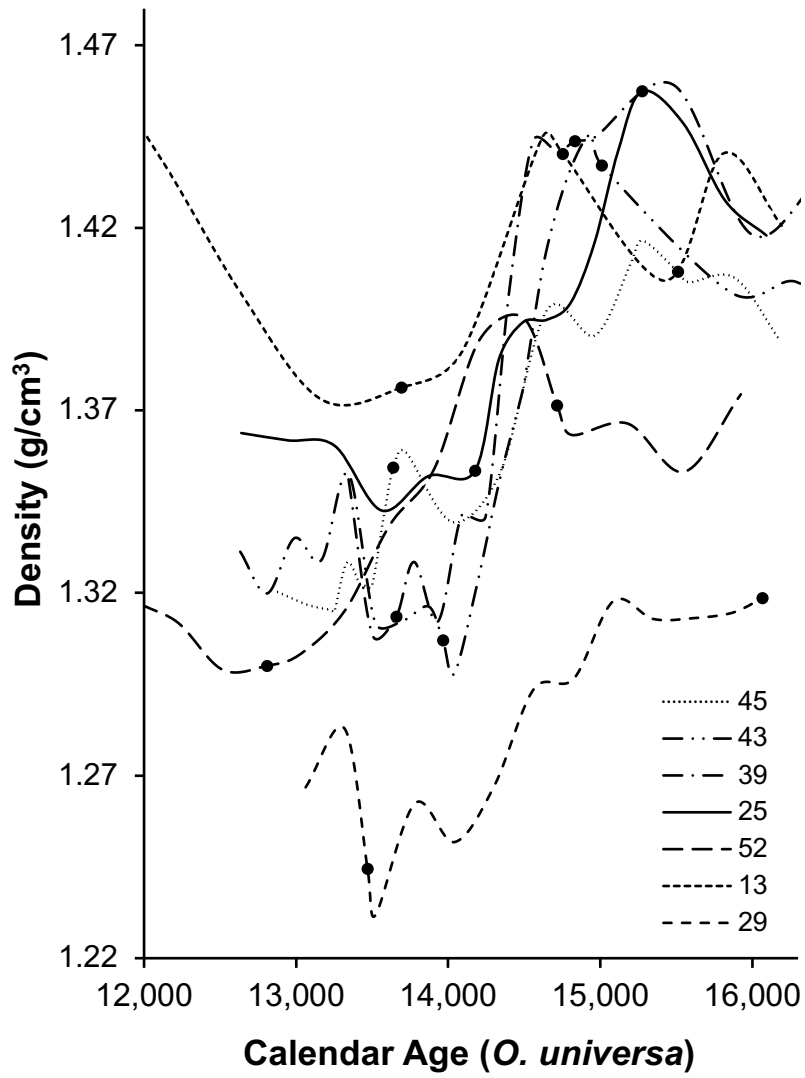
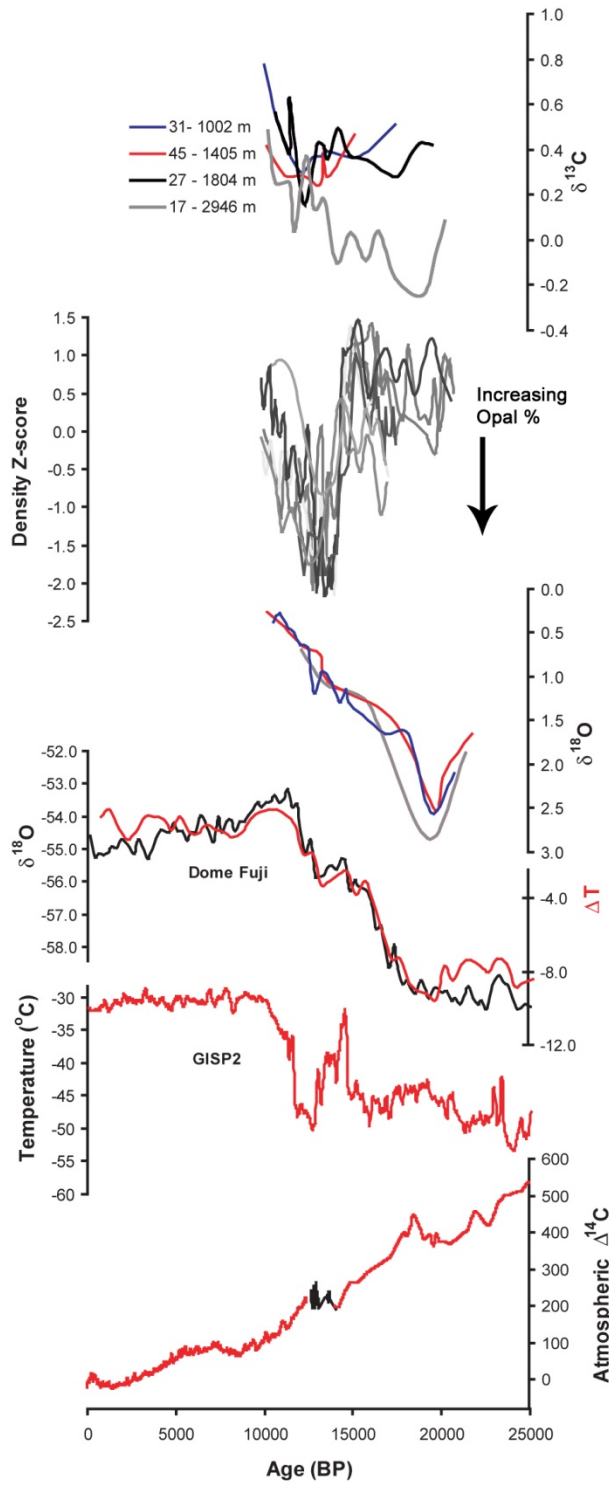


Figure 2.8. Density profiles from cores 13, 25, 29, 39, 43, 45, and 52 plotted on a calendar age scale. Black circles indicate intervals that were radiocarbon dated.

Figure 2.9. Bulk density z-scores for cores 13, 25, 29, 39, 43, 45, and 52; planktonic $\delta^{18}\text{O}$; benthic $\delta^{13}\text{C}$; temperature records from Greenland and Antarctica; and atmospheric $\Delta^{14}\text{C}$ are plotted versus calendar age. Benthic $\delta^{13}\text{C}$ was stacked using the age scale for core 45.



Chapter 3

A core top assessment from the southeastern Atlantic for the planktonic/benthic
foraminiferal radiocarbon proxy

Abstract

We present radiocarbon results from a geographically constrained depth transect of sediment cores from water depths spanning 400-3500 meters in the southeastern Atlantic. The distribution of radiocarbon is a tracer of the ventilation history of mid-depth water and can delineate water of North Atlantic versus Southern sources. Coexisting benthic and planktonic foraminifera pairs in the sedimentary record have been used to reconstruct past changes in ventilation, yet the fidelity of the method has been called in to question due to potential problems and biases. Thus, before interpretation of past changes to the ocean's interior can be made, it is important to assess the validity of using benthic/planktonic pairs to distinguish the essential features of modern seawater radiocarbon distribution. Here we present radiocarbon and stable isotope results from twenty-seven, high sedimentation rate, modern samples from the southeastern Atlantic, an area where the seafloor intersects all the principal water masses involved in the thermohaline circulation of the Atlantic. We use two cosmopolitan planktonic species, from different habitats, and with a ^{14}C age of less than 2000 years and find several consistent trends; it is these consistent trends that provide quantitative insight to the benthic-planktonic radiocarbon method. In all cases, the *G. bulloides* ^{14}C ages are older than *O. universa*. However, this age offset between *O. universa* and *G. bulloides* is not consistent at all water depths – the ages diverge significantly in the 2000-1500 water depth range, in parallel with the shifts in sedimentary organic carbon %. This inter-species variability is large enough to overwhelm any possible radiocarbon differences in deep water masses (benthic foraminifera). Clearly, even among the most abundant taxa, planktonic foraminifera do not provide an interchangeable chronological reference for the benthic foraminiferal radiocarbon. Restricting the analysis to planktonic foraminifera that are most likely to be “surface dwelling”—in our case,

O. universa—results in a benthic-planktonic radiocarbon depth profile that bears the same structure as modern seawater nutrient profiles (especially dissolved silica) in the region. However, the benthic minus planktonic radiocarbon depth profile does not reproduce the features of the closest dissolved inorganic carbon $\Delta^{14}\text{C}$ (modern seawater) profile. In particular, with respect to modern DIC $\Delta^{14}\text{C}$ measurements, the benthic-planktonic depth profile gives the impression of significantly “older” water bathing mid depth sediments (600-800 meters) and abyssal depth sediments (greater than 2500 meters). The consistency of the trends with water depth provides a measure of the fidelity of the method for reconstructions over the interval since the last glacial maximum.

Introduction

The distribution of radiocarbon in the ocean's interior potentially offers one of the best available tracers of changes of both the geometry and the ventilation history of the major water masses. A variety of sediment proxies – for example, benthic foraminiferal $\delta^{13}\text{C}$ (*Sarnthein et al.*, 1994), Cd/Ca (*Boyle and Keigwin*, 1985), and sedimentary neodymium isotopes (*Piotrowski et al.*, 2005) – are sensitive to changes in the distribution of water masses (or, more precisely, nutrients). However, these tracers do not resolve rates of overturning (*LeGrand and Wunsch*, 1995). As a result, while many tracers allow inference of major changes to the chemistry of the ocean's interior, they cannot speak directly to cause or climatic effect. Radiocarbon is ostensibly different because it carries an inherent clock.

Over the past few decades, there have been a variety of attempts to use ^{14}C values from coexisting benthic and planktonic foraminifera as a measure of the ventilation age of water masses (e.g. *Broecker et al.*, 2004a; *Keigwin*, 2004). To track deep water changes, this method assumes that planktonic foraminiferal radiocarbon bears a consistent relationship with atmospheric radiocarbon content and, therefore, that it can be used as a chronological reference point. However, this method features a number of possible problems and biases (reviewed by *Broecker et al.*, 2004b). Bioturbation, for example, has the potential to mix together foraminiferal shells that were not originally contemporaneous. Other forms of reworking (e.g. downslope or downcurrent transport of sediments) can also occur. The habitat of many taxa of planktonic foraminifera is also not necessarily constrained to surface waters of uniform radiocarbon content. Finally, the addition of secondary calcite can contaminate the original radiocarbon content of any foraminiferal test. These potential problems have been difficult to gauge (or even rule out) when applied to different sedimentary sequences, and, consequently, it is often possible to arrive at a

highly skeptical view of the practical application of paired planktonic-benthic foraminiferal radiocarbon (e.g. *Broecker et al.* 2004b).

The purpose of this paper is to describe a core top assessment for the planktonic/benthic foraminiferal radiocarbon proxy. Various models suggest that the distribution of radiocarbon in the ocean should be altered substantially if the intermediate-deep ocean circulation changed dramatically over the ice ages or the abrupt climate shifts of the late Pleistocene (e.g. *Toggweiler and Samuels*, 1998; *Meissner et al.*, 2003). Thus, it becomes important to establish the capacity of foraminiferal radiocarbon to delineate the essential features of modern seawater radiocarbon distribution. Here we present radiocarbon results from a geographically constrained depth transect of sediment cores from the southeastern Atlantic, all with relatively high sedimentation rates and sufficient abundance of two cosmopolitan planktonic species with different habitats. Despite the limited geographic domain, the depth transect spans a wide range of sedimentary environments and water column radiocarbon content. Thus, the results offer as yet one of the best opportunities to determine the sensitivity, biases and errors of the benthic-planktonic radiocarbon method.

Core Locations and Oceanographic Setting

The southeastern Atlantic is an especially suitable location to carry out a radiocarbon core top analysis because the seafloor intersects all the principal water masses involved in the thermohaline circulation of the Atlantic. Water masses from high-latitude northern and southern sources are stacked vertically and can be distinguished on the basis of density and nutrient concentrations (figure 3.1). For example, thermocline water of southern hemisphere origin (100-500 meters) overlies Antarctic Intermediate Water and Upper Circumpolar Deep Water (500-1500 meters), which in turn overlies the constituents of North Atlantic Deep Water (notably

Labrador Sea Water in the 1700-2000 meter depth range) (*Schlitzer, R., 2000; Stramma and England, 1999*).

The stable carbon isotopic composition of DIC reflects these various water masses (figure 3.1). Two profiles, one at 12° 0.0'S and one at 29° 44.05'S (MelVan station 95 located north of Walvis Ridge in the Angola Basin approximately 400km from shore and BEAGLE station 87 located south of the Walvis Ridge in the Cape Basin approximately 600 kilometers from shore) illustrate the main features. An intense $\delta^{13}\text{C}$ minimum, broadly overlapping with the oxygen minimum zone and the Antarctic Intermediate Water, underlies the surface layer; this $\delta^{13}\text{C}$ minimum is bounded at depth (around 1500 meters) by the high $\delta^{13}\text{C}$ characteristic of northern source waters. MelVan 95 profile (closer to the continent) shows lower $\delta^{13}\text{C}$ values between 0-1400 meters compared to the profile from BEAGLE87; however, both profiles indicate a very strong gradient in the upper 200 meters (more so in the waters closer to shore), a depth range that could certainly encompass the seasonal habitat for deeper dwelling planktonic foraminifera. Thus, carbon isotopic composition of planktonic foraminiferal tests might be sensitive to the large upper ocean gradients in carbon.

The origin and characteristics of these various water masses are also imprinted on the $\Delta^{14}\text{C}$ of dissolved inorganic carbon (DIC) in the South Atlantic Ocean (figure 3.2). In the modern ocean, high latitude southern source waters have lower initial radiocarbon concentrations than North Atlantic source waters because these southern source waters are not as fully equilibrated with the atmosphere prior to sinking. For example, though there must be some downstream "aging" of the inorganic carbon pool in the Atlantic in accordance with the transit times of water masses, the $\Delta^{14}\text{C}$ of Antarctic Intermediate Water is approximately 60 ‰ lower than that of NADW at the latitude of our depth transect (in other words, AAIW has a radiocarbon age that is

approximately 250 years older than the northern source waters) (*Broecker and Peng, 1982*). In the western South Atlantic, the tongue of NADW stands out clearly as a maximum of radiocarbon, because, in addition to the overlying radiocarbon minimum associated with AAIW, there is also a gradient of about 50‰ between 2 km and 5 km associated with an enhanced presence of deep southern source water. In the eastern basins, the available radiocarbon profiles all feature a prominent intermediate water minimum, but do not show a substantial gradient at depth.

Radiocarbon produced by the atmospheric bomb testing in the 1950's and 1960's has entered the ocean through air-sea gas exchange, altering the natural radiocarbon distribution in the ocean. The pre-bomb surface radiocarbon values were approximately -60‰ (*Broecker and Peng, 1982*) and have been raised by the bomb contamination at our field site to almost 100‰. It was shown in the 1990's that "the bomb-produced radiocarbon signal had not penetrated significantly below 1000 m except in the North Atlantic through the formation of North Atlantic Deep Water and immediately adjacent to Antarctica wherever Antarctic Bottom Water is formed" (Matsumoto and Key, 2004). The upper 1000 meters of the BEAGLE 87 profile plotted in figure 3.2 is therefore enriched in radiocarbon from the bomb spike. Pre-bomb surface values were probably around -60‰, as opposed to the 100‰ observed in post-bomb surveys. The exact significance of bomb radiocarbon in the upper 1000 meters of the profile is unknown; disentangling the bomb influence in the interior of the ocean requires a realistic model of the ocean carbon cycle. However, it is important to note that the intermediate depths in the southern Atlantic represent a direct conduit to the atmosphere and the gas exchange rates in sub-Antarctic waters are the highest anywhere in the global ocean; therefore, it is plausible that the modern

seawater profile is offset substantially from that which sedimentary foraminifera (even young core tops) would ever reconstruct.

Dissolved silica profiles are often used to evaluate the mixing ratios of northern and southern source waters and to distinguish bomb radiocarbon effects; dissolved silica tends to follow the same trends as radiocarbon in the modern ocean (*Broecker and Peng, 1982*).

GEOSECS station 103 and BEAGLE 87 silica measurements are plotted in figure 3.3. The slight differences in nutrient concentrations in the southeast Atlantic, along with the possibility of bomb contamination, serves as a reminder that our core top profile does not constitute a true radiocarbon calibration. Nevertheless, the broad features in recent foraminiferal radiocarbon should at least lead us to a more meaningful interpretation of past changes.

Materials and Methods

The majority of the twenty-seven cores presented here were collected aboard the R/V Melville in March 2003 (MelVan09), south of the Walvis Ridge on the continental slope of Africa. In addition, twenty-four water samples were taken at 11° 59.9'S, 9° 25.0'E ranging from 0 to 4300 meters. Of the MelVan09 cores, nineteen are gravity cores, two are trigger cores, and two are multi-cores. All but four were collected along three depth transects within an area defined by 19° 43.3'S and 21° 33.1'S and 9° 54.1'E and 12° 48.1'E and range in depth from 326 to 3678 meters. Three other cores (63, 73, and 108) were taken south of the transect at 24° 28.0'S, 12° 26.0'E, 24° 28.9'S, 12° 51.299'E, and 28° 45.0'S, 13° 50.0'E in water depths of 2646, 1708, and 1987, respectively. In addition to the MelVan09 cores, we used samples from two ODP holes: Sites 1078 (11° 55.2'S, 13° 24.0'E) and Site 1079 (11° 55.7'S, 13° 18.5'E) at 427 and 737 meters respectively. We also use one core donated to Texas A&M University (TAMU 04) from 1000 meters collected at 11° 55.0'S and 13° 12.0'E. We were forced to use cores from this

region of the South Atlantic, because we were unable to find suitable cores south of the Walvis Ridge in this depth range (which is bathed by Antarctic Intermediate Water).

Generally, samples were taken from the top three centimeters of the cores (except where noted in table 3.1), wet sieved through 63 μ m mesh, and picked for foraminifera. The tests of planktonic and benthic foraminifera were then analyzed for $\delta^{13}\text{C}$, $\delta^{18}\text{O}$, and ^{14}C . For the stable isotope analysis, specimens of *Orbulina universa* were picked from the 355-425 μ m size fraction and *Planulina* (all species) were picked from the >250 μ m size fraction. Isotopic analyses were performed using a common acid-bath, Carousel-48 automation carbonate preparation device coupled to a Finnigan MAT 252 mass spectrometer. Estimated analytical precision, deduced from the concurrent measurement of 24 NBS 19 standards, was 0.05 to 0.07 per mil for $\delta^{13}\text{C}$ and $\delta^{18}\text{O}$, respectively.

Radiocarbon measurements were made at the Center for Accelerator Mass Spectrometry at Lawrence Livermore National Laboratory on *Globigerina bulloides*, *O. universa*, and mixed benthic samples. Foraminifera tests were sonicated in a .0001N HCl solution; planktonics were sonicated briefly to avoid having the shells explode, whereas benthics were sonicated for 1 minute. The HCl was then pipetted off and the samples were dried, weighed, and graphitized. Sample sizes varied between .4 and 8 mg. The $\delta^{13}\text{C}$ of the samples used for radiocarbon analysis was not measured, but we assigned a $^{13}\text{C}/^{12}\text{C}$ ratio of 1.5‰ for planktonic samples, and 0‰ for the benthic samples to correct for the mass-dependent fractionation. To convert the benthic foraminifera age to $\Delta^{14}\text{C}$, the values were decay-corrected to 1950 using the coexisting planktonic foraminiferal $\Delta^{14}\text{C}$ as an estimate of calendar age, and then calculated as $\Delta^{14}\text{C}$ using the equations in Stuiver and Polach (1977).

Total carbon of bulk sediment and carbon isotope values of water were measured using a Thermo-Finnigan Delta XP Isotope Ratio Mass Spectrometer at Scripps Institution of Oceanography. Total inorganic carbon values were obtained by acidification of bulk sediment using 1N HCl.

Results

We analyzed radiocarbon in thirty-eight core tops; nineteen for mixed benthics, *G. bulloides*, and *O. universa*, eighteen for mixed benthics and *O. universa*, and one for mixed benthics and *G. bulloides*. Of the core tops dated, eleven were found unsuitable for our purposes here. For example, several core tops had benthic and planktonic ages greater than 9,000 ¹⁴C years and three others had widely discordant (>5000 year) dates among the different components-- which we took as an indication that the samples were not representative of modern sediments.

We have stratigraphic information (for example, the thickness of sediment to the last glacial maximum) for a subset of the cores used. These observations suggest that sedimentation rates are between 5 and 12 cm/kyr, except in the case of our two shallowest cores where they are much higher (table 3.1). In any case, the smoothest depth profile of planktonic-benthic radiocarbon is produced when we include only those core tops younger than 1800 years (radiocarbon age). Three core top samples had *O. universa* ¹⁴C ages of 2355, 1980, and 2285 years. Although there was no obvious stratigraphic problem with these samples, the benthic-planktonic radiocarbon values fell well off the trend defined by the other twenty-seven younger samples. Therefore, for the purposes of our discussion we institute a cutoff age of approximately 1800 ¹⁴C years. Though the general strategy of culling only the youngest core tops is logical, the exact cutoff we employ here is, of course, completely arbitrary. This process does, however,

illustrate the sensitivity of planktonic-benthic radiocarbon method to the careful screening of cores and the importance of multiple replication.

The resulting radiocarbon profile is complemented by other sedimentary variables. The oxygen isotope values of benthic foraminifera show the expected trend from lower values in the warmer shallow water to higher values in colder deep water near 1500 meters. At approximately 1700 meters water depth, both the weight % organic carbon in the bulk sediment and the carbon isotope values of benthic foraminifera show a pronounced shift: the change is from low $\delta^{13}\text{C}$, high organic carbon that is characteristic of shallow depths, to higher $\delta^{13}\text{C}$, low organic values that characterize the deeper cores. The bulk carbon chemistry of the surficial sediments suggests substantial heterogeneity in sedimentary environments captured. For example, high sedimentary organic carbon content occurs beneath the regions of pronounced upwelling in the surface waters. This influence diminishes greatly as one moves off shore and, therefore, to greater depths of the continental slope. Nevertheless, these stable isotope tracers suggest that the broad physical and nutrient characteristics of the ambient bottom water are captured by the epibenthic foraminifera.

The most obvious feature of the benthic-planktonic radiocarbon profile is the age offset between the planktonic species. In all cases, the *G. bulloides* ^{14}C ages are older than *O. universa*. However, this age offset between *O. universa* and *G. bulloides* is not consistent at all water depths – the ages diverge significantly in the 2000-1500 water depth range, in parallel with the shifts in sedimentary organic carbon %, and, in the extreme cases, the *G. bulloides* ^{14}C ages are older than that of the corresponding benthic foraminifera.

Considering only the *O. universa* minus benthic profile, there is an apparent radiocarbon minimum in the intermediate water zone (1500-500 meters), an apparent radiocarbon maximum

at about 2000 meters, and an apparent gradual decline of deep radiocarbon from 2000-4000 meters. This foraminiferal radiocarbon profile can be compared with the $\Delta^{14}\text{C}$ of seawater DIC (figure 3.2) from the closest CTD casts. To facilitate this comparison, foraminiferal radiocarbon dates are expressed both as a simple difference and as $\Delta^{14}\text{C}$. Between 1300 and 1800 meters in the upper NADW, we have eight reconstructed $\Delta^{14}\text{C}$ values that match the measured water column values. Below this depth range, our reconstructed values are depleted in radiocarbon, with an average offset of 50‰ when compared to the nearest BEAGLE profiles, station 87 located at 29° 44.05'S, 9° 17.7'E. The magnitude of this offset is highly significant with respect to the range of $\Delta^{14}\text{C}$ values in deep water. It is important to note that this trend in the deeper cores must be the product of benthic foraminiferal radiocarbon variability, given that the trend in apparent $\Delta^{14}\text{C}$ is the same for both planktonic species used.

$\delta^{13}\text{C}$ values of *planulina* from our core tops (figure 3.1) distinguish between northern and southern source waters, with a similar pattern as the radiocarbon data in the upper 2000 meters. For example, the benthic foraminiferal $\delta^{13}\text{C}$ data, like the benthic-planktonic $\Delta^{14}\text{C}$, show a pronounced gradient at mid-depths, in agreement with modern water column profiles between 1300 and 1800 meters. Below 2000 meters, $\delta^{13}\text{C}$ values become slightly and progressively lower, though not nearly to the same extent implied by a simple scaling of the foraminiferal radiocarbon. Clearly, the stable carbon and radiocarbon content of benthic foraminifera are not equally sensitive to the same influences in cores at all water depths.

To probe the possible bias of the radiocarbon age pairs derived from sediment mixing, we measured foraminiferal abundance in the upper 2 meters of four piston cores whose corresponding gravity core-top formed part of the radiocarbon profile (figure 3.4). The downcore abundance variability was remarkably consistent in these cores that span water depths of 1000-

2500 meters. *O. universa* abundance in all four cores was high in the late Holocene, with a steady increase from low values during the LGM. The total benthic abundance (mixed assemblage) has the exact opposite trend – low during the late Holocene, with a significant increase during the LGM. The *G. bulloides* data indicates a maximum during the early Holocene (and deglaciation), with a steady decline to the present. These variations in abundance can be referenced to a typical downcore stable isotope profile to illustrate the possible influences of bioturbation. For example, it is important to note that the maximum in *G. bulloides* abundance corresponds to an intense early Holocene minimum in $\delta^{13}\text{C}$.

Discussion

The fidelity of the benthic-planktonic foraminiferal radiocarbon method has been assessed in various ways previously. However, our results here are unique in that the sedimentary radiocarbon depth transect from a limited area was constructed with a large number (27) of essentially modern samples (less than 2000 ^{14}C yrs). Most of the results from cores in adjacent water depths are reproducible and therefore define several consistent trends; it is these consistent trends that provide quantitative insight to the benthic-planktonic radiocarbon method (these consistent trends also allow us to rule out randomizing influences such as downslope transport or secondary calcite addition). The most obvious result is that the radiocarbon content of the two most abundant planktonic foraminifera is significantly offset; the core tops are characterized by inter-species variability that is large enough to overwhelm any possible radiocarbon differences in deep water masses (benthic foraminifera). Clearly, even among the most abundant taxa, planktonic foraminifera do not provide an interchangeable chronological reference for the benthic foraminiferal radiocarbon. Restricting the analysis to planktonic foraminifera that are most likely to be “surface dwelling”—in our case, *O. universa*—results in a

benthic-planktonic radiocarbon depth profile that bears the same structure as modern seawater nutrient profiles (especially dissolved silica) in the region. However, the benthic-planktonic radiocarbon depth profile does not reproduce all the features of the closest dissolved inorganic carbon $\Delta^{14}\text{C}$ (modern seawater) profile. In particular, with respect to modern DIC $\Delta^{14}\text{C}$ measurements, the benthic-planktonic depth profile gives the impression of significantly “older” water bathing mid depth sediments (600-800 meters) and abyssal depth sediments (greater than 2500 meters). We argue that the explanation for these trends cannot involve simply sedimentary artifacts; they must also reflect the oceanographic distribution of radiocarbon. This is evident in the strong resemblance between the structure of the benthic-*O. universa* radiocarbon difference and the dissolved nutrient (silica) profiles from the region. The salinity profile from our field site agrees with the radiocarbon depleted water we observe below 3200 meters – presumably circumpolar deep water. Highlighted in figure 3.3 is a salinity discontinuity at 21° S which would be diffused unless it is the boundary between water masses.

G. bulloides and *O. universa* were chosen for this study because they were the two most abundant planktonic species in the sediment, and they had been used as a calendar age indicator in previous studies (Roark *et al.*, 2003; Schefuss *et al.*, 2005). In the case of our core top profile, some of the observed age differences between the two species may be the result of sediment mixing. The abundance profiles for the two species—maximized for *O. universa* and *G. bulloides* in recent and early Holocene sediments, respectively—would tend to promote an age offset in the same sense as that observed, given intense mixing. However, a notable feature of the benthic minus planktonic radiocarbon data is that the offset between the two planktonic species increases dramatically between approximately 1300 and 2000 meters water depth. This aspect cannot be explained by mixing: there is no difference in *G. bulloides* abundance values and

trends between our two shallower cores and two deeper cores to account for the anomalously old *G. bulloides* ages we observe between 1300 and 2000 meters. Furthermore, the coupling between abundance and bioturbation cannot explain the extreme cases of core top *G. bulloides* ages that are older than coexisting benthic foraminifera, because the *G. bulloides* abundance peak is younger than the benthic abundance peak.

Instead, we believe that the most likely explanation for the age distribution of *G. bulloides* in the core tops is its deeper habitat. The $\delta^{13}\text{C}$ DIC profile indicates an intense $\delta^{13}\text{C}$ minimum just below the surface mixed layer at relatively shallow depths (<100 meters). If *G. bulloides* were calcifying within this $\delta^{13}\text{C}$ minimum, it is likely that they would be calcifying in ^{14}C depleted (old) waters as well. We can only say “likely”, because the hypothesized radiocarbon-depleted waters in the upper part of the water column undoubtedly would have been obscured in seawater measurements by the bomb radiocarbon transient. The intersection of this ^{13}C and ^{14}C -depleted water mass with the habitat of *G. bulloides* should be more substantial as one moves landward, because the isopycnal surfaces have a significant east-west slope. In fact, taken at face value, the results from the shallowest cores (1300 meters) would demand that *G. bulloides* calcified in water that was older than the corresponding bottom water. While such circumstances are not common in the modern ocean, it is at least conceivable that a poorly ventilated thermocline “shadow zone” that is near to the surface ocean overlies better-ventilated water. The $\delta^{13}\text{C}$ DIC profiles allow this possibility, and the $\delta^{13}\text{C}$ of *G. bulloides* is universally low in all the recent sediments of the Benguela region. However, it is important to point out that the implication from $\delta^{13}\text{C}$ is that this shallow “shadow zone” may not always have existed—the $\delta^{13}\text{C}$ of *G. bulloides* in all cores from the region decreased abruptly at the close of the last ice age

(figure 3.4)—and, therefore, the benthic-planktonic radiocarbon age difference may not have always been subject to this influence.

Plankton tow and core top evidence suggest that *O. universa*, unlike *G. bulloides*, is much more restricted to the surface mixed layer, even in upwelling environments (*Field, 2004*), perhaps because it has photosynthetic symbionts that constrain its habitat to the shallow photic zone. This fact, combined with *O. universa*'s abundance peak during the latest Holocene, leads us to conclude that *O. universa* is the most suitable of all the possible planktonic foraminifera to use as a radiocarbon reference for recent benthic foraminiferal dates in this region.

Summary and Conclusions

On the one hand, it may seem encouraging that the structure of the benthic-*O. universa* radiocarbon difference strongly resembles dissolved nutrient (silica) profiles from the region. On the other hand, it may seem problematic that the implied radiocarbon age of the intermediate and deep water from these sedimentary measurements is much larger than suggested by the closest radiocarbon measurements of modern seawater. What are we to make of these seemingly conflicting observations?

The most obvious suggestion might be that older benthic foraminifera are mixed upward to the core top through bioturbation. However, this possible explanation is not especially satisfying, given that virtually the same sedimentary characteristics apply to the core tops at 1800 meters (where there is reasonable agreement between foram and seawater radiocarbon measurements) as to core tops at 2500 meters (where there is 50‰ difference between foram and seawater profiles). Furthermore, the trend toward older ¹⁴C ages in the deeper core tops is reproduced using either of the planktonic foraminiferal species as reference. And one would predict that the early Holocene *G. bulloides* abundance maximum should be manifested more

strongly in the radiocarbon difference if bioturbation were a pervasive influence. Thus, while we cannot rule out the possibility of selective bioturbation—for example, if the mixing characteristics of small benthic foraminifera were different than for *G. bulloides*—the evidence for significant bioturbation influence is not compelling.

A more likely possibility is that the modern seawater radiocarbon values recorded from locations closest to our study site are not in fact representative of the time-averaged (2000 year) seawater chemistry we presented here. The bomb radiocarbon transient comes to mind immediately, and that contamination could certainly explain any upper ocean (<1000 meters) discrepancies between sedimentary and modern seawater measurements. But it is difficult to imagine a significant influence of bomb carbon at depth in the radiocarbon profiles.

Nevertheless, bomb-¹⁴C contamination is not the only factor to consider. It is also conceivable that the deep water in this far northeastern quadrant of the Cape Basin—bounded to the north and west by the Walvis Ridge and to the east by the continental margin—is isolated to the extent that the available radiocarbon profiles to the south of the region do not capture its true radiocarbon age (as inferred from the benthic foraminifera). Recirculation of water masses has been observed in intermediate waters at approximately 27°S in the Cape Basin (*Duncombe Rae*, 2005) and could extend to deeper waters as well. Therefore, it is plausible that deeper waters are recirculating in our sheltered location of the northern Cape Basin, leading to an aged $\Delta^{14}\text{C}$ signal. While our core-top radiocarbon profile cannot be extrapolated to a larger geographical area of the southeastern Atlantic, we believe the internal consistency between our twenty-seven cores is accurately reflecting the radiocarbon distribution in our geographically constrained field area. This conclusion will allow us to interpret past changes in ventilation recorded deeper in the sediments at our core locations.

Acknowledgments

We acknowledge the technical assistance of Dana Vukolovich and Bruce Deck. This work was supported by an NSF award to CDC and SEGRF fellowship at LLNL to JM. Sample material used in this project provided by the Ocean Drilling Program Bremen Core Repository.

References

- Arhan, M., Herlé Mercier, Young-Hyang Park (2003), On the deep-water circulation of the eastern South Atlantic Ocean, *Deep-Sea Research Part I-Oceanographic Research Papers*, 50(7), 889-916.
- Boyle, E. A., and L. D. Keigwin (1985), Comparison of Atlantic and Pacific paleochemical records for the last 215,000 years - changes in deep ocean circulation and chemical inventories, *Earth and Planetary Science Letters*, 76(1-2), 135-150.
- Broecker, W., Katsumi Matsumoto, Elizabeth Clark, Irka Hajdas, Georges Bonani (1999), Radiocarbon age differences between coexisting foraminiferal species, *Paleoceanography*, 14(4), 431-436.
- Broecker, W., Stephen Barker, Elizabeth Clark, Irka Hajdas, Georges Bonani, Lowell Stott (2004a), Ventilation of the glacial deep Pacific Ocean, *Science*, 306(5699), 1169-1172.
- Broecker, W. S., and T.-h. Peng (1982), *Tracers in the Sea*, Lamont-Doherty Geological Observatory, Palisades, NY, USA.
- Broecker, W. S., Elizabeth Clark, Irena Hajdas, Georges Bonani (2004b), Glacial ventilation rates for the deep Pacific Ocean, *Paleoceanography*, 19(2), 12.
- Cain, W., N.C. Slowey, D.J. Thomas, C.D. Charles (2006), Neodymium as a tracer of glacial to interglacial change in Atlantic water column structure, edited, Fall Meet. Suppl., Abstract #PP31A-1737, Eos Trans. AGU.
- Duncombe Rae, C.M., 2005. A demonstration of the hydrographic partition of the Benguela upwelling ecosystem at 26°40', *South African Journal of Marine Science*, 27(3): 617-628.
- Field, D. B. (2004), Variability in vertical distributions of planktonic foraminifera in the California Current: Relationships to vertical ocean structure, *Paleoceanography*, 19(2), 27.
- Keigwin, L. D. (2004), Radiocarbon and stable isotope constraints on Last Glacial Maximum and Younger Dryas ventilation in the western North Atlantic, *Paleoceanography*, 19(4).
- Legrand, P., and C. Wunsch (1995), Constraints from paleotracer data on the North Atlantic circulation during the last glacial maximum, *Paleoceanography*, 10(6), 1011-1045.
- Meissner, K. J., A. Schmittner, A. J. Weaver, J. F. Adkins (2003), Ventilation of the North Atlantic Ocean during the Last Glacial Maximum: A comparison between simulated and observed radiocarbon ages, *Paleoceanography*, 18(2), 23.
- Piotrowski, A. M., Steven L. Goldstein, Sidney R. Hemming, Richard G. Fairbanks (2005), Temporal relationships of carbon cycling and ocean circulation at glacial boundaries, *Science*, 307(5717), 1933-1938.

Roark, E. B., Lynn Ingram, John Southon, James P. Kennett (2003), Holocene foraminiferal radiocarbon record of paleocirculation in the Santa Barbara Basin, *Geology*, 31(4), 379-382.

Ruhlemann, C., Carsten Rühlemann, Stefan Mulitza, Gerrit Lohmann, André Paul, Matthias Prange, Gerold Wefer (2004), Intermediate depth warming in the tropical Atlantic related to weakened thermohaline circulation: Combining paleoclimate data and modeling results for the last deglaciation, *Paleoceanography*, 19(1), 10.

Sarnthein, M., Kyaw Winn, Simon J. A. Jung, Jean-Claude Duplessy, Laurent Labeyrie, Helmut Erlenkeuser, Gerald Ganssen (1994), Changes in east Atlantic deepwater circulation over the last 30,000 years: Eight time slice reconstructions. *Paleoceanography*, 9(2), 209-267.

Schefuß, E., Stefan Schouten, Ralph R. Schneider (2005), Climatic controls on central African hydrology during the past 20,000 years, *Nature*, 437(7061), 1003-1006.

Schlitzer, R. (2000), Electronic Atlas of WOCE Hydrographic and Tracer Data Now Available, edited, Eos Trans. AGU.

Speer, K., G. Siedler, Lynne Talley (1995), The Namib Col Current, edited, pp. 1933-1950, Deep Sea Research I Oceanographic Research Papers.

Stramma, L., and M. England (1999), On the water masses and mean circulation of the South Atlantic Ocean, *Journal of Geophysical Research-Oceans*, 104(C9), 20863-20883.

Stuiver, M., and H. A. Polach (1977), Reporting of C-14 data - discussion, *Radiocarbon*, 19(3), 355-363.

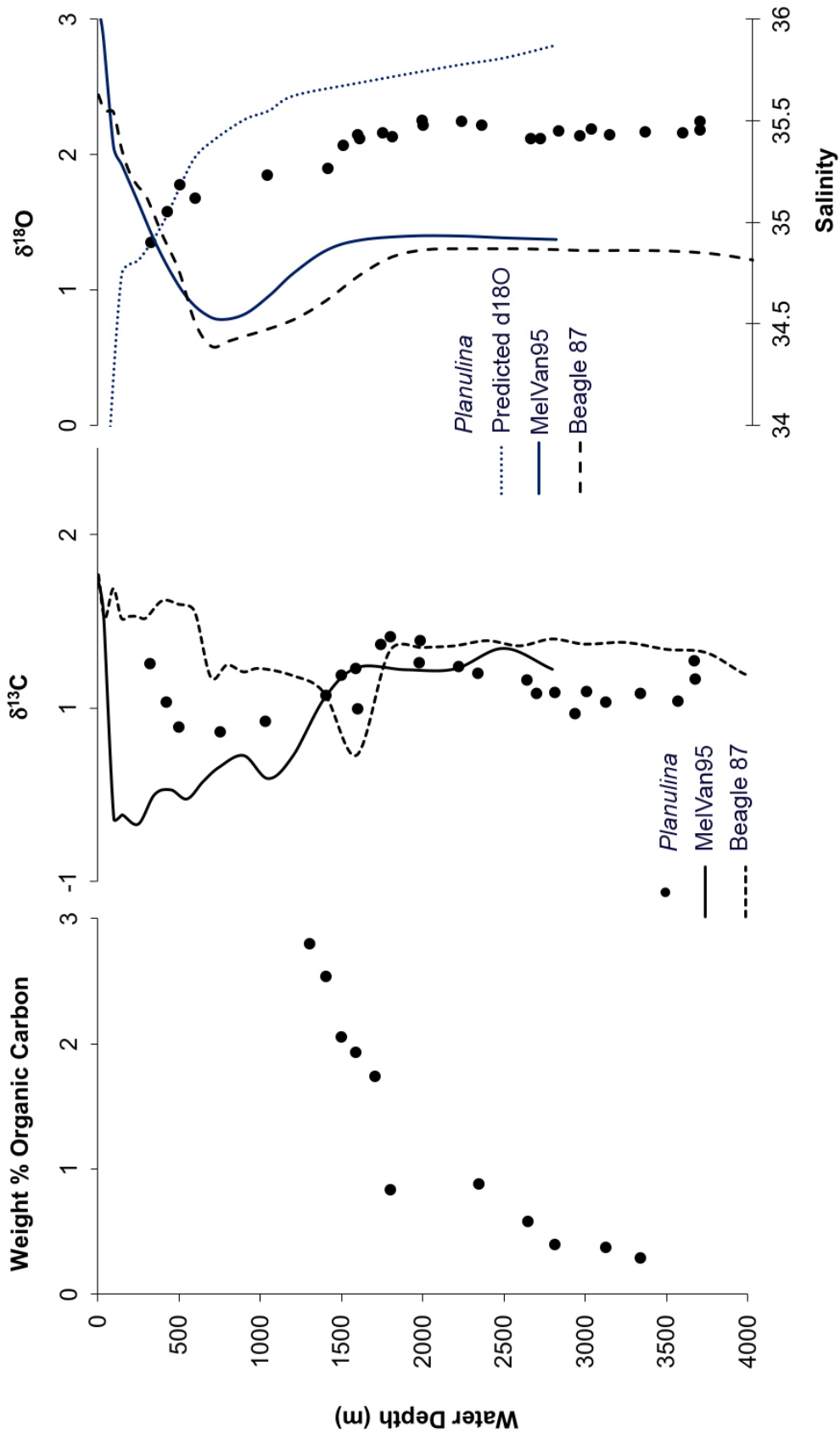
Toggweiler, J. R., and B. Samuels (1998), On the ocean's large-scale circulation near the limit of no vertical mixing, *Journal of Physical Oceanography*, 28(9), 1832-1852.

Table 3.1. Core type, depth, core top radiocarbon ages, and core depth to the LGM

Core	Core Type	Core Depth (m)	<i>Orbulina universa</i> (¹⁴ C age)	<i>Globigerina bulloides</i> (¹⁴ C age)	<i>G.bulloides</i> – <i>O. universa</i> ¹⁴ C age difference	Mixed Bethics (¹⁴ C age)	Depth to LGM (cm)
1078D (1.5-5.5cm)	Piston	427	615			1020	*970
1078D	Piston	427	455			1080	*970
1079C (3.5-7.5 cm)	Piston	737	260			1295	735
TAMU4		1000	905			1985	**235
56	Multicore	1037	625	----	----	1400	----
46	Gravity	1303	1630	----	----	2060	165
44	Gravity	1405	1120	----	----	1710	145
42	Gravity	1501	655	2275	1620	1205	145
55	Gravity	1590	505	----	----	1145	----
40	Gravity	1601	1495	2925	1430	1770	140
73	Gravity	1708	370	----	----	1120	----
38	Gravity	1742	1030	----	----	1485	155
26	Gravity	1803	1815	2840	1025	2255	100
22	Gravity	1980	1460	2725	1265	2140	110
108	Gravity	1987	910	1620	710	1870	----
53	Gravity	2224	1195	1305	110	1790	195
51	Gravity	2345	1705	2200	495	2750	160
63	Gravity	2646	1360	1920	560	2505	----
20	Gravity	2705	1560	2340	780	2550	120
18	Gravity	2813	1080	----	----	2050	120
16	Gravity	2942	690	1465	775	1770	130
14	Gravity	3012	600	1370	770	1685	----
12	Gravity	3127	805	1350	545	1770	115
11	Gravity	3342	670	1855	1185	2165	----
48	Trigger	3571	1150	----	----	2370	----
50	Multicore	3677	1070	----	----	2910	----
49	Trigger	3678	1145	1920	775	2995	----

* Data from core 1078C (Rühlemann et al., 2004); **Interpolated from a ¹⁴C age of 28,850

Figure 3.1. (left) weight % organic carbon of bulk sediment from core tops
(center) dissolved inorganic carbon $\delta^{13}\text{C}$ from MelVan station 95 and from BEAGLE station 87,
and measured $\delta^{13}\text{C}$ of benthic foraminifera.
(right) salinity values from MelVan station 95 and from BEAGLE station 87, $\delta^{18}\text{O}$ values from
the benthic foraminifera species *Planulina*, and predicted foraminiferal $\delta^{18}\text{O}$ values from water
column temperature and $\delta^{18}\text{O}$ data at GEOSECS site 107.
The salinity data and water samples for inorganic carbon analysis were collected aboard the R/V
Melville at station 95 at 12° 0.0'S, 9° 25.2'E. BEAGLE water samples were collected at station
87 at 29° 44.05'S, 9° 17.7'E. GEOSECS water samples were collected at station 107 at 12°0.0'S
and 1° 57.6'E. Benthic foraminifera were collected from the south slope of the Walvis Ridge.



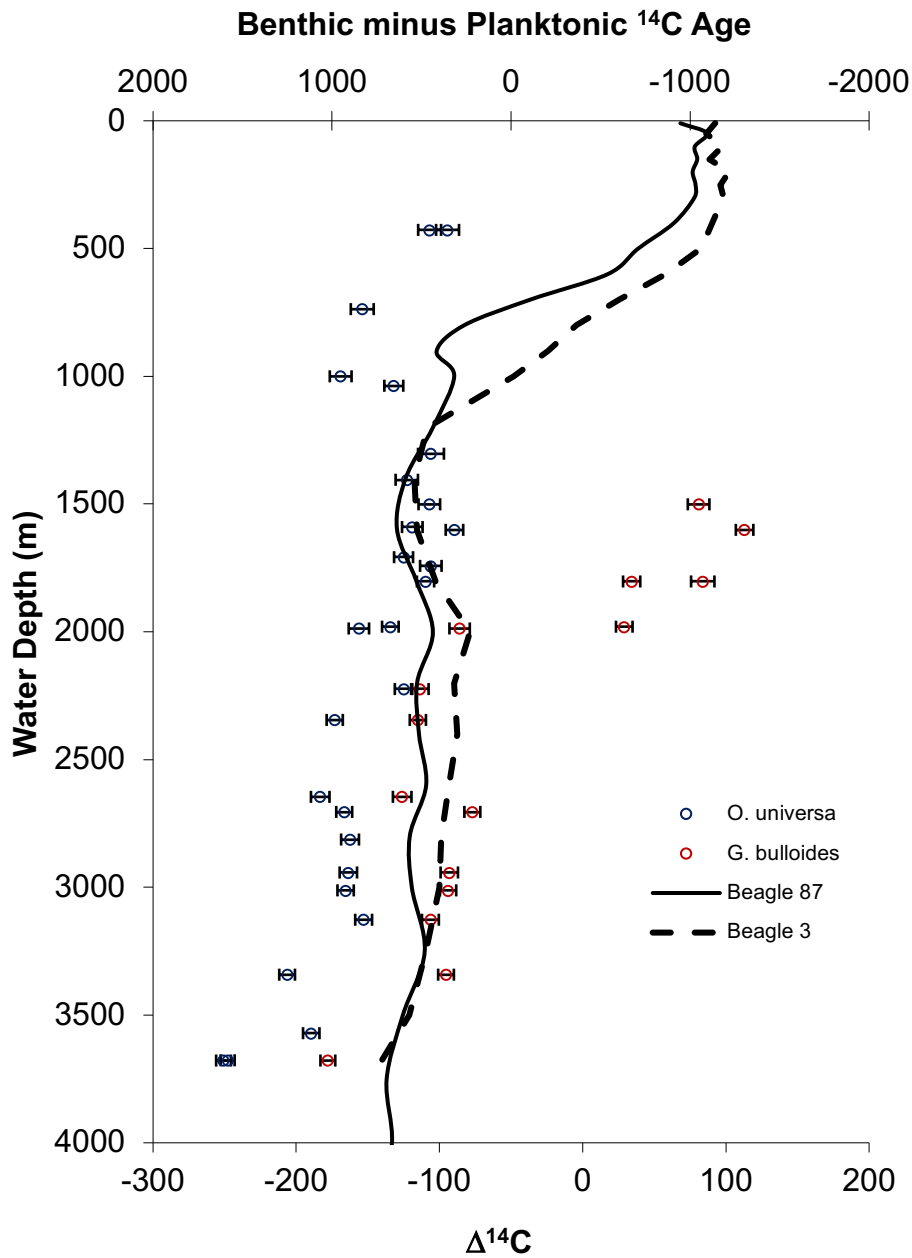


Figure 3.2. Benthic minus planktonic ^{14}C ages from cores tops. *Orbulina universa* in blue and *Globigerina bulloides* in red plotted versus the water depth of the core. $\Delta^{14}\text{C}$ values are shown on the bottom x-axis for a more direct comparison to the published BEAGLE water column profile of dissolved inorganic carbon $\Delta^{14}\text{C}$ values for stations 87 (29° 44.05'S, 9° 17.7'E) and 3 (28° 50.04'S, 43° 35.22'E).

Figure 3.3. (left) $\Delta^{14}\text{C}$ values of benthic foraminifera and $\Delta^{14}\text{C}$ of dissolved inorganic carbon of water from BEAGLE site 87. Silica (μmol) values from GEOSECS stations 103 and BEAGLE site 87

(right) Salinity data from MELVAN Stations 95 and 83.

Benthic foraminifera are from the south slope of the Walvis Ridge. BEAGLE 87 is located at $29^{\circ} 44.05'S$, $9^{\circ} 17.7'E$ and Geosecs 103 is located at $23^{\circ} 59.0'S$, $8^{\circ} 30.0'E$. MelVan 95 is located at $12^{\circ}0.0'S$, $9^{\circ} 25.2'E$ and MelVan 83 is located at $21^{\circ} 17.21' S$, $10^{\circ} 8.45' E$.

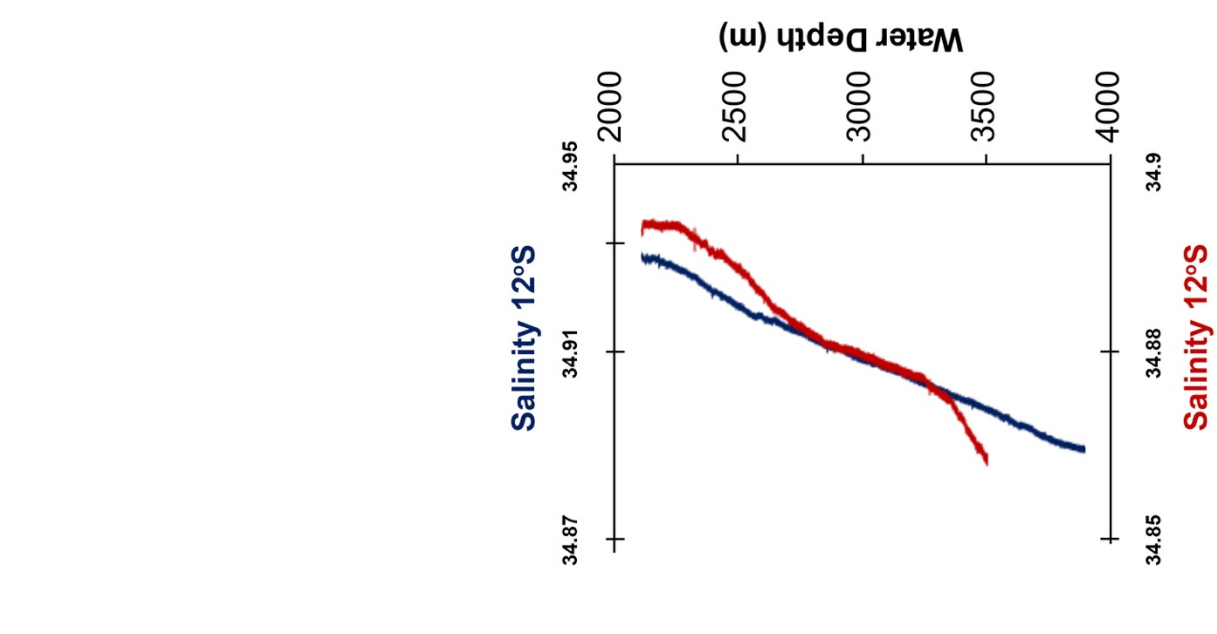
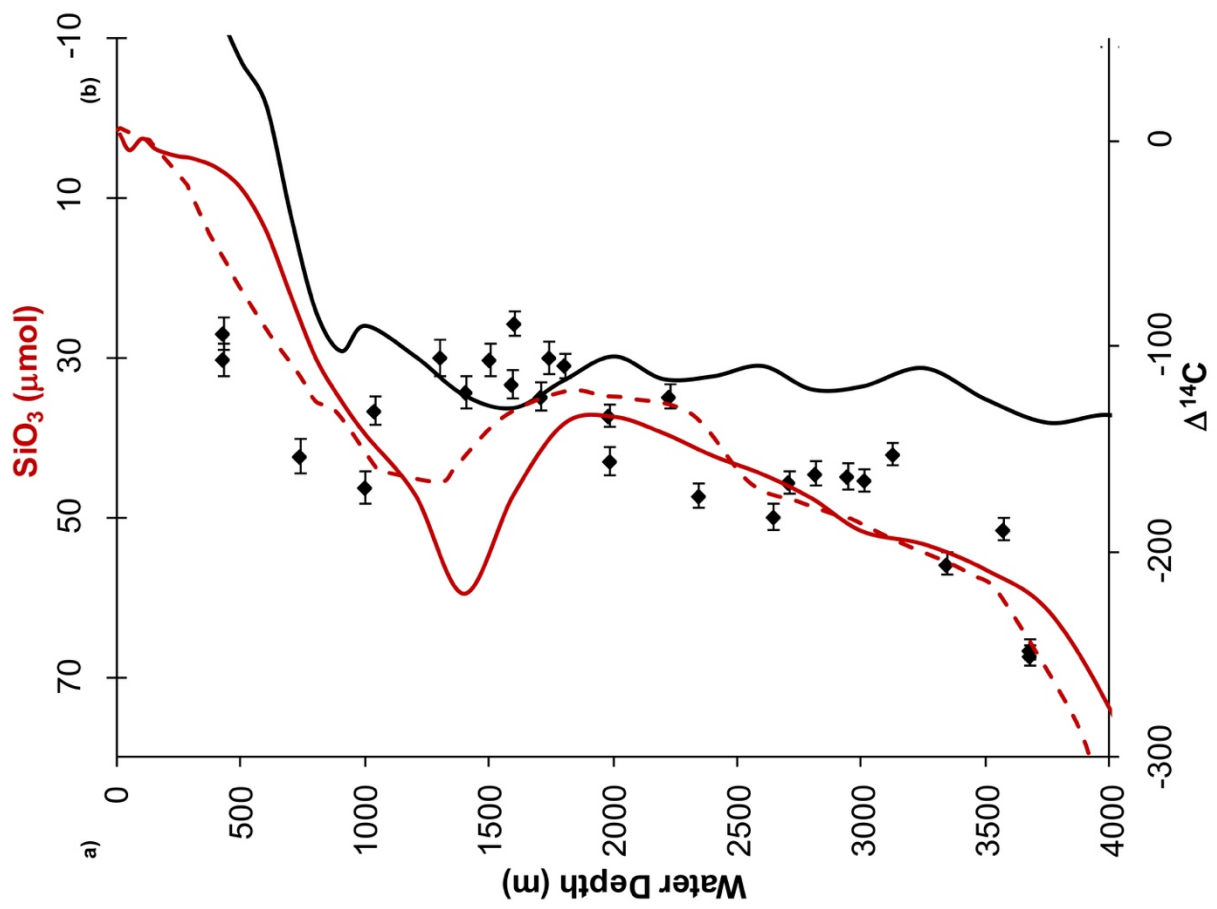
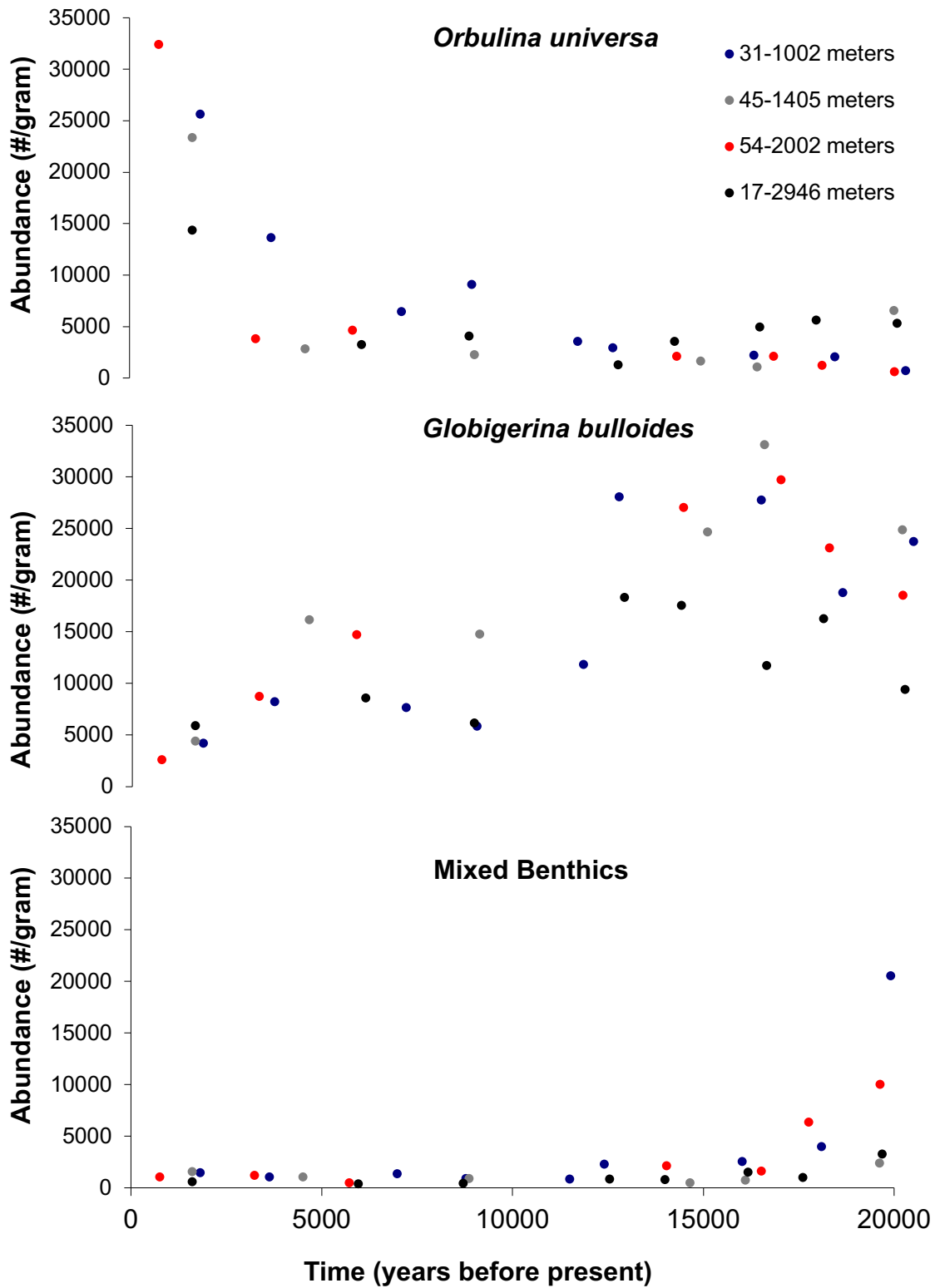


Figure 3.4. Abundance data (#/gram) for *O. universa*, *G. bulloides*, and mixed benthics from the present to the LGM for four cores: 31, 45, 54, and 17. The *depth in core* of 45, 54, and 17 was scaled to match core 31 using bulk density profiles and planktonic foraminifera stable isotope data. All cores were then plotted on a linearly interpolated age scale from core 31 planktonic radiocarbon dates.



Chapter 4

Water mass distribution from the past 20,000 years reconstructed from radiocarbon
and stable isotopes in the southeastern Atlantic

Abstract

Reconstructions of sedimentary nutrient proxy and stable carbon isotopes indicate substantial changes to the structure of the interior of the ocean at the Last Glacial Maximum (LGM) and throughout the last deglaciation. Yet there is debate about the interpretations of this altered geometry because the possible explanations for the redistribution of sedimentary tracers are not unique. Here we compare radiocarbon and stable carbon isotope results collected from a depth transect in the southeastern Atlantic, where presently the seafloor intersects all principal water masses involved in the thermohaline circulation of the Atlantic. Sediment cores ranging in water depth from 882 to 3092 meters are stratigraphically and chronologically correlated to three distinct time horizons – two during the deglacial period and one at the end of the last ice age. The benthic foraminiferal radiocarbon from the LGM suite of cores displays increasing age with depth between 800 and 2600 meters, a profile that is markedly different from that of the modern ocean. The radiocarbon results are entirely compatible with other sedimentary proxies suggesting that old (presumably Southern-sourced) water filled the deep Atlantic basin at the close of the last ice age. They further demonstrate that the altered glacial nutrient proxy and carbon isotope distribution did not result from non-conservative or “nutrient trapping” effects.

Introduction

It is widely believed that the geometry of the deep-water masses in the Atlantic Ocean during the Last Glacial Maximum (LGM) through the deglacial period differed substantially from that of the modern ocean. At the LGM, $\delta^{13}\text{C}$, Cd/Ca, and Zn/Ca tracers from the North Atlantic reconstruct a pattern of apparently nutrient (and carbon) depleted water overlying nutrient (and carbon) rich water (SSW) with a boundary between 2000 and 2500 m (*Boyle and Keigwin*, 1982 and 1987; *Duplessy et al.*, 1988; *Marchitto*, 2002). Such reconstructions have been refined in areas where the observations allow vertical discrimination—for example, *Curry and Oppo* (2005) found evidence for a three-water-mass structure in the southwestern Atlantic—but generally, the patterns (*Curry and Oppo*, 2005; *Duplessy et al.*, 1988; *Marchitto et al.*, 2002) lead overwhelmingly to the conclusion that (i) much of the deep Atlantic Ocean was occupied by waters of Southern Ocean origin; and (ii) this change in the deep ocean was accompanied by, if not caused by, a weakening and shoaling of North Atlantic Deep Water (NADW) overturning circulation. Additionally, abrupt changes in the global climate and deep-ocean systems punctuated the last deglacial period. One of the best documented of these abrupt shifts is the transition to the Bolling-Allerod warm period about 14.5 ka, when, as the Greenland ice core evidence demonstrates, temperatures over central Greenland rose by roughly 10°C over the course of several decades (*Dahl-Jensen*, 1998). The role of the ocean's meridional overturning circulation in promoting or amplifying this abrupt change is hotly debated. There is little doubt that this climate shift was accompanied by a rearrangement of the pattern of nutrient-like sedimentary tracers of deep ocean circulation. Prior to 14.5 ka, tracers such as benthic foraminiferal $\delta^{13}\text{C}$ and sedimentary Nd data indicate that the deep Atlantic Ocean was still in its ice age-like state of apparent nutrient enrichment (*Sarnthein et al*, 1994; *Charles and Fairbanks*,

1992; *Piotrowski*, 2004). These reconstructions stand in stark contrast to the state of the ocean during the Bolling-Allerod (BA), when $\delta^{13}\text{C}$, Cd/Ca, and Nd, tracers in the deep Atlantic were distributed in a state that is similar to that of the modern ocean (*Alley and Clark*, 1999; *Piotrowski*, 2004). Thus, from these considerations, one might conclude that the ocean's overturning circulation flipped from ice age to modern modes at the time of the Bolling-Allerod. However some tracer evidence (*Marchitto*, 2007; *McManus*, 2004) also suggests that the most anomalous state of the deep ocean period occurred just after the close of the last ice age during an episode of extreme iceberg discharge to the North Atlantic Ocean—an episode known as Heinrich Event I. Thus, it may be inappropriate to view the deglaciation history in the deep ocean as essentially a binary shift in modes of operation.

The validity of these interpretations, however, has been called into question (e.g. *Legrand and Wunsch*, 1995) because the most common sedimentary tracers available to define the water mass geometry can be affected by a number of processes aside from the vigor of circulation and the mixing in the interior of the ocean (e.g. *Mix and Fairbanks*, 1985; *Piotrowski et al.* 2004). In fact, analysis of other tracers such as $^{231}\text{Pa}/^{230}\text{Th}$ – which is sensitive to nuclide export from the deep Atlantic and therefore is less directly tied to nutrient cycling – tend to suggest a relatively minor slowdown of the meridional overturning during the LGM compared to the Holocene, with the largest anomaly during the post-glacial interval (*McManus et al.*, 2004).

How might these apparent contradictions be resolved? Radiocarbon offers perhaps the most readily available additional constraint, because dateable benthic materials are ubiquitous throughout the global oceans and because the radiocarbon concentration of various water masses is potentially more diagnostic of ventilation history. Existing radiocarbon results in the Atlantic are concentrated in the western North Atlantic and derive from the dating of both benthic

foraminifera and deep-sea corals. At the LGM, the benthic and planktonic foraminifera pairs reconstruct apparent ventilation ages over 1000 years old below 3000 m, reaching their oldest values of approximately 1500 years below 4000 m (*Keigwin, 2002 and 2005*). As with the $\delta^{13}\text{C}$ reconstructions, these North Atlantic radiocarbon observations suggest an influx of old, southern source water (SSW) to the deep North Atlantic during the LGM. Shallower ventilation ages, reconstructed at 1700 meters by *Robinson et al. (2005)* using deep-sea corals and paired benthic and planktonic foraminifera, indicate a well-ventilated northern source water mass. *Robinson et al.* concluded the SSW was circulating vigorously and the radiocarbon depletion of southern source waters resulted from increased sea-ice cover in the Southern Ocean. However, comparable reconstructions must be built in other regions of the global ocean for a full mechanistic understanding of the role of the deep ocean in the climate of the last ice age.

Here we present radiocarbon and stable isotope results collected from a depth transect in the southeastern Atlantic where, presently the seafloor intersects all the principal water masses involved in the thermohaline circulation of the Atlantic. Our previous core top study results indicate radiocarbon and $\delta^{13}\text{C}$ can be used to distinguish different water masses, although the sensitivity of the paired planktonic-benthic foraminiferal radiocarbon method requires careful culling of cores. Sediment cores ranging in water depth from 882 to 3092 meters can be stratigraphically and chronologically correlated at three distinct horizons.

Here we use three well-defined stratigraphic markers in Southeastern Atlantic sediment cores—the shift from high to low sediment bulk density (increased opal concentration) that is coincident with the Bolling-Allerod event and a $\delta^{18}\text{O}$ high preceding an abrupt excursion to lower values (essentially the close of the last ice age) – to build depth transects of benthic-planktonic foraminiferal radiocarbon age pairs before and after these climatic transitions. These

radiocarbon measurements, along with accompanying stable isotopic profiles, provide a firm anchor for reconstruction across two of the most dramatic climatic transitions of the last deglaciation – the end of the LGM and the BA transition.

Materials and Methods

All piston cores analyzed for radiocarbon and presented here were collected aboard the R/V Melville in March 2003 (MelVan09), south of the Walvis Ridge on the continental slope of Africa. All were collected along two depth transects within a square area defined by 20° 4.99'S and 21° 18.52'S and 10° 38.3'E and 11° 44.50'E and range in depth from 1002 to 3092 meters. These cores were also analyzed for $\delta^{18}\text{O}$ and $\delta^{13}\text{C}$, along with one additional core – 1079 from ODP leg 175 (11° 55.7'S and 13° 18.54'E, 755 meters). Three datasets are described further in this chapter – “The Last Glacial Maximum Dataset”, the “15.2 kyr dataset”, and the “13.7 kyr” dataset.

15.2 kyr and 13.7 kyr Datasets:

As described in chapter one, the bulk density profiles of six cores align at the prominent shift from high to low values using the *O. universa* calendar age scale for each core. From these six cores spanning 1405 to 3092 meters water depth, there are two well-dated and distinct time slices where benthic $\Delta^{14}\text{C}$, $\delta^{13}\text{C}$, and $\delta^{18}\text{O}$ measurements were made – these are marked with black circles on the density graph in figure 4.1. The dataset at the density high before the shift consists of six cores and will be referred to as the 15.2 kyr dataset and the dataset from the density low following the density shift will be referred to as the 13.7 kyr dataset. The samples used from each core for radiocarbon and stable isotope measurements are presented in table 4.1.

Benthic foraminifera stable isotope analysis were performed on *Planulina* (all species) from all size fractions, each sample weighing between 150 and 190 μg .

LGM Dataset:

Initially, twenty-three cores were sampled in two-centimeter sections at five or ten-centimeter intervals and wet sieved through 63 μ m mesh. The tests of the planktonic foraminifera species *Orbulina universa* or *Globigerina bulloides* from the 250-425 μ m size fraction were analyzed for $\delta^{18}\text{O}$ and $\delta^{13}\text{C}$. From the $\delta^{18}\text{O}$ stratigraphies, thirteen cores were selected to radiocarbon date the apparent last glacial maximum interval. As opposed to only dating samples with a benthic foraminifera abundance peak (Keigwin, 2002), our strategy was to date all cores whose stratigraphy implied a reasonable chance of having a robust LGM point. Subsequently we determined which of these points we felt had recorded an LGM signal based on the selected radiocarbon date, the radiocarbon dates above the apparent LGM point from the deglacial period, and other sedimentological indices. While this strategy will date more samples than suitable, we feel with stable isotope and radiocarbon data and careful core selection, it allows us to maximize the number of cores for our study as opposed to only identifying those with benthic abundance peaks.

Benthic foraminifera stable isotope analysis was performed on *Cibicides pachyderma*, *Planulina* (all species), *Uvigerina akitaensis*, and *Uvigerina urnula* picked from the 150-425 μ m size fraction.

All Samples:

All isotopic analyses were done using a common acid-bath, Carousel-48 automation carbonate preparation device coupled to a Finnigan MAT 252 mass spectrometer. Estimated analytical precision, deduced from the concurrent measurement of 175 NBS 19 standards, was 0.05 to 0.07 per mil for $\delta^{13}\text{C}$ and $\delta^{18}\text{O}$, respectively.

Radiocarbon measurements were made at the Center for Accelerator Mass Spectrometry at Lawrence Livermore National Laboratory on *Globigerina bulloides* and mixed benthic samples. Foraminifera tests were sonicated in a .0001N HCl solution; planktonics were sonicated briefly to avoid having the shells explode, whereas benthics were sonicated for 1 minute. The HCl was then pipetted off and the samples were dried, weighed, and graphitized. Sample sizes varied between .4 and 8 mg. We assigned a $^{13}\text{C}/^{12}\text{C}$ ratio of 0‰ for all samples to correct for the mass-dependent fractionation. Planktonic radiocarbon ages were converted to calendar ages with the CALIB 5.0.2 program, which uses a marine reservoir correction of 408 years.

Results

All cores were analyzed for bulk density, stable carbon and oxygen isotopes and radiocarbon. In addition to the modern sediments analyzed (chapter 2), we identified three well-defined stratigraphic markers – the shift from high to low sediment bulk density during the deglacial period and the Last Glacial Maximum (LGM). The radiocarbon dated deglacial points are indicated by black circles in figure 4.1 – these points were also analyzed for benthic $\delta^{13}\text{C}$ values. The deglacial bulk density shift can also be seen compared to the downcore measurements of benthic $\delta^{13}\text{C}$ from four cores at 1002, 1405, 1804, and 2946 meters that were presented in chapter 2 (figure 2.2). Last glacial maximum points chosen for radiocarbon and benthic $\delta^{13}\text{C}$ and $\delta^{18}\text{O}$ analysis were determined from *Globigerina bulloides* $\delta^{18}\text{O}$ values. These selected LGM points are indicated in figure 4.3.

$\delta^{18}\text{O}$

Modern and LGM oxygen stable isotope data for benthic foraminifera and $\delta^{18}\text{O}$ values of two *Uvigerina* species are plotted in figure 4.4. The *Uvigerina* species values have been corrected using correction values obtained from duplicate *Planulina* and *Uvigerina* runs from our samples and the offset is similar to the 0.64‰ correction of Shackleton (1974). $\delta^{13}\text{C}$ values from *Uvigerina* species were not plotted as these values have been shown to be representative of pore water values as opposed to seawater values (McCorkle *et al.*, 1990).

$\delta^{13}\text{C}$

$\delta^{13}\text{C}$ from the 13.7 kyr, 15.2 kyr., LGM, and modern (chapter 2) datasets, are plotted in figure 4.5. Both the 13.7 kyr and 15.2 kyr datasets shows an enrichment of $\delta^{13}\text{C}$ from deeper to shallower waters between 3100 and 1900 meters, although this is only constrained by three points (two for the 15.2 kyr. dataset and one for the 13.7 kyr. dataset). Between 1400 and 1900 meters, both profiles indicate little significant change.

Other than core 31 (1002 m), it is apparent from these graphs that the shift to modern values takes place after the density shift in cores 45, 27, and 17 (1405, 1804, and 2946 meters, respectively), although core 45 is closer to modern values than cores 27 and 17. Core 17 does show an initial shift of approximately .25‰ from lower to higher $\delta^{13}\text{C}$ values at approximately the same time as the density shift – although it is hard to constrain this timing as core 17 has a 10 cm sampling interval for stable isotope data.

Our LGM $\delta^{13}\text{C}$ values are significantly depleted below 3600 meters and gradually increase from 3000 meters (-.201 ‰) to 1400 meters (.63 ‰). Here, the mid-depth $\delta^{13}\text{C}$ maximum shoaled from 1800 meters in the Holocene to 1400 meters during the LGM. Above this point, we have one value at 635 meters that remains relatively high at .61 ‰. LGM and

Holocene values converge between 1700 and 1400 meters, whereas there is an increasingly large offset between our LGM and Holocene values between 1700 and 3000 meters ranging from .45 to .70 ‰ and a larger offset of .80 to 1.0‰ below 3600 meters. Above 1400 meters, our LGM values remain consistent, as opposed to returning to lower values as Curry and Oppo found in their Brazilian Margin cores. Our coverage in this intermediate depth between 600 and 1400 meters is sparse, but as with our $\delta^{18}\text{O}$ values, we find no evidence for an intermediate water structure in $\delta^{13}\text{C}$ akin to that associated with modern Antarctic Intermediate Water. This is in contrast to Curry and Oppo's stable isotope ($\delta^{18}\text{O}$ and $\delta^{13}\text{C}$) results indicating a third, shallow, southern source water mass during the LGM whose northward extent is not constrained. In this regard it is also interesting to note our highest $\delta^{13}\text{C}$ values are only .63‰, lower than the .9‰ measured on the Brazil margin for the equivalent water depths.

Radiocarbon

The 15.2 kyr dataset at the density high before the shift consists of six cores and has an average calendar age of 15,235 years BP. Of the six points, five are tightly constrained to within 550 years of each other – ranging from 14,714 to 15,275 years BP. An additional point in the dataset from core 45 (1405 m) is dated at 15,509 years BP. This point is slightly older than the rest of the dataset, but core 43 (1505 meters - dated to 15.0 kyr) provides a second data point at this depth range for verification.

The 13.7 kyr dataset from the density low following the density shift has an average calendar age of 13,727 years BP. Of the six points in this dataset, five have tightly constrained calendar ages within 500 years of each other – ranging from 13,640 to 14,171 years BP. One data point from core 52 was dated at 12,809 years BP and will be disregarded from further

discussion as this is after the onset of the Younger-Dryas interval when large-scale Atlantic circulation changes have been inferred from other proxies (*Came et al. 2003*).

Benthic radiocarbon from both datasets are plotted in figure 4.6. Values are plotted as the $\Delta^{14}\text{C}$ relative to the atmosphere ($\Delta^{14}\text{C}_{\text{sample}} - \Delta^{14}\text{C}_{\text{atmosphere}}$), along with the modern profile reconstructed from core tops (chapter 2). Atmospheric $\Delta^{14}\text{C}$ values prior to 14,000 calendar years BP are from the Intcal dataset, whereas values younger than 14,000 calendar years BP are from the Fairbanks 2005 dataset.

Our six $\Delta^{14}\text{C}$ values from the 15.2 kyr dataset indicate a substantial difference in values compared with the core top reconstructions. At 1405 and 1503 meters, the offset from the modern profile is constrained to between approximately 75‰ and 120‰, respectively. The offset from modern values becomes more depleted (greater than 200‰) at the depths of 1724, 1902, and 2343 meters. At 3092 meters, the $\Delta^{14}\text{C}$ value falls near the modern profile.

Compared to the modern profile, the 15.2 kyr profile has a much shallower, larger magnitude, and more abrupt offset between the radiocarbon enriched and depleted waters below. This transition of approximately 100‰ (from enriched to depleted waters) takes place between 1500 and 1725 meters. This in contrast to the modern profile, where the transition from enriched to depleted waters starts at 1800 meters and is much more gradual with depth, with an initial transition of 50‰ over 500 meters water depth.

The five $\Delta^{14}\text{C}$ values from the 13.7 kyr dataset exhibit very little change through the water column. The three shallowest points (1405 to 1902 meters) have essentially the same $\Delta^{14}\text{C}$ value (average = -180‰), taking into account the errors imposed by both the planktonic and benthic ^{14}C dates. The deepest point at 3092 is slightly more depleted (-245‰). These five

values are close to the modern profile and more enriched in radiocarbon than the profiles from the 15.2 kyr dataset.

We do not observe a radiocarbon depleted water mass overlying our shallowest, more enriched points in either profile, but it is possible that our cores are not shallow enough to capture the signature of this water mass as the modern boundary between northern and southern water recorded in our core tops is at 1000 meters, shallower than any of our cores from this time period.

Of the twelve cores radiocarbon dated, seven had tightly constrained *G. bulloides* radiocarbon ages, ranging from 16,710 to 16,990, at the stratigraphic level of the LGM (defined by planktonic foraminiferal $\delta^{18}\text{O}$ values). This tight age constraint made these seven an ideal choice for reconstructing the southeastern Atlantic LGM water mass distribution. Planktonic ages, sedimentation rates, stratigraphic features, and additional radiocarbon ages above and below the apparent LGM point were used to disqualify the seven other cores. The planktonic $\delta^{18}\text{O}$ stratigraphies of these seven cores used for our LGM reconstruction are plotted in figure 4.7 and the ^{14}C ages and distance to the LGM (as a proxy for sedimentation rate) are indicated in table 4.2. As shown by our core-top calibration at this site, core-top *G. bulloides* radiocarbon content may be significantly offset from the radiocarbon content of surface waters. Nevertheless, we chose to date and present *G. bulloides* because they have higher abundances during the LGM than in core top sediments. Furthermore, the behavior of *G. bulloides* during the LGM may be very different from that of the modern ocean (for one thing, there is no indication of older *G. bulloides* dates than the corresponding mixed benthics in the ice age samples). Therefore, instead of plotting our values as either $\Delta^{14}\text{C}$ as we did with core top sediments, or as a projection ages (*Adkins and Boyle, 1997*), our values are plotted in figure 4.7

as the mixed benthic ^{14}C date minus the *G. bulloides* ^{14}C date. It is important to note that although the *G. bulloides* ^{14}C dates may be difficult to translate into a precise calendar age, our tightly constrained planktonic dates are at least internally consistent with one another. Although the benthic minus planktonic scale is floating and does not provide us with an absolute ventilation age, the apparent $\Delta^{14}\text{C}$ gradient with water depth is unaffected by the issue of absolute value.

Data from core MD07 (3770 meters in the South Atlantic) from *Skinner et al* is plotted on figure 4.7 as well. The addition of this deeper data point indicates there is very little change in the benthic minus planktonic values during the LGM between this deep core and our data between 1900 and 2600 meters.

Discussion

Deglacial Results

The most obvious anomaly from our $\delta^{13}\text{C}$ and radiocarbon profiles is the 15.2 kyr $\delta^{13}\text{C}$ values are not depleted with respect to the LGM like the radiocarbon results. Our LGM and modern $\Delta^{14}\text{C}$ and $\delta^{13}\text{C}$ data suggest $\delta^{13}\text{C}$ closely follows the $\Delta^{14}\text{C}$ pattern and both proxies characterize the water mass distribution, whereas this relationship is uncoupled at our 15.2 kyr time slice. There is no evidence for benthic $\delta^{13}\text{C}$ and $\Delta^{14}\text{C}$ uncoupling and when our deglacial cores are more closely scrutinized, it becomes obvious these cores are sedimentologically disrupted.

Our downcore abundance graphs from chapter 1 show the following pattern: *O. universa* abundance in all four cores was high in the late Holocene, with a steady increase from low values during the LGM. The total benthic abundance (mixed assemblage) has the exact opposite trend –

low during the late Holocene, with a significant increase during the LGM. The *G. bulloides* data indicates a maximum during the early Holocene (and deglaciation), with a steady decline to the present. These abundance maxima can help explain our flawed deglacial data. Core 27's "calendar age" versus "depth in core" for two planktonic species is plotted in figure 4.8 to illustrate one way to identify flawed core sequences. If only *G. bulloides* had been radiocarbon dated, there would appear to be no sedimentological disturbances in the core. When the *O. universa* radiocarbon dates are added, problems within the core become apparent. It appears that downward mixing from the *O. universa* abundance peak has given four dated points in the core artificially young radiocarbon ages. This could be one explanation for the highly depleted radiocarbon ages observed in the 15.2 kyr dataset. Downward mixing of young *O. universa* from a modern abundance peak would produce a larger benthic minus planktonic ^{14}C age for past reconstructed water masses. Additionally, upward mixing of old benthic foraminifera from the LGM abundance peak would further enhance the benthic minus planktonic ^{14}C age. Therefore downward mixing of young planktonic foraminifera and the upward mixing of old benthic foraminifera could both be combining to produce the artificial, highly depleted benthic minus planktonic ^{14}C ages we calculated for the deglacial. Although it is disappointing to not have reliable water mass reconstructions from the deglacial period, the results stress the importance of dating abundance peaks and the importance of benthic $\delta^{13}\text{C}$ data as a verification of the benthic minus planktonic values – two criteria that were both met with our Last Glacial Maximum Data.

LGM density gradients obtained from $\delta^{18}\text{O}$

Our LGM oxygen isotope data demands a significant cooling of the interior of the ocean, relative to modern temperatures in this region. For example, our deepest $\delta^{18}\text{O}$ sample (3000

meters) indicates a Holocene to LGM $\delta^{18}\text{O}$ difference of 2.1‰. If one assumes that the global ice volume effect is on the order of 1.0 per mil, then the residual (2.1-1.0 = 1.1‰) must be mainly the result of temperature change—as much as 4°C cooling. A change this large in the $\delta^{18}\text{O}$ at 3000 meters from a measured modern temperature of 2.49°C supports Adkins (2002) proposal that the glacial deep ocean was everywhere close to the freezing point. However, the $\delta^{18}\text{O}$ measurements also suggest a change in the density structure between 1400 and 1600 meters: we see no inflection of higher $\delta^{18}\text{O}$ values in the intermediate water as Curry and Oppo (2005) do in their Brazilian Margin cores which they cite as evidence for a third water mass, AAIW, in the South Atlantic during the LGM.

Our oxygen stable isotope values are useful for adding to the Lynch-Stieglitz *et al.* (2006) $\delta^{18}\text{O}$ data set reconstructing cross basin density gradients and the vertical shear associated with the north and southward flow of waters in the Atlantic. Our values are plotted with Lynch-Stieglitz's in figure 4.4. It was determined through intercalibration studies done at Woods Hole Oceanographic Institution (WHOI) for Lynch-Stieglitz's study that an offset of .18‰ exists between values run at WHOI and those run at Scripps. In this paper, I have subtracted .18 ‰ from the values published in Lynch-Stieglitz *et al.* Lynch-Stieglitz has less coverage from the eastern (African) margin below 1000 meters (four LGM and Holocene data points) as opposed to above 1000 meters (ten Holocene and nine LGM data points). Our data fills in the gaps, especially below 1000 meters where we have nine Holocene and eleven LGM data points. Additionally, using data from our suite of cores may overcome many of the problems Lynch-Stieglitz *et al.* pointed out with the eastern margin cores used in their study: low sedimentation rates, changes in abundance from *Planulina* and *Cibicides* dominating during the Holocene to a dominance of *Bolivina* during the LGM, and bioturbation. Our cores have sedimentation rates

above 5 cm/1000 kyrs (which may reduce bioturbation effects), planktonic stratigraphies and ^{14}C dates that well define the LGM, and a sufficient amount of either *Planulina* or *Uvigerina* for reliable stable isotope values. All of our Holocene samples are *Planulina*, which allows for a robust LGM comparison to *Uvigerina* values as the offset between *Planulina* and *Uvigerina* is documented and we were able to run both species from the sample to verify these offsets.

Our findings differ from Lynch–Stieglitz’s below 1000; we find consistently lower eastern margin $\delta^{18}\text{O}$ values in both the Holocene and LGM as opposed to higher eastern margin $\delta^{18}\text{O}$ values in the Holocene and similar eastern and western margin values in the LGM. Above 1000 meters, our few data points are consistent with Lynch-Stieglitz’s finding of higher densities from the eastern margin during the Holocene and a reversal during the LGM of higher density waters from the western margin. Our data (lower eastern margin densities below 1000 meters) may indicate that geostrophic shear reconstructions, in regard to the strength of meridional overturning, can be confined to above 1000 meters. If this is the case, our data is consistent with a reversal in the cross-basin density gradient above 1000 meters, yet show little change below 1000 meters.

South Atlantic $\delta^{13}\text{C}$

The $\delta^{13}\text{C}$ results from the Southeastern Atlantic depth transect are consistent, at least in a relative sense, with other reconstructions that depict a water mass that is high in $\delta^{13}\text{C}$ in the modern intermediate water depth zone, a strong gradient towards lower $\delta^{13}\text{C}$ values between 1400 and 2500 meters, and uniformly low values below 2500 meters water depth. These results therefore serve to reinforce the concept of the “two-layer” Atlantic Ocean during the last ice age, with the deep Atlantic occupied by much colder, more nutrient and carbon-rich water.

However, while these results expand the geographic extent of the $\delta^{13}\text{C}$ observations, they do not, by themselves, contribute much more to the debate on the forces that produced this altered geometry of nutrient-like tracers in the ice age ocean. For example, it is not possible with these results alone to discriminate among the relative influences of air-sea gas exchange (which creates the potential for “pre-formed” $\delta^{13}\text{C}$ shifts of up to a 0.5 per mil), nutrient “trapping” phenomena that might concentrate nutrients at lower depths in the ocean, “whole ocean” $\delta^{13}\text{C}$ effects resulting from the variable land-sea partitioning of carbon, and the mixing and ventilation of water masses. Thus the joint evidence from radiocarbon is important because all of these possible influences on $\delta^{13}\text{C}$ should be differentially expressed in radiocarbon.

LGM radiocarbon

Our seven radiocarbon benthic minus planktonic values indicate a substantial shift in the distribution of water masses during the Last Glacial Maximum compared with the core top reconstructions (figure 4.9). Our core top data indicates an apparent radiocarbon minimum in the intermediate water zone (1500-500 meters), an apparent radiocarbon maximum at about 2000 meters, and an apparent gradual decline of deep radiocarbon from 2000-4000 meters. In contrast, the LGM radiocarbon crude ages (crude ages refer to the benthic minus planktonic age of coexisting foraminifera – this calculation does not take into account the different surface $\Delta^{14}\text{C}$ values of the warm waters overlying core locations and the polar source waters the benthics are bathed in) suggest water age increasing with depth between 800 and 2600 meters. This shallow shift to younger waters may be the result of the shoaling of NADW to form a water mass has been termed Glacial North Atlantic Intermediate Water (GNAIW) (*Boyle and Keigwin 1987*). This water mass is presumed to be radiocarbon enriched, as well as fresher (and therefore less

dense) than contemporary NADW. Our LGM water mass reconstruction can be reconciled with various models of LGM circulation. Keeling and Stephens (2001) proposed a glacial “off” mode during the LGM, during which there is a permanent collapse of the conveyor in which GNAIW overlies denser, salty, southern source waters. This reconfiguration is possible if GNAIW is insufficiently dense to sink below southern source waters whose density increased as enhanced sea ice cover increased their salinity. This collapsed state in which AAIW directly overlies AABW requires that a significant portion of the deep ocean be filled with AABW to the sill depth of the Drake Passage – between 1500 and 2500 meters (*Keeling and Stephens, 2001*). Kwon *et al* (2012) propose an alternate theory of the deep, South Atlantic being southern-sourced, but still containing and increased fraction of North Atlantic ventilated water. This theory reconciles LGM data showing the Atlantic being bathed in presumably southern sourced low, $\delta^{13}\text{C}$ waters and an LGM reduction in atmospheric CO_2 – presumably due to an increase in North Atlantic ventilated water..

The deepest benthic minus planktonic age from our LGM dataset is 1085 years at 2560 meters. To compare LGM crude ages at our study location to those measured by Broecker at 3200 meters in the Pacific, we use the LGM radiocarbon trend (increasing crude ages with increasing depth) to extrapolate a crude age at 3200 meters of 1640 years. During the LGM, this would require ~900 years of aging between deep southeastern Atlantic values and those of the deep Pacific. Currently, SSW waters in the deep South Atlantic have a $\Delta^{14}\text{C}$ value of -160‰ (data courtesy of Robert Key from SAVE, located at 30°0'S, 12°15'E), corresponding to a crude age of 1100 years. The difference between these values and the modern radiocarbon of the Pacific (1625 years crude age) requires aging between the basins of ~525 years. Although the

difference in ages between the basins is larger during the LGM, Broecker's deep Pacific results are consistent with the radiocarbon trend in our cores.

Keigwin concludes from his additional, older LGM samples that because the radiocarbon values are the same as the radiocarbon in the modern deep north Pacific, it is plausible the same water mass, probably of southern origin, flowed deep within each basin during the LGM.

Robinson proposes, based on the synchronicity of the pattern of LGM deep Atlantic $\Delta^{14}\text{C}$ and the atmospheric $\Delta^{14}\text{C}$ that the SSW filling the deep Atlantic basin is circulating vigorously and the cause of the radiocarbon depleted values is extensive sea-ice coverage in the Southern Ocean.

This conclusion agrees with Keeling and Stephen hypothesis that there was an increase in sea-ice cover in the Southern Ocean during the LGM. Our result of LGM crude ages being older than current values by approximately 400 to 800 years below 2000 meters do not allow us to differentiate radiocarbon depletion due to increased sea ice cover from depletion due to increased ventilation ages. But, if, as Robinson proposes, SSW was circulating vigorously and there was enhanced sea-ice cover, our LGM radiocarbon results would agree with this scenario. In contrast, based on benthic $\delta^{18}\text{O}$ and $\delta^{13}\text{C}$ data, Lund et al. (2011) propose that southern-sourced Antarctic Bottom water shoaled to 2000 meters during the LGM and reduced vertical mixing resulted in the sequestration of significant quantities of carbon during glacial times. Our radiocarbon data is also consistent with this interpretation of the Atlantic LGM Ocean – we see a shift to highly depleted radiocarbon values right at 2000 meters.

As observed in our core top reconstruction, the LGM radiocarbon and $\delta^{13}\text{C}$ patterns are in agreement, indicating the $\delta^{13}\text{C}$ values are recording the inorganic carbon signal of the water in which they are growing. The agreement between the two proxies cannot rule out $\delta^{13}\text{C}$ being affected by the variable land-sea partitioning of carbon or air-sea gas exchange, as these would

affect the profile at all depths. However, the results do suggest processes that would affect only part of the $\delta^{13}\text{C}$ profile (i.e. confined to deep or shallow water), such as nutrient trapping, are not incorporated into the benthic foraminifera $\delta^{13}\text{C}$ signal. The agreement between the two proxy patterns indicates both radiocarbon and $\delta^{13}\text{C}$ are reflecting the changed water mass geometry at the LGM. This confirms our assertion that the Atlantic LGM deep ocean was filled with an old, nutrient enriched water mass, above which the concentration of radiocarbon increased and nutrients decreased with decreasing depth.

Summary and Conclusions

We used seven cores from the southeastern Atlantic, whose concurrent stratigraphy was verified by planktonic $\delta^{18}\text{O}$ values and ^{14}C ages, to characterize the LGM water mass distribution. Our results showing water ages increase with depth between 800 and 2600 meters was verified using both $\delta^{13}\text{C}$ and ^{14}C . This verification was deemed crucial after analyzing two distinct time periods during the deglacial period whose $\delta^{13}\text{C}$ and ^{14}C was uncoupled. Upon further examination, these cores were found to have sedimentological problems during the deglacial period and we concluded it is vital to have $\delta^{13}\text{C}$ verify radiocarbon results, as well as only interpret periods of foraminifera abundance peaks.

Our LGM results enhance our understanding of the Atlantic LGM ocean from an integral, and heretofore missing, geographical location. They are consistent with north Atlantic $\delta^{13}\text{C}$, Cd/Ca, and Zn/Ca records and south Atlantic Nd records which indicate the deep Atlantic basin filled to the sill depth of the Drake Passage with southern source radiocarbon depleted waters that were overlain by a weaker, shoaled northern source water mass of radiocarbon enriched waters. This interpretation conflicts with Pa/Th data suggesting NADW was vigorously overturning at the LGM.

The agreement between the $\delta^{13}\text{C}$ and $\Delta^{14}\text{C}$ patterns suggests at the LGM, $\delta^{13}\text{C}$ distribution is a reflection of the changed water mass geometry. Our core top $\Delta^{14}\text{C}$ and $\delta^{13}\text{C}$ values followed the same pattern as well, suggesting that accompanying $\delta^{13}\text{C}$ data can be used as a check of the validity of $\Delta^{14}\text{C}$ reconstructions, or in the absence of $\Delta^{14}\text{C}$ values, benthic $\delta^{13}\text{C}$ measurements can be used as a proxy for water mass distribution.

Acknowledgments

This work was supported by an NSF award to CDC and SEGRF fellowship at LLNL to JM. Sample material used in this project provided by the Ocean Drilling Program Bremen Core Repository.

References

- Adkins, J. F., and E. A. Boyle (1997), Changing atmospheric Delta C-14 and the record of deep water paleoventilation ages, *Paleoceanography*, 12(3), 337-344.
- Adkins, J. F., Katherine McIntyre, Daniel P Schrag (2002), The salinity, temperature, and delta O-18 of the glacial deep ocean, *Science*, 298(5599), 1769-1773.
- Boyle, E. A., and L. D. Keigwin (1982), Deep circulation of the North-Atlantic over the last 200,000 years - geochemical evidence, *Science*, 218(4574), 784-787.
- Boyle, E. A., and L. Keigwin (1987), North-Atlantic thermohaline circulation during the past 20,000 years linked to high-latitude surface temperature, *Nature*, 330(6143), 35-40.
- Broecker, W., Stephen Barker, Elizabeth Clark, Irka Hajdas, Georges Bonani, Lowell Stott (2004b), Ventilation of the glacial deep Pacific Ocean, *Science*, 306(5699), 1169-1172.
- Broecker, W. S. (2002), Constraints on the Glacial Operation of the Atlantic Ocean's Conveyor Circulation, *Israel Journal of Chemistry*, 42(1), 14.
- Broecker, W. S., Elizabeth Clark, Irena Hajdas, Georges Bonani (2004a), Glacial ventilation rates for the deep Pacific Ocean, *Paleoceanography*, 19(2), 12.
- Duplessy J.-C., N. J. Shackleton, R. G. Fairbanks, L. Labeyrie, D. Oppo, and N. Kallel, 1988: Deepwater source variations during the last climate cycle and their impact on the global deepwater circulation. *Paleoceanography*, 3, 343–360.
- Keeling, R. F., and B. B. Stephens (2001), Antarctic sea ice and the control of Pleistocene climate instability, *Paleoceanography*, 16(1), 20.
- Keigwin, L., Marley Bice, Nancy J Copley, (2005), Seasonality and stable isotopes in planktonic foraminifera off Cape Cod, Massachusetts, *Paleoceanography*, 20(4).
- Keigwin, L. D., and M. A. Schlegel (2002), Ocean ventilation and sedimentation since the glacial maximum at 3 km in the western North Atlantic, *Geochemistry Geophysics Geosystems*, 3.
- Keigwin, L. D. (2004), Radiocarbon and stable isotope constraints on Last Glacial Maximum and Younger Dryas ventilation in the western North Atlantic, *Paleoceanography*, 19(4), 15.
- Kwon, E.Y., Mathis P. Hain, Daniel M. Sigman, Eric D. Galbraith, Jorge L. Sarmiento, and J.R. Toggweiler, (2012), North Atlantic ventilation of “southern-sourced” deep water in the glacial ocean, *Paleoceanography*, 27.
- Legrand P., and C. Wunsch, 1995: Constraints from paleotracer data on the North-Atlantic circulation during the last glacial maximum. *Paleoceanography*, 10, 1011–1045.

Lund, D. C., J. F. Adkins, and R. Ferrari (2011), Abyssal Atlantic circulation during the Last Glacial Maximum: Constraining the ratio between transport and vertical mixing, *Paleoceanography*, 26.

Lynch-Stieglitz, J., William B. Curry, Delia W. Oppo, Ulysses S. Ninneman, Christopher D. Charles, Jenna Munson (2006), Meridional overturning circulation in the South Atlantic at the last glacial maximum, *Geochemistry Geophysics Geosystems*, 7, 14.

Marchitto, T. M., Delia W. Oppo, William B. Curry (2002), Paired benthic foraminiferal Cd/Ca and Zn/Ca evidence for a greatly increased presence of Southern Ocean Water in the glacial North Atlantic, *Paleoceanography*, 17(3), 16.

McCorkle, D. C., L. Keigwin, B. Corliss, S. Emerson (1990), The influence of microhabitats on the carbon isotopic composition of deep-sea benthic foraminifera, *Paleoceanography*, 5(2), 25.

McManus, J. F., J.-M. Gherardi, L. D. Keigwin, S. Brown-Leger, R. Francois (2004), Collapse and rapid resumption of Atlantic meridional circulation linked to deglacial climate changes, *Nature*, 428(6985), 834-837.

Mix A. C., and R. Fairbanks, 1985: North Atlantic surface-ocean control of Pleistocene deep-ocean circulation. *Earth Planet. Sci. Lett.*, 73, 231-243.

Shackleton, N. (1974). Attainment of isotopic equilibrium between ocean water and the benthic foraminifera genus *uvigerina*: isotopic changes in the ocean during the last glacial. In *Les méthodes quantitatives d'étude des variations du climat au cours du pléistocène*, pages 203-209. J. Labeyrie, CNRS, Paris.

Skinner, L. C., S. Fallon, C. Waelbroeck, E. Michel, and S. Barker (2010) *Ventilation of the Deep Southern Ocean and Deglacial CO₂ Rise*. *Science*, 328 (5982). pp. 1147-1151.

Ostlund, H. G. (1988), GEOSECS Atlantic, Pacific, Indian, and Mediterranean Radiocarbon Data, in *NDP-027*, edited, Carbon Dioxide Information Analysis Center, Oak Ridge, TN.

Piotrowski, Alexander M., Steven L. Goldstein, Sidney R. Hemming, Richard G. Fairbanks (2004), Intensification and variability of ocean thermohaline circulation through the last deglaciation, *Earth and Planetary Science Letters*, 225(1-2), 205-220.

Robinson, L. F., Jess F. Adkins, Lloyd D. Keigwin, John Southon, Diego P. Fernandez, S-L Wang, Daniel S. Scheirer (2005), Radiocarbon variability in the western North Atlantic during the last deglaciation, *Science*, 310(5753), 1469-1473.

Yu, E.-F., R. Francois, and P. Bacon, 1996: Similar rates of modern and last-glacial ocean thermohaline circulation inferred from radiochemical data. *Nature*, 379, 689-694.

Table 4.1. Samples used from each core for radiocarbon and stable isotope measurements

Water Depth (m)	Core/Section/Interval	Depth in Core (m)	<i>O. universa</i> calendar age BP	$\Delta^{14}\text{C}$ (‰)	$\delta^{13}\text{C}$ (‰)	$\delta^{18}\text{O}$ (‰)
1405	45/1/90-92 cm	.910	13,640	-135	0.28	2.66
1503	43/1/111.5-113.5 cm	1.145			0.13	3.34
1724	39/2/62-64 cm	1.030	13,657	-106	0.39	
1902	25/2/13-14 cm	.585	14,171	-154	0.35	2.67
2343	52/1/87-89 cm	.880	12,809**	-271**	0.37**	3.13**
3092	13/1/64-66 cm	.650	13,695	-156	0.09	3.33
1405	45/1/100-102 cm	1.010			0.47	2.88
1405	45/1/102-104 cm	1.030	15,509	-208		
1503	43/1/125.5-127.5 cm	1.265	15,013	-208		
1724	39/2/77-79 cm	1.180	14,831	-297	0.22	3.35
1902	25/2/20-22 cm	.655	15,275	-319	0.29	3.83
2343	52/1/100-102 cm	1.01	14,714	-329	0.14	
3092	13/1/72-74 cm	.730	14,756	-162	0.24	3.50

**this interval was not used as it dated younger than the rest of the dataset

Table 4.2. ^{14}C ages and distance to the LGM (as a proxy for sedimentation rate)

Core Type	Core Depth (m)	Glacial Core	<i>Globigerina bulloides</i> (^{14}C age)	Mixed Bethics (^{14}C age)	Benthic – <i>G. bulloides</i> ^{14}C age difference	centimeters to the LGM
31	Piston	882	16,840	16,985	145 years	210
45	Piston	1285	16,990	17,460	470 years	145
43	Piston	1383	16,825	17,305	480 years	145
27	Piston	1684	16,985	17,500	515 years	100
23	Piston	1857	16,710	17,735	1025 years	110
52	Piston	2223	16,835	17,715	880 years	160
21	Piston	2560	16,850	17,935	1,085 years	120

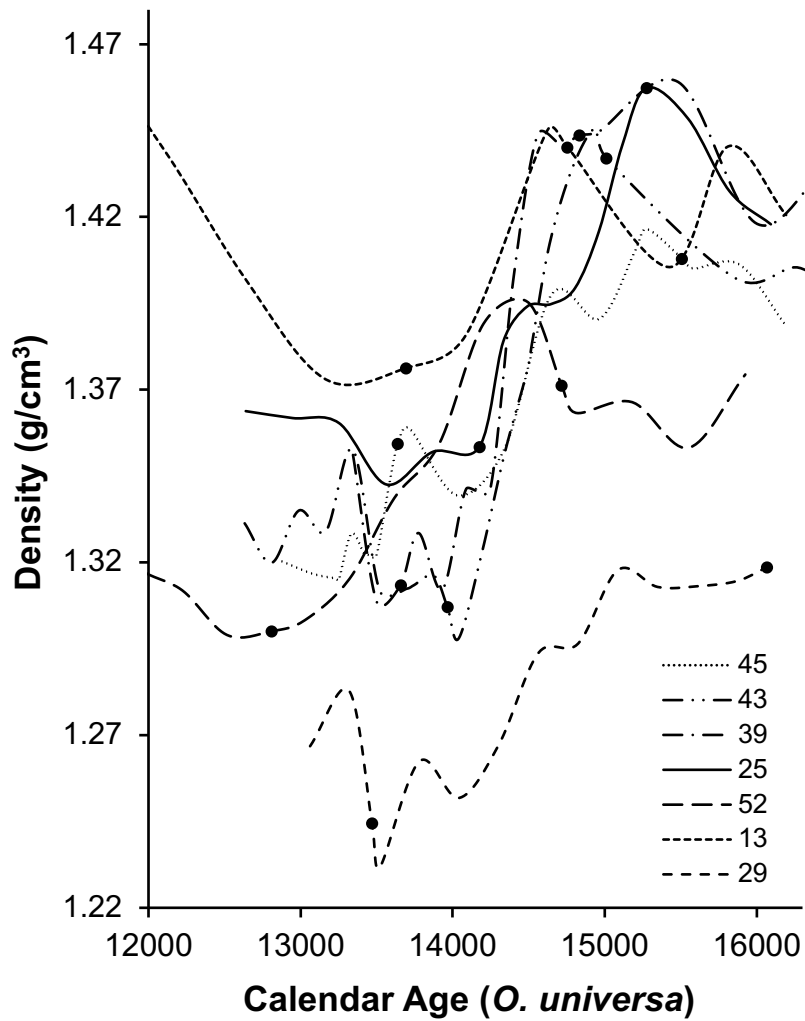


Figure 4.1. Stacked density profiles of seven cores spanning the density high to low transition plotted with calendar age. Black circles indicate radiocarbon dated intervals

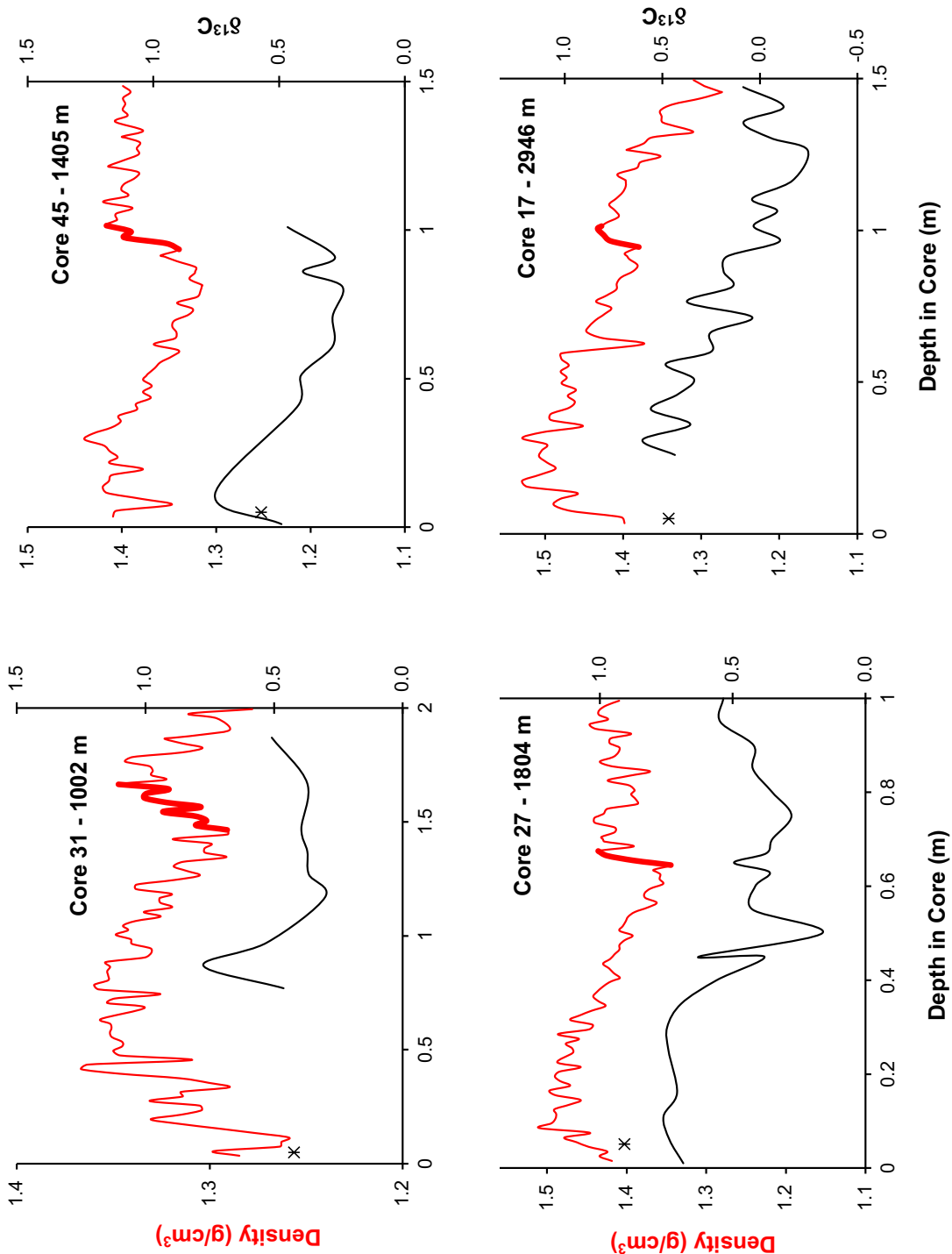


Figure 4.2. Downcore $\delta^{13}\text{C}$ and bulk density values plotted versus depth in core for cores 31, 45, 27, and 17. The black asterisk (*) on the graph is the modern $\delta^{13}\text{C}$ value measured from gravity core tops.

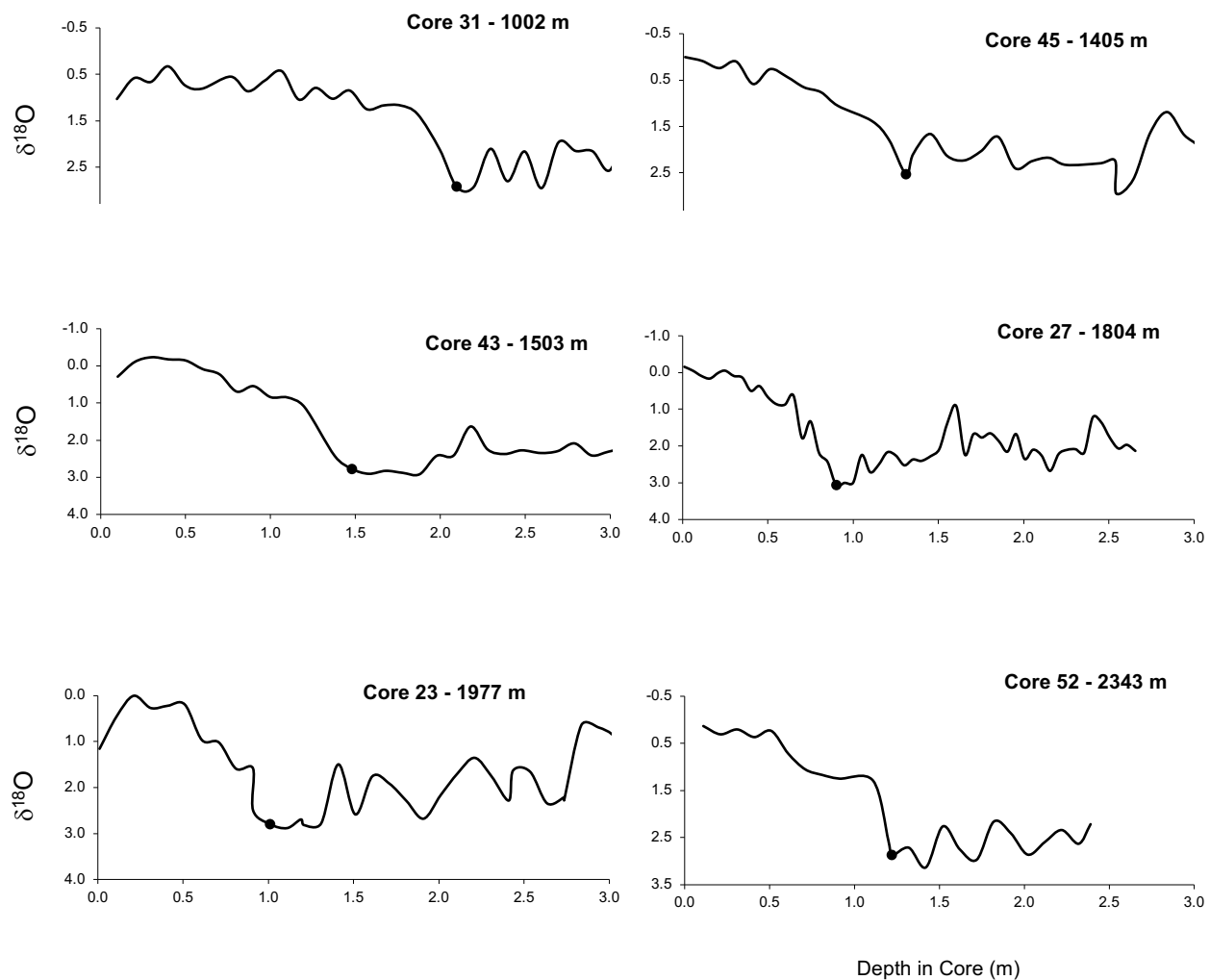
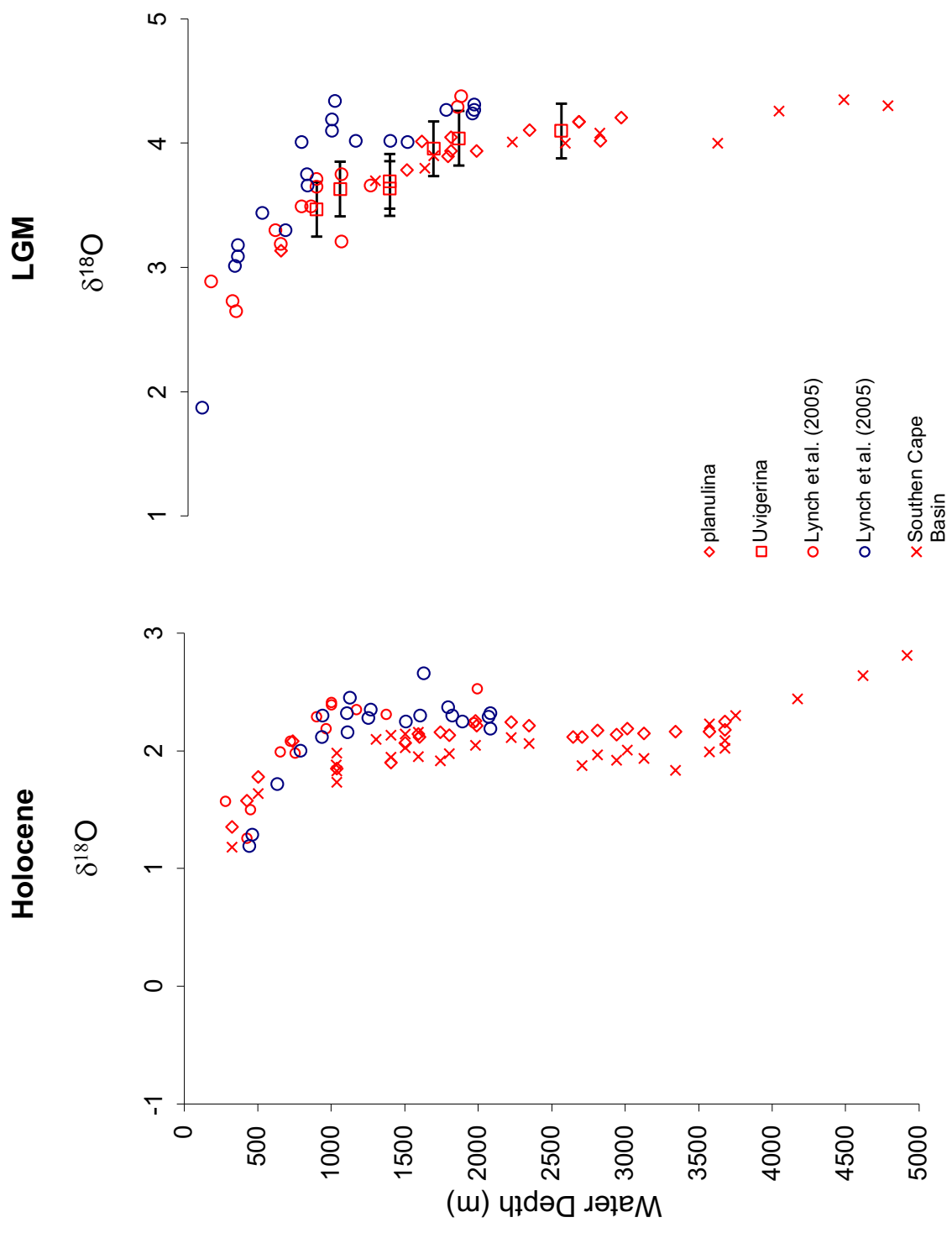


Figure 4.3. *Globigerina bulloides* $\delta^{18}\text{O}$ values plotted versus depth in core. All cores were sampled at a 10 cm interval except core 27, which had a 5 cm sampling interval. Black circles indicate where the Last Glacial Maximum was radiocarbon dated.

Figure 4.4. Modern and Last Glacial Maximum benthic foraminifera $\delta^{18}\text{O}$ values plotted versus core water depth (m) from our samples, data from the Southern Cape Basin (from C. Charles), and data from *Lynch-Stieglitz et al.* (2005).

Red points are from the eastern South Atlantic off the African margin and blue points are from the western South Atlantic off the Brazilian Margin. 120 meters were subtracted from the actual water depth of the LGM samples to account for Last Glacial Maximum sea-level change.

Analytical precision for $\delta^{13}\text{C}$ measurements is .05‰ and .07‰ for $\delta^{18}\text{O}$ measurements. Error bars are indicated for *Uvigerina* samples as larger errors were introduced when correcting for the offset between *planulina* and *Uvigerina*



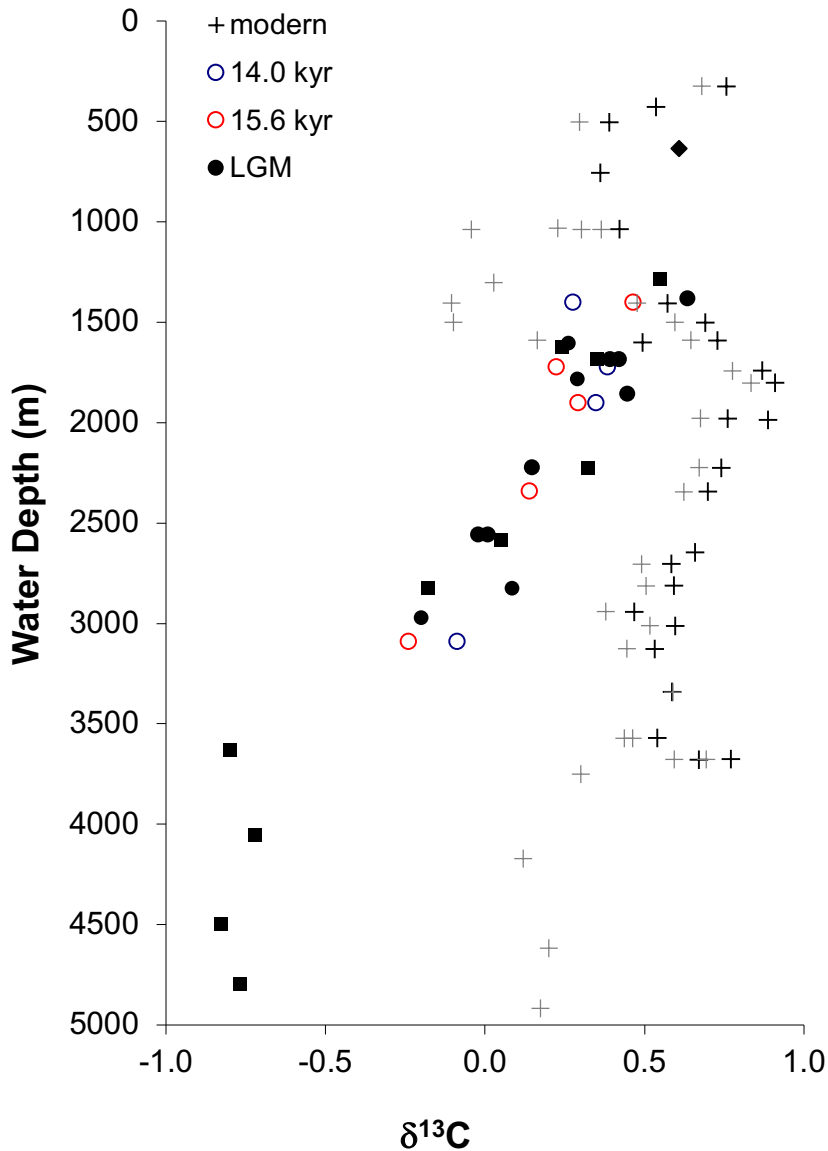


Figure 4.5. Benthic $\delta^{13}\text{C}$ values from, modern LGM, 15.2 kyr, and 13.7 kyr datasets. 120 meters were subtracted from the actual water depth of the LGM samples to account for Last Glacial Maximum sea-level change. Error is $\pm .05$ per mil.

Modern data in black are from results presented in chapter 2 and grey data points are from additional Southern Cape Basin data.

Diamond (\blacklozenge) points indicate samples from the seven cores presented with radiocarbon data in this paper, (\blacksquare) points are from additional radiocarbon dated southern Cape Basin cores, and circle (\bullet) points indicate samples from other cores whose LGM point was determined stratigraphically.

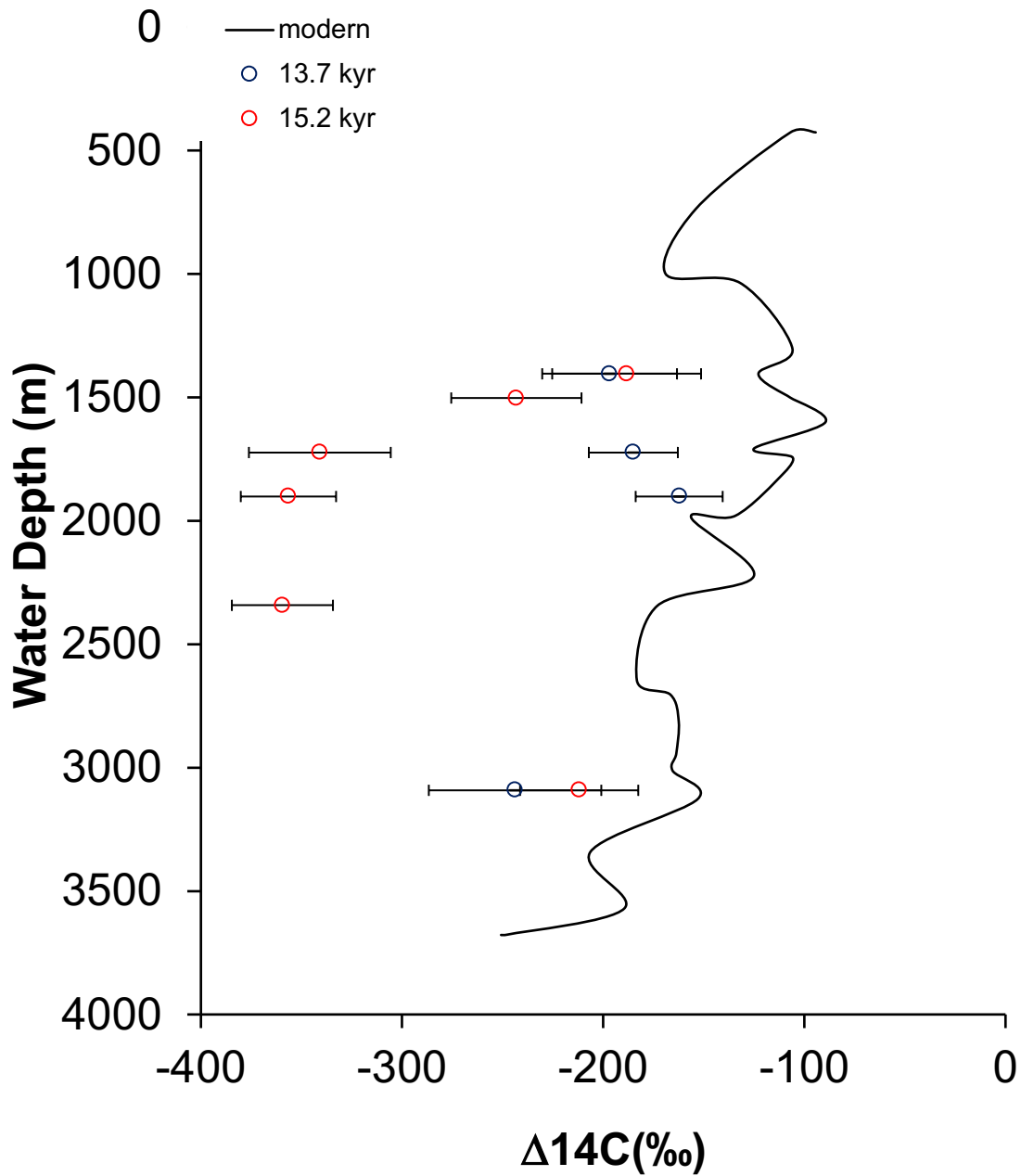
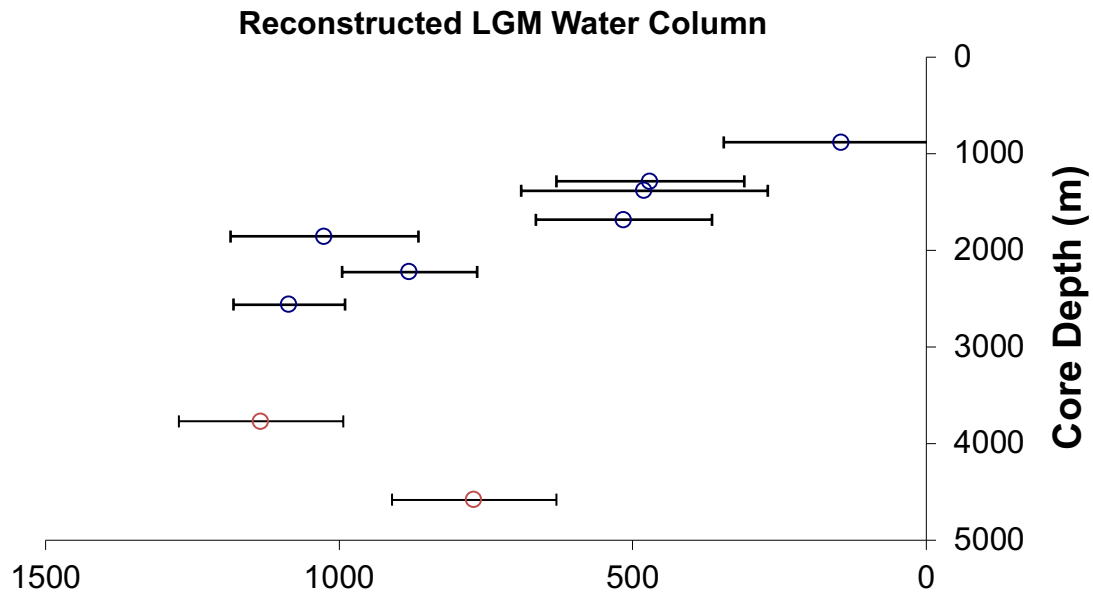


Figure 4.6. $\Delta^{14}\text{C}$ values measured on *O. universa* plotted relative to the atmosphere from the 15.2 kyr, 13.7 kyr, and modern datasets.

Atmospheric $\Delta^{14}\text{C}$ values prior to 14,000 calendar years BP are from the Intcal dataset, whereas values younger than 14,000 calendar years BP are from the Fairbanks 2005 dataset.



Benthic ^{14}C Age minus planktonic ^{14}C Age

Figure 4.7. Benthic minus planktonic ^{14}C dates plotted versus the water depth of the core. Blue points are from data presented in this chapter and red points are from additional South Atlantic cores: MD07 (3770 meters) from *Skinner et al.* and unpublished data from TNO57-5 (4700 meters)

120 meters was subtracted from the actual water depth of the core to account for Last Glacial Maximum sea-level change

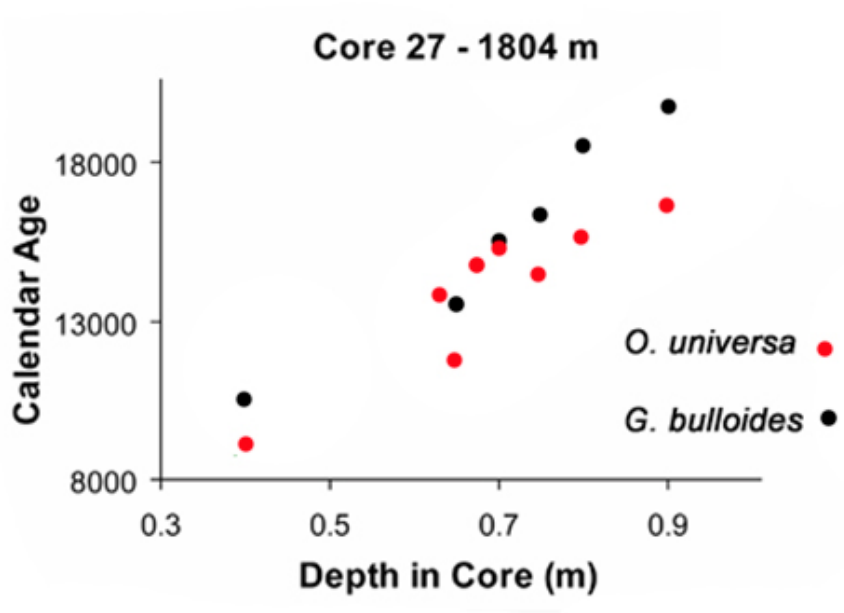


Figure 4.8. Calendar age plotted versus *depth in core* for two planktonic species, *O. universa* and *G. bulloides* of core 27.

